DISTINCT TRANSCRIPTIONAL REGULATION OF HUMAN NEUTRAL AMINO ACID TRANSPORTER SNAT2 BY ENDOPLASMIC RETICULUM STRESS AND AMINO ACID LIMITATION

By

ALTIN GJYMISHKA

A DISSERTATION PRESENTED TO THE GRADUATE SCHOOL
OF THE UNIVERSITY OF FLORIDA IN PARTIAL FULFILLMENT
OF THE REQUIREMENTS FOR THE DEGREE OF
DOCTOR OF PHILOSOPHY

UNIVERSITY OF FLORIDA

2008

To my father, Niazi Gjymishka (1937-2004)

ACKNOWLEDGMENTS

These years of Ph.D. studies in biomedical sciences here at the University of Florida have represented a great opportunity for me to expand my scientific knowledge. It has been a unique learning experience and I want to thank all the people who contributed to and supported me during this period. I will start acknowledging the person who has had the biggest impact on my education and scientific training during this period, my mentor Dr. Michael S. Kilberg. To me he has always represented the tireless teacher, the great educator and most of all, the passionate scientist. His dedication and professionalism to the graduate student training have always been a source of inspiration to me. Also, I want to thank my distinguished committee members Dr. Brian D. Cain, Dr. Jorg Bungert, Dr. Maureen M. Goodenow and Dr. Stephen Hunger for their service, advice and contribution to bring my work to completion. I want to thank present and past members of the Kilberg laboratory that I had the opportunity to work with during the years. I address special thanks to Elizabeth who has been an excellent colleague and a great friend to me.

The support I received from my family, who lives in Albania where I am proudly from, has been of enormous importance. Especially, I want to acknowledge my father Niazi Gjymishka, a person of exceptional intellect and character, and a great believer in education. His support and motivation have always represented the solid foundation of my academic achievements. Also, I thank my mother Kumrie and my brother Ilir, who visited me here at UF during this period, for their unlimited support. Finally, I want to dedicate this work to my wonderful daughter Erina and to my wife and my best friend Roxana. They have been my strongest supporters and we together, during this period, have endured the implicit sacrifices of an intense graduate training. They represent the joy and the motivation in my life. Because of them, my accomplishments are greater and bear plenty of significance.

TABLE OF CONTENTS

LIST OF TABLES

LIST OF FIGURES

Figure

page

LIST OF ABBREVIATIONS

AAR	amino acid response
AARE	amino acid response element
ASNS	asparagine synthetase
ATF	activating transcription factor
BiP/GRP78	immunoglobulin-heavy-chain-binding protein/glucose regulated protein 78
C/EBP	CCAAT/enhancer-binding protein
ChIP	chromatin immunoprecipitation
CHOP	C/EBP homology protein
ERSE	endoplasmic reticulum stress element
ERSR	endoplasmic reticulum stress response
GAPDH	glyceraldehyde-3-phosphate dehydrogenase gene
GCN2	general control non-derepressible 2
GTF	general transcription factor
HisOH	histidinol
LAP	liver-enriched activating protein
LIP	liver-enriched inhibitory protein
mTOR	mammalian target of rapamycin
NSRE	nutrient sensing response element
NSRU	nutrient sensing response unit
PERK	double-stranded RNA-activated protein kinase – like endoplasmic reticulum kinase
qRT-PCR	quantitative real-time PCR
RT-PCR	reverse transcriptase-polymerase chain reaction

SNAT2	System A sodium-dependent neutral amino acid transporter 2
TBP	TATA-box binding protein
TFII	general transcription factor II
Tg	thapsigargin
Tu	tunicamycin
UPR	unfolded protein response
XBP1	X-box binding protein 1

Abstract of Dissertation Presented to the Graduate School
of the University of Florida in Partial Fulfillment of the
Requirements for the Degree of Doctor of Philosophy

DISTINCT TRANSCRIPTIONAL REGULATION OF HUMAN NEUTRAL AMINO ACID TRANSPORTER SNAT2 BY ENDOPLASMIC RETICULUM STRESS AND AMINO ACID LIMITATION

By

Altin Gjymishka

December 2008

Chair: Michael S. Kilberg
Major: Medical Sciences--Biochemistry and Molecular Biology

Accumulation of malfolded proteins in the ER lumen triggers an adaptive response known as the unfolded protein response (UPR), which comprises signal transduction pathways that slow protein synthesis, increase the ER folding capacity, and ultimately, provoke cell death. Whereas, amino acid deprivation leads to the activation of a signaling cascade of events called the Amino Acid Response pathway (AAR). Activating transcription factor 4 (ATF4) mediates the transcriptional activation of target genes for both AAR and UPR. The two *cis*-acting elements, Nutrient Sensing Response Elements-1, 2 (NSRE-1, NSRE-2) in the promoter region of human asparagine synthetase gene (*ASNS*) are the genomic elements that mediate the transcriptional response of the gene to both AAR and UPR pathway activation. In contrast, the system A neutral amino acid transporter 2 (SNAT2) gene enhancer is composed of a single intronic C/EBP-ATF composite site called Amino Acid Response Element (AARE). Chromatin immunoprecipitation (ChIP) analysis of HepG2 human hepatoma cells revealed that ATF4 binds the *SNAT2* C/EBP-ATF following either AAR or UPR pathway activation, and yet, SNAT2 transcription activity was increased only during the AAR, but not UPR pathway activation. Hyperacetylation of histone H3 and recruitment of the general transcription factors at the HepG2 *SNAT2* promoter

occurred in response to the AAR, but not the UPR. Concurrent activation of the AAR and the UPR pathways revealed that the UPR actually generates a repressive signal that acts downstream of ATF4 binding. The ChIP analysis also showed that HDACs 1-3 are constitutively bound to the SNAT2 and ASNS promoters and their binding decreases upon activation of the AAR or UPR pathways, whereas the use of HDAC inhibitor trichostatin A led to the inhibition of the AAR induced SNAT2 transcription. The DNase I hypersensitivity assay showed that in HepG2 cells there are six constitutive hypersensitive sites in the scanned region of the *SNAT2* gene. The characterization of the *ASNS* transcriptional regulation by ChIP demonstrated the involvement of PERK/eIF2α/ATF4 arm of the UPR acting on the NSRU in the *ASNS* gene. The siRNA strategy revealed the independence of *ASNS* transcriptional regulation from the ATF6 and IRE1/XBP1 arms during the UPR.

CHAPTER 1
INTRODUCTION

Extending our current knowledge regarding the transcription regulation of human neutral amino acid transporter 2 (*SNAT2*) and asparagine synthetase (*ASNS*) genes under celluar stress, represented the major goal of this study. Particularly, strong emphasis was put on the differential transcriptional regulation of the *SNAT2* gene by endoplasmic reticulum stress (ER stress) and amino acid limitation. The human *SNAT2* gene transcriptional control represents a very good model for the investigation of the fundamental mechanisms of transcription regulation.

Transcriptional Regulation in Eukaryotes

Nuclear Compartments

In eukaryotes the process of transcription occurs in the nucleus which is composed of distinct compartments including nucleoli, speckles, Cajal bodies, RNA POL II foci, pore containing nuclear envelope and nuclear lamina (1-4). Nucleoli are the site of rRNA transcription, whereas speckles and Cajal bodies represent the splicing factor compartments (5). Transcription factories are RNA POL II foci that also colocalize with actively transcribing genes (6,7). The genomic material inside the nucleus is organized into the compact heterochromatin containing inactive genes and euchromatin containing actively transcribing genes (8). As part of the chromatin organization, chromosomes are positioned in so-called chromosome territories that extend loops in the interchromatin compartments (2,9). These loops often contain actively transcribing genes. Most of the active transcription occurs in the nucleoplasm toward the center of the nucleus whereas inactive or repressed genes are positioned or migrate to the periphery in proximity of nuclear lamina (10). The functional role that nuclear architecture plays in the control of gene expression is the subject of intense investigation (10,11).

Transcription Control

Gene expression in eukaryotes includes multiple steps that occur inside the nucleus such as opening of chromatin, transcription initiation, elongation and termination (12,13). The processing and transport of the mRNA are intranuclear as well(5). Once transported to the cytoplasmic compartment, the mRNA is subject to degradation or translation into protein through the contribution of translation initiation factors and ribosomes. Most of gene expression regulation occurs at the level of transcription (13). Numerous studies both at the level of a single gene and genome wide have been conducted to bring more insights to the fundamentals that govern gene expression with special focus on transcription regulation. Experiments performed on 1% of human genome in the ENCODE pilot project led to some striking observations: 1) most of the genome is transcribed in coding and noncoding transcripts that show overlapping sequences, 2) many novel transcription start sites (TSSs) were identified, 3) specific chromatin modifications represent a very good indicator of TSSs, 4) distal DNaseI hypersentive sites show distinct histone modification patterns when compared to promoters(14). Transcription control involves multiple components such as chromatin conformation, *cis*-acting regulatory elements and *trans*-acting regulatory factors including general transcription factors (GTFs) and enhancer or silencer binding proteins. The *cis*-acting regulatory elements are represented by promoter elements, proximal regulatory sequences (e.g., CAAT or GC boxes), and distal regulatory sequences – enhancer/silencer sites, which bind *trans*-acting factors and thereby, recruit complexes that increase/decrease the transcriptional activity. Promoters are *cis*-acting elements that represent the site of pre-initation complex assembly (GTFs and RNA Polymerase II), whereas enhancers are DNA sequences that can exercise their function in an orientation and position independent manner and can confer responsivity to a heterologous promoter. A protein complex that binds the enhancer element and influences the rate of transcription from the

promoter is called an enhanceosome (15,16). This term was introduced to underline the fact that this complex can be defined by specific structural and functional characteristics. A well-characterized enhanceosome is described for the protein complex that binds the viral inducible enhancer of interferon beta (INFβ) gene. This enhanceosome is composed of the architectural protein high mobility group protein isoform I and Y (HMGI/Y) and the coordinated binding of nuclear factor kB (NF-κB), interferon regulatory factors (IRFs) and activating transcription factor 2 (ATF2) and c-Jun heterodimer (17). The multitude of DNA sequences and the binding transcription factors constitutes the combinatorial mechanism of gene regulation that confers the specificity of expression of a gene in a particular cell type. The *trans*-acting regulatory factors are specific binding proteins, such as ATF4, which bind an enhancer element (e.g. a CAAT enhancer binding protein (C/EBP) –activating transcription factor (ATF) or general transcription factors (TATAAA (TATA) binding protein (TBP), TBP associated factors (TAFs), transcription factor IIA (TFIIA), TFIIB, TFIIF, RNA ploymerase II (RNA POLII), TFIIE, TFIIH), which bind in a temporally sequential manner to form the preinitiation complex (PIC) at the promoter region of any given gene (18,19). TBP is thought to be the first GTF recruited to the promoter and together with TAFs, TBP forms the TFIID complex, which is responsible for the recognition and subsequent binding of the promoter region (20,21). The binding of TBP to the TATA box bends the DNA at 90° and this makes it possible for critical upstream and downstream sequences to come in close proximity, and thus create a suitable binding site for TFIIB(22,23). A recent study revealed that the majority of genes are TATA-less genes (20% of yeast genes are TATA containing genes) (24). In that study it was concluded that the presence of a TATA box was associated with genes that responded to stress and were highly regulated. In the case of TATA-less genes, it seems that TAFs play a central role in anchoring the TFIID complex in the

promoter region (25). TFIID binding to DNA is also followed by TFIIA binding to the amino terminus of TBP, thereby protecting TFIID from inhibition by transcriptional repressors. TFIIB joins the PIC by binding the DNA next to the TATA box and it represents the "conductor" protein during the assembly of the PIC (13). TFIIB recruits to the complex RNA POL II, which is associated with TFIIF (26). RNA POL II itself is a complex of up to 12 subunits(27). TFIIE and TFIIH are the last GTFs that join the PIC. The role of the structural protein TFIIE is to recruit and anchor TFIIH, which is a kinase that phosphorylates the RNA POL II C-terminal domain (CTD) at Ser 5 (28). Helicase activity then unwinds the DNA strands making possible the "melting" of a 10-nucleotide sequence at the transcription start site. This process requires energy, which is provided in the form of ATP molecules. In this way, the "closed" PIC transforms into an "open" complex. The presence of rNTPs and phosphorylation of the RNA POL II CTD at Ser5 triggers transcription elongation (29). Ser5 phosphorylation is seen at promoters while, ser2 phosphorylation occurs at coding regions as an important modification of RNA POL II CTD during elongation (29,30). RNA POL II and TFIIF form the elongation complex, which travels downstream of the promoter synthesizing the new RNA transcript (31).

The main component of the transcription machinery is the enzyme RNA polymerase which transcribes the DNA template into RNA in the nucleus. There are three RNA polymerases that are responsible for the synthesis of RNA: RNA POL I which synthesizes ribosomal RNA (rRNA), RNA POL II that synthesizes messenger RNA (mRNA) and RNA POL III that transcribes transfer RNA (tRNA) and small nuclear RNAs (snRNA). The RNAs that encode and are translated into proteins in the cytosol are represented by mRNA molecules. In eukaryotes these are synthesized under the form of pre-mRNAs that contain introns, which are latter spliced by the splicing machinery in the nucleus. Spliced mRNAs are then transported through the

nuclear pores in the cytosol where the translation machinery is ready for the synthesis of polypeptide chains.

The Role of Chromatin and Epigenetics in Transcription Regulation

The genomic DNA present in every cell of an organism undergoes the process of transcriptional control by epigenetic mechanisms that allow for differential expression of genes in different tissues. Epigenetic modifications such as DNA methylation and posttranslational modifications of histone tails establish and are responsible for the modality of expression of the underlying DNA sequence (8). These mechanisms contribute to the control of differential gene expression during physiological and pathological processes including cancer (32).

The fundamental unit of chromatin is represented by the nucleosome which is formed by an histone octamer wrapped almost twice in a left-handed helix by 147 bp of DNA (27,33). The histone octamer is composed of two subunits of each of the H2A, H2B, H3 and H4 proteins. Nucleosomes give the DNA the aspect of "beads in a string". Higher order chromatin structure represented by the 30nm fiber and chromosome loops are also important, not only for the packing of the genomic material inside a limited space in the nucleus, but seem to be critical in the regulation of gene transcription by controlling the accessibility of the gene locus to transcription factors (34). The conformational state of chromatin (condensed, heterochromatin - inactive transcriptional state or opened, euchromatin - able to be activated) dictates the transcriptional status of the underlying genes. Chromatin modifications include the following. 1) Post-translational modifications of histone tails such as acetylation, methylation, ubiquitination, phosphorylation, sumoylation, ADP-ribosylation, glycosylation and the proteins that recognize such histone modifications (e.g. bromo and chromodomain containing proteins) all together represent the histone/epigenetic code (8,35). 2) Nucleosome remodeling by complexes such as switch/sucrose nonfermenting (SWI/SNF) or imitation switch (ISWI), which remodel

nucleosomes, and are involved in nucleosome sliding, nucleosome displacement or replacement (12). ChIP-on-chip technology has allowed genome wide analysis of protein (including histones) -DNA interactions (36,37). This method involves the hybridization of the DNA obtained through chromatin immunoprecipitation (ChIP) procedure with DNA sequences in a microarray representing the DNA regions of the genome that will be investigated. This technology has led to the mapping of histone modifications and nucleosomes across the entire genome(38). As a result of this type of analysis it is thought that transcriptionally active genes have nucleosome free promoter regions (39). The *cis*-acting elements and the corresponding TFs, in combination with chromatin conformation and nucleosomes, establish the status of transcription of a specific gene. The interplay of these elements represents the "transcriptional regulatory code" in eukaryotic cells (40).

The most accepted model of transcriptional activation implies that the recruitment of GTFs is preceded by chromatin modifications. Lately, this model has been challenged by interesting findings which describe the recruitment of GTFs to the promoter prior to chromatin modifications in a gene whose expression is developmentally regulated (41).

Metabolite Control of Transcription in Eukaryotic Cells

Mammalian Integrated Stress Response

Figure 1-1 shows two of the signal transduction pathways activated by amino acid limitation or endoplasmic reticulum (ER) stress. Several stress signals result in protein misfolding and consequent accumulation in the ER triggering an adaptive response known as the Unfolded Protein Response (UPR). The amino acid response pathway (AAR) is a signaling cascade of events in response to amino acid limitation. One of the first steps of the cascade is represented by the activation of the general control non-derepresible 2 (GCN2) protein kinase by accumulated uncharged tRNA (42,43). Both UPR and AAR pathways converge on a single

event, which is phosphorylation of the translation initiation factor eIF2alpha (eIF2α-P) at serine 51. Double-stranded RNA-activated protein kinase - like endoplasmic reticulum kinase (PERK) and GCN2 are the respective kinases involved in this process (44). Phosphorylation of eIF2α causes global inhibition of translation, but a paradoxical increase in translation of the bZIP transcription factor ATF4. The increase in transcriptional activity of the target genes responsive to either the AAR [system A neutral amino acid transporter (SNAT2) and asparagine synthetase (ASNS)] or UPR (ASNS) is associated with the increased binding of ATF4 to enhancer elements within these genes (45,46). The differential response of the target genes is depicted in Fig. 1-1. The ASNS gene transcription is induced by both AAR and UPR, whereas SNAT2 transcription is increased only during amino acid limitation, but not ER stress.

Amino Acid Response Pathway

Starvation of cultured cells for even a single essential amino acid slows the synthesis of cellular proteins, except for the specific target proteins of the AAR pathway (e.g. bZIP transcription factors, CCAAT/enhancer binding protein (C/EBPβ), activating transcription factor 3 (ATF3) and ATF4; membrane transporter, SNAT2; metabolic enzyme, ASNS), which are induced (47-49). A similar response is observed in intact animals during protein deprivation (50). Re-introducing the missing amino acid into the cell culture media or refeeding the fasted animals with protein-containing meals returns the protein synthesis rates back to normal (fed state levels). Amino acid sufficiency activates the mammalian target of rapamycin (mTOR) pathway (51,52). Activation of the mTOR kinase cascade causes phosphorylation of ribosome-associated S6 kinase and 4E-BP1, which causes an increase in translation of ribosomal proteins. So, the mTOR pathway coordinates the rate of protein synthesis to amino acid sufficiency. In contrast, amino acid deficiency is detected by the AAR pathway. Deprivation of cells for an essential amino acid

will cause an increase in the uncharged tRNA. A current model in yeast shows that Gcn1p and Gcn20p (which form a complex with the translating ribosome) sense the uncharged tRNA bound at ribosome "A" site and assist its binding to the HisRS domain of Gcn2p (53). This process activates the Gcn2 protein kinase activity. Gcn2 binds the different uncharged tRNAs with similar affinities, but has reduced affinity for the charged form of a tRNA molecule (54). Consistent with this mechanism, inhibition of any one of the aminoacyl-tRNA synthetases triggers the AAR pathway, even in the presence of normal intracellular levels of that particular amino acid. For example, L-histidinol activates the AAR pathway by inhibiting the histidyl-tRNA synthetase (55,56). Activated GCN2 protein kinase phosphorylates eIF2α at Ser51 and eIF2α-P then binds to and inhibits the activity of eIF2B, which is a guanine nucleotide-exchange factor for eIF2 (converts the eIF2-GDP into eIF2-GTP; the latter is part of the ternary complex, eIF2-GTP-$tRNA_i^{Met}$). During the translation initiation, the ternary complex, initiation factors and mRNA bind the 40S ribosomal subunit forming the 43S complex, which is recruited to 5' end-capped mRNAs and then scans the 5' UTR where it recognizes the AUG-start codon. The 60S ribosomal subunit joins the complex to form the translation competent 80S ribosome. The inhibition of eIF2B results in low levels of ternary complexes and therefore, blocks the translation of most mRNAs. However, the translation of ATF4 mRNA, which has two upstream open reading frames (uORFs) that mediate translational control via a re-initiation mode is stimulated (57). In the fed state, the uORFs are inhibitory to the translation of ATF4 and to its yeast counterpart, GCN4(58). Under starvation conditions, low levels of ternary complexes increase the probability of translation initiation at the ATF4/GCN4 start codon. These events result in elevated ATF4 protein synthesis. The interplay between structural characteristics of an mRNA (e.g., uORFs) and the activity of a general initiation factor (e.g., eIF2α) can convert the

global translational regulation to a gene-specific one (58). ATF4 induction is mainly translationally controlled, although some transcription regulation (2- to 3- fold mRNA induction) under amino acid limitation or ER- stress is observed as well (59). As mentioned above, amino acid deficiency in yeast determines an increase in the GCN4 translation affecting the transcription of hundreds of genes, which has led Hinnebusch to characterize it as a "master regulator" (60,61). Array analysis in yeast and mice revealed similar targets for GCN4 and ATF4, including genes involved in amino acid transport and metabolism (60). Both the AAR and UPR induce phosphorylation of eIF2α and therefore, include ATF4-mediated transcription as a crucial component of the integrated stress response (59). ATF4 is a member of the ATF subfamily of the bZIP transcription factor super family. ATF members are known to heterodimerize within the ATF group as well as with other bZIP transcription factors, including members of the C/EBP family (62). The crystal structure of the C/EBPβ-ATF4 bZIP domains has been resolved at 2.6Å (63).

Mammalian Unfolded Protein Response

The endoplasmic reticulum (ER) is a cellular organelle that is responsible for the synthesis, folding and processing of newly synthesized secretory and membrane proteins. ER is a network of tubules, vesicles and sacs that are interconnected and that are continuous with the nuclear envelope. Regions of the ER with ribosomes attached to the cytosolic side of the membrane represent the rough ER and regions without ribosomes represent the smooth ER. In some cells, the primary protein product of rough ER is cell type specific. For example, in B-lymphocytes a major product is antibodies (immunoglobulins), whereas in pancreatic beta cells a primary product is insulin. Proteins made by the rough ER go into the smooth ER and from there travel to their final destination. The smooth ER function, besides being a transitional location for transport

vesicles loaded with ER products, mediates lipid synthesis. Alterations in the ER status by a number of stress conditions, such as perturbation in calcium homeostasis, glucose deprivation or expression of misfolded proteins, lead to accumulation of unfolded or misfolded proteins in the ER lumen triggering signal transduction pathways that decrease protein synthesis, increase folding capacity, activate ER-associated protein degradation and ultimately, if the ER homeostasis cannot be restored, provoke cell death (64). The imbalance between the protein load and the folding capacity of the ER is defined as ER-stress (64,65).

The following ER resident trans-membrane proteins serve as ER-stress sensors: inositol requiring kinase 1 (IRE1), PERK, and ATF6 (44). They recognize an increase in unfolded proteins or other ER-stress signals and transduce them across the ER membrane. Upon accumulation of malfolded proteins, the ER lumenal chaperone glucose-regulated protein 78 (GRP78) /BiP dissociates from the lumenal domains of the sensors and binds the unfolded proteins that start accumulating. BiP binding does not induce protein folding, but rather maintains the proteins in a folding-competent state. The ATP-bound form of BiP has low affinity for the unfolded substrates compared to the ADP-bound form, which shows high affinity for the bound polypeptide. Substrate binding stimulates the ATPase activity of BiP to generate the ADP-bound form. IRE1, PERK and ATF6 are all activated after dissociation from BiP (66). However, the time interval before they become fully activated is different (67). BiP release permits activation of IRE1 and PERK through dimerization and *trans*-autophosphorylation, whereas for ATF6, dissociation from BiP allows its translocation to the Golgi complex followed by proteolysis to the functional form. The PERK mediated pathway exists only in metazoans, whereas the GCN2 protein is found in all eukaryotes.

PERK: The PERK /eIF2α signaling pathway is responsible for both translational and transcriptional control during activation of the UPR (68). The PERK protein contains regions that through their function define the role that the protein plays in the UPR. Starting from the lumenal N-terminus of PERK protein there is a signal sequence, a dimerization region, a domain that binds the chaperone BiP, a transmembrane and a kinase domain that phosphorylates eIF2α. The activation of PERK /eIF2α represents the first branch of the UPR that is activated when ER-stress is present (68,69). Similarly to GCN2 kinase activity PERK phosphorylation of eIF2α at serine 51 leads to inhibition of eIF2B and a decrease in GTP-eIF2 complexes, which are required for translation initiation. The reversible step of eIF2α phosphorylation allows for flexibility and adaptibility of translation rates to stress. PERK activation does not depend on translocation, transcription or translation and as a result, global translation inhibition represents an early event (aproximately 30 min) in the UPR process. The main consequence of this activation is a decrease in global protein synthesis that reduces the protein load that undergoes folding in the ER contributing to the alleviation of ER stress. Similar to the activation of the AAR pathway, the slowing of general protein synthesis as a consequence of the eIF2α phosphorylation by PERK is associated with the paradoxical increase in translation of the ATF4 mRNA. ATF4 protein is a potent transcriptional activator that migrates inside the nucleus where it binds and activates the ER stress target genes (70).

NF-E2 related factor 2 (Nrf2) is the other direct substrate of PERK (71,72). In unstressed cells, Nrf2 is maintained in inactive cytosolic complexes by the cytoskeleton anchor Keap1. ER-stress triggers phosphorylation of Nrf2 by PERK and dissociation from Keap1 followed by Nrf2 nuclear import. Once in the nucleus, Nrf2 heterodimerizes with Maf proteins or ATF4 and binds to antioxidant response elements (ARE) promoting expression of phase 2 detoxification enzymes

which are involved in maintaining cellular redox homeostasis and in the repression of genes that promote apoptosis.

ATF6: During UPR activation the membrane-bound precursor form of ATF6 is translocated from the ER to the Golgi apparatus where is cleaved in the lumenal domain by a serine protease, site 1 protease (S1P) (73,74). The N-terminal half is then cleaved by a metalloprotease, site 2 protease (S2P). As a result of these proteolytic events, the cytosolic bZIP domain of ATF6 is free to travel to the nucleus where it activates transcription by binding the ER stress response elements, ERSE-I, CCAAT-N9-CCACG, or ERSE-II, ATTGG-N-CCACG in the presence of constitutively bound nuclear factor Y (NF-Y), a CCAAT/binding factor (CBF). There are two well known isoforms of ATF6 protein: alpha and beta (CREBL1). These isoforms arise from two different genes localized in two different chromosomes, 1 and 6, respectively. Recently, a novel finding reported that ATF6α undergoes alternative splicing, which involves the removal of exon 7 in lymphocytes that are HLA-B27 positive when ER stress is triggered by dithiothreitol (DTT) but not tunicamycin (75). This new isoform of ATF6α is thought to have regulatory function during UPR activation. Given the fact that the ATF6α spliced isoform lacks part of the DNA binding domain, it is possible that dimerization with other bZIP proteins (including full length ATF6α) prevents the latter's binding the DNA by a sequestering mechanism. Although ATF6α and ATF6β are similar in structure, some published studies have suggested that they play opposite roles in transcription of target genes, ATF6α behaving as an activator, whereas ATF6β acts as a repressor of transcription (76). The results of these studies have been questioned by other groups which did not observe the antagonizing effects of ATF6β on transcription (77).

IRE1: ER-stress induces dimerization, autophosphorylation, and activation of the RNase activity of the ER-bound protein IRE1 (78,79). A precursor X-box binding protein 1 (XBP1) mRNA is uniquely spliced by IRE1 and ligated by tRNA ligase in response to ER stress (80,81). The spliced XBP1 mRNA encodes the protein XBP1 which is a bZIP transcription factor of the ATF/CREB family that binds the mammalian UPRE (mUPRE) sequence or to the 3' end of the ERSE I element in the presence of NF-Y bound at the 5' end. The IRE1/XBP1 signal transduction pathway is the only branch of the UPR that is conserved from yeast (IRE1/HAC1) to mammalian cells (82). A recent study conducted by Hollien and Weissman revealed a novel mechanism that involves the ribonuclease activity of IRE1 in cells undergoing ER stress(83). It was shown in this particular work that besides the XBP1 mRNA, IRE1 has also other substrates represented by specific target mRNAs that encode for secreted and membrane proteins. These target mRNAs are subject to degradation by IRE1. This mechanism contributes to the alleviation of ER stress by eliminating an mRNA pool that would otherwise be translated. David Ron describes this IRE1-mediated mRNA degradation as a third UPR effector mechanism which is in addition to the well known short-term translational and long-term transcriptional effector mechanisms (84).

A recent article published by the Mori group addressed the role that ATF6 has in XBP1 transcriptional activation during UPR (77). ATF6 alpha and beta knockout mouse embryonic fibroblast cell lines were produced and tested for induced expression of XBP1 in the presence of ER stress. In these cell lines, transfected with a plasmid reporter containing ERSE I sequences, XBP1 transcription was induced upon ER stress, demonstrating that XBP1 induction during UPR activation is ATF6 independent (77).

The phenotypes of knockout mice lacking specific ER stress sensors/transducers have produced evidence for the critical roles the respective proteins play (Table 1-1) (85). The cell lines obtained from the knockout mice provide good models of human disease caused by loss of gene function.

ERAD: Proteins that are defective undergo degradation as an essential process to maintain cell homeostasis by avoiding intracellular toxic effects of aggregates that form and extracellular malfunctions of secreted proteins (86). Approximately 30% of de novo synthesized proteins that misfold and/or contain mutations are subject to degradation (87). Protein targeting to the ER is under the direction of signal peptides localized at the N-terminus of secretory proteins or a C-terminal KDEL (Lys-Asp-Glu-Leu) sequence, which dictates the ER localization. Protein translocation into the ER occurs through the channel formed by the sec61 complex (88). Translocated proteins in the ER lumen are subjected to chaperone-assisted folding. Proteins in the ER, depending on their specific features, can also undergo oligomerization, formation of disulfide bonds or modifications such as N-linked glycosylation, which contribute to the processing to a fully matured protein (89). Accumulation of malfolded proteins in the ER lumen triggers the UPR as part of an adaptive response to redress the malfunction by assisting the folding process. Proteins that fail to fold properly during the UPR phase associated with increased induction of ER chaperones are subject to ER-stress Associated Degradation (ERAD) (86). ERAD involves the transport of defective proteins to the cytoplasm where they are subject to proteosomal degradation. ATF4 and ATF6 are involved in induction of homocysteine-responsive protein (Herp), which is thought to recruit the 26S proteasome to the ER membrane during ER-stress (90). ER degradation-enhancing α-mannosidase-like protein (EDEM), 3-hydroxy-3-methylglutaryl-CoA reductase (HMG-R) degradation (HRD) 1 and uridine

diphosphate (UDP)-glucose: glycoprotein glucosyl transferase (UGGT) UGGT.EDEM are genes involved in ERAD that require the IRE1/XBP-1 pathway for induction (91,92). Degradation of the unfolded/malfolded proteins through ERAD reduces the load of the ER during stress.

Human *SNAT2* Transporter and Its Regulation

The System A and System N are part of the *SLC38* family of sodium-coupled amino acid transporters (93,94). System A was first described by Oxender and Christensen in 1963 (95) and studies to characterize neutral amino acid transport were performed in the early 1970s (96,97). The system A amino acid transporter is encoded by three *SLC38* genes SNAT1, SNAT2 and SNAT4 (94). Amino acid transport by SNAT2 is a Na^+ coupled cotransport with 1 sodium :1 amino acid stoichiometry (98-100). System A transport activity is increased by amino acid limitation, and SNAT2 is largely responsible for this up-regulation (97,101,102). SNAT2 mRNA levels increase following amino acid starvation and Hyde *et al*. have shown that there is an increase in plasma membrane SNAT2 protein following amino acid limitation of skeletal muscle cells or 3T3-L1 mouse adipocytes (103). In addition to amino acid limitation, adaptive regulation of SNAT2 expression is observed in response to hypertonicity, changes in cell volume and pH (104,105). The SNAT2 gene is ubiquitously expressed. The SNAT2 transport of alanine, which represents a substrate of gluconeogenesis in the liver constitutes a rate limiting step in diabetes (102). The alanine transport and the induction by insulin in muscle and L6 myotubes, and glucagon in the liver make SNAT2 a potential attractive therapeutic target in diabetes (106). In breast cancer cells, which are estrogen receptor positive, SNAT2 expression is under the influence of estrogen (107), whereas in vascular smooth muscle cells it is subject to regulation by transforming growth factor-β1 (TGFβ-1) to up-regulate proline transport to enhance the production of collagen (108).

The SNAT2 adaptive regulation by amino acid deprivation occurs through the activation of the AAR pathway (GCN2/p-eIF2α/ATF4), whereas the investigation of the increase in transcription during hypertonic conditions has revealed that it is p-eIF2α independent (109). SNAT2 expression is controlled transcriptionaly, translationally and post-translationally. During AAR activation, SNAT2 undergoes cap-independent translation with the contribution of an IRES sequence in the 5' UTR (109). Recent work in muscle cells has revealed that during amino acid limitation there is a redistribution of SNAT2 protein from intracytoplasmic pools in endosomes to the plasma membrane (103,110).

The C/EBP-ATF Composite Site (AARE)

A cis-element that was required for the transcription up-regulation of the ASNS gene during amino acid deprivation was first identified by Guerrini *et al*. in the promoter of the ASNS gene and was called the amino acid response element (AARE). The authors located the AARE sequence at approximately 60 bp upstream of the major trascription start site of ASNS(111). Barbosa-Tessmann *et al.* through deletion and mutagenesis analysis and *in vivo* footprinting identified two regulatory elements (site V (nt −79/−53) and VI (nt −55/−26); later the core sequences were refined by mutagenesis analysis and referred as nutrient response element (NSRE)-1, 5'- TGATGAAAC-3', nt −68/−60; and NSRE–2, 5'-GTTACA-3' nt –48/-43; respectively) within the ASNS gene promoter that mediate the adaptive response to both the AAR and UPR pathways (112,113). Later AARE sequences were characterized for many genes such as CHOP, SNAT2, TRB3, VEGF, Cat-1 and HERP. Identification by Palii *et al*. of an AARE sequence within the first intron of the SNAT2 gene strengthens the concept that transcriptional control is an important modality of regulation of the SNAT2 gene expression (114). The *cis*-acting elements of the SNAT2 gene are represented by conserved sequences of a

C/EBP-ATF composite site (AARE), the CAAT box, and the purine-rich element - PuR). The sequence of the AARE is identical to that in the C/EBP homology protein (CHOP) promoter (115). The SNAT2 C/EBP-ATF composite site, in association with the adjacent CAAT box, has enhancer activity, which means that it functions in an orientation and position independent manner and can increase transcription of a heterologous promoter (114).

It was shown by Chen *et a*l. that ATF4 plays a central role in the transcriptional regulation of the ASNS gene during amino acid limitation (45). It was reported by these authors that ATF4 binding that occured at an early phase (0-4 h) paralleled histone acetylation, GTF recruitment, including Pol II, and the transcription activity of the gene (Fig. 1-2) (45). Whereas, increased ATF3 and C/EBPβ binding to the ASNS C/EBP-ATF site occured later (after 4 h) and corresponded with a decrease in transcription (Fig. 1-2) (45,116). The increase in protein abundance of these TFs was correlated with their binding to the ASNS C/EBP-ATF site (NSRE-1). Recently, was reported by Palii *et al*. that the sequential binding of ATF4, ATF3, and C/EBPβ at the *SNAT2* C/EBP-ATF site controls the increase of *SNAT2* transcription during amino acid limitation (46). It is the interplay between the TFs ATF4, ATF3 and C/EBPβ that controls the ASNS and SNAT2 transcription during amino acid starvation. Despite the fact that ATF4 binding to the *SNAT2* C/EBP-ATF site has been documented during AAR activation (46), whether or not there is ATF4 binding to *SNAT2* during UPR activation has not been investigated. Reported results by Bain *et al*. have documented the insensitivity of the SNAT2 gene (the SNAT2 mRNA content and transport activity) to UPR activation. Given the increase in ATF4 protein abundance during ER stress and the lack of response of the SNAT2 gene to UPR activation this study adresses the ATF4 binding to the C/EBP-ATF site and the transcriptional control of the *SNAT2* gene during UPR.

Table 1-1. Phenotype of the knockout mice for the ER stress sensors and transducers (adapted from Zhao *et al*.).

Protein	Phenotype
ER stress sensors	
PERK	*Perk*$^{-/-}$ mice exhibit type I diabetes, bone abnormalities, small body size
IRE1α	*Ire1*α$^{-/-}$ mice are embryonic lethal
ATF6α	Develop normally, sensitive to ER stress
ATF6β	Develop normally
ATF6α/β	ATF6α/β double knockout mice are embryonic lethal
UPR transducers	
XBP1	*Xbp1*$^{-/-}$ mice are embryonic lethal; *Xbp*$^{+/-}$ mice show insulin resistance and type II diabetes on high fat diet
eIF2α	Homozygous eIF2αS51A mice die perinatally with diabetes and pancreatic β cell deficiency
ATF4	*Atf4*$^{-/-}$ mice exhibit embryonic or perinatal lethality

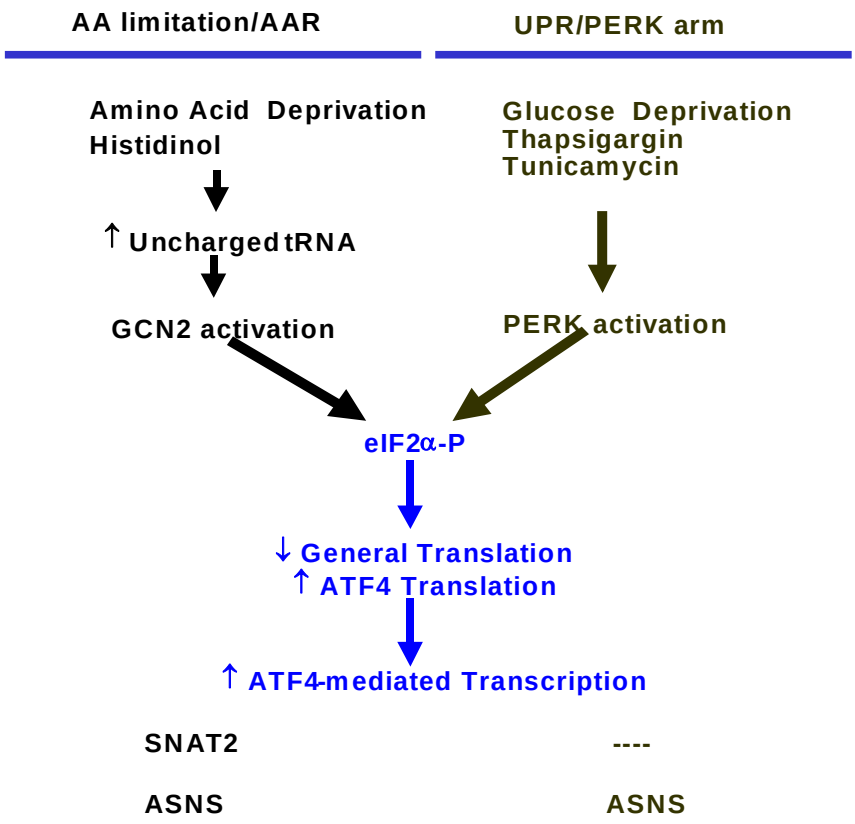

Figure 1-1. Mammalian integrated stress response. ATF4 translation is elevated by both AAR and UPR (PERK/eIF2α arm) pathways. ASNS transcription is induced by both AAR and UPR activation. In contrast, SNAT2 transcription is not induced during ER stress.

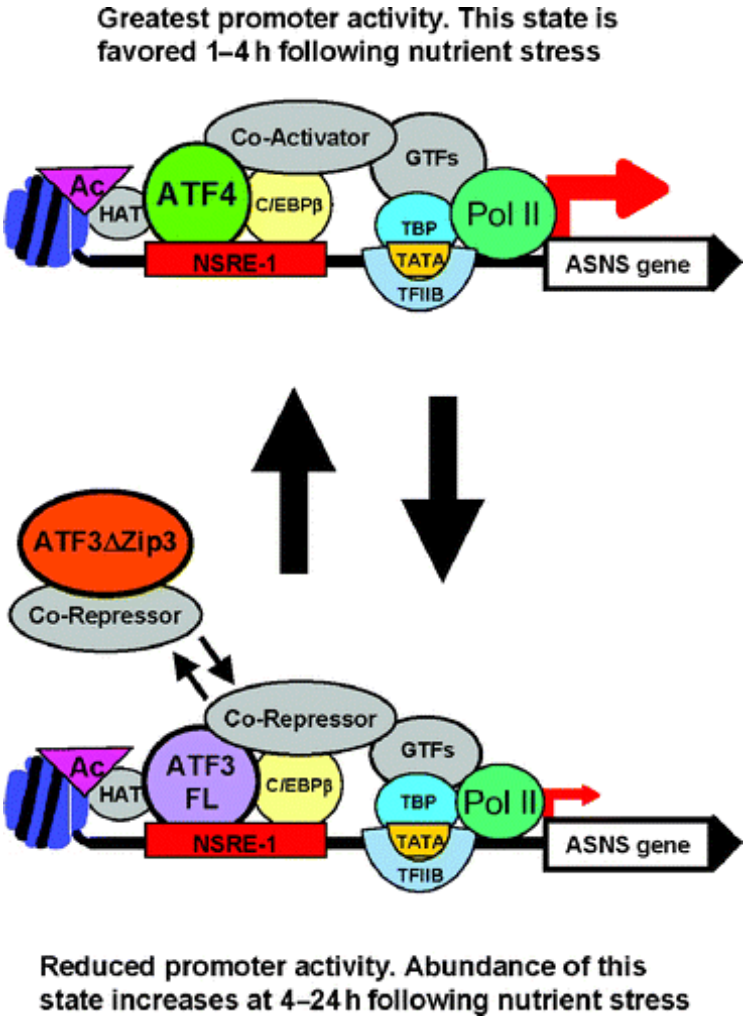

Figure 1-2. Working model for control of the asparagine synthetase (*ASNS*) gene. Transcription factors shown in color have been localized to the ASNS promoter by chromatin immunoprecipitation analysis. Unidentified proteins are shown in gray. (Kilberg et al. Annu. Rev. Nutr. 2005)

CHAPTER 2
MATERIALS AND METHODS

Cell Culture

Cell Lines

HepG2 Human hepatoma cells; Mouse embryonic fibroblasts (MEFs) that are wild type or ATF3$^{-/-}$ cells; Bnl-Cl2 immortalized mouse fetal hepatocytes.

Cell Culture Conditions

Cells were first cultured in T-175 flasks and later seeded on a 60 mm or 150 mm dishes and incubated in modified Eagle's MEM (minimal essential medium; pH 7.4) (Mediatech, Herndon, VA) at 37°C in a humidified atmosphere of 5% CO2 and 95% air until they reach ~70% confluence. The medium consisted of MEM supplemented with 1X nonessential amino acids, 2 mM glutamine, 100 μg/ml streptomycin sulphate, 100 units/ml penicillin G, 0.25 μg/ml amphotericin B and 10%(v/v) FBS (fetal bovine serum). To ensure that the cells were in an optimal fed state at the beginning of the experiment, fresh complete medium was provided to cells 12 h before the initiation of either drug treatment or starvation period. The AAR pathway was triggered by incubating cells in medium lacking the amino acid histidine (InVitrogen, Carlsbad, CA) supplemented with 10% dialyzed fetal bovine serum (Sigma, St. Louis, MO).

Inhibitors Used and Their Final Concentrations

Thapsigargin (TG)

Thapsigargin inhibits the ER Ca^{2+} ATPase causing the depletion of ER calcium deposits. Calcium is an element that is required during protein folding and its absence leads to the accumulation of unfolded or missfolded proteins in the ER lumen (117). The final concentration of TG was 300nM.

Tunicamycin (Tu)

Tunicamycin inhibits the N-glycosylation of proteins which is required for proper protein folding in the ER (118). The final concentration of Tu was 5μg/ml.

Histidinol (HisOH)

Histidinol is an alcohol analog of the amino acid histidine that inhibits reversibly the histidyl-tRNA synthase, the ezyme responsible for the charging of amino acid histidine to its respective tRNA (55). The final concentrations of HisOH were 1 and 2mM. Histidinol mimics the action of MEM medium lacking amino acid histidine (-His) which triggeres the AAR pathway.

MEK Inhibitors

PD98059 and U0126 are inhibitors of MEK1/2 kinases. As part of the MAP kinase signaling cascade MEK activates the substrate ERK through a phosphorylation event. The final concentration of PD98059 was 50 μM, whereas that of U0126 was 10 μM.

Total RNA Isolation

Total RNA was isolated using a Qiagen RNeasy kit according to the company's recommended protocol (Qiagen, Valencia, CA). In summary, at each time point of the experiment, cells from a 60 mm dish were washed with PBS (after the media was aspirated) and lysed with RLT buffer supplemented with 10 μl/ml β-mercaptoethanol. Each sample was homogenized by applying it to a Qiagen "shredder column" after which the sample was stored at -80°C till further processed. After thawing, the samples were diluted to a1:1 ratio with 70% ethanol and applied to an RNeasy column that binds the RNA. DNase I digestion was performed for each sample for 15 min at room temperature to make sure that no DNA was present in the final elution. RNA was eluted in 100 μl RNase free H_20. Following the elution step,

measurement of RNA concentration by spectrophotometer analysis and preparation of dilutions to 20 ng/μl was done. The amount used for reverse transcriptase PCR (RT-PCR) was equal to 100 ng (5 μl from each sample). A standard RNA set was prepared from one of the RNA eluted samples, starting from 80 ng/μl and making serial dilutions to respectively to 40, 20, 10, 5, 2.5, 1.25 and 0.625 ng/μl.

Determination of Transcriptional Activity

After the isolation of total RNA the determination of transcription activity consisted of amplification of the short-lived unspliced hnRNA using primers (sequences are listed in Table 2-1) that span the junction of exon 4 with intron 4 in the case of SNAT2 gene (Fig. 2-1), intron 12 with exon 13 of the ASNS gene or exon 2 with intron 2 of BiP/GRP78 gene. This approach is adapted from the method described by Lipson and Baserga (119). The reverse transcriptase RT-PCR was performed for the measurement of the hnRNA levels. Each reaction with a total volume of 25 μl contained: 5 μl of RNA template (20ng/μl), 1.25 μl (50 Units/μl) reverse transcriptase, 1.25 μl (20 Units/μl) RNase inhibitor, 1.25 μl (5 μM) of each primer (sense and reverse), 12.5 μl SYBR Green mastermix and 2.5 μl RNase free water. The RT-PCR values were referred to a standard curve ranging from 400 to 3.125 ng that was constituted using RNA samples with a previously determined amount of RNA. The PCR parameters were: incubation of the reaction mixtures at 48°C for 30 min followed by 95°C for 15 min to activate the Taq polymerase and amplification of 35 cycles of 95°C for 15 s, and 60°C (ASNS and BiP/GRP78) or 63°C (SNAT2) for 60 s. Reactions without reverse transcriptase were run as negative controls to rule out any residual genomic DNA amplifications. No amplification was observed under these conditions (data not shown). After every PCR, melting curves were acquired by stepwise increase of the temperature from 55 to 95°C to ensure that a single product is amplified in the

reaction. Values of GAPDH mRNA from the same RNA samples were measured by RT-PCR (primers listed in Table 2-1) and used for the normalization of the values and as an RNA loading control. For each of the 3-4 samples per condition, all PCR reactions were run in duplicate.

Determination of mRNA Levels

Reverse transcriptase qRT-PCR was used to measure the mRNA levels for the ASNS, SNAT2, ATF6α, ATF6β (CREBL1) and XBP1 genes. The approach includes the use of primers that amplify a specific region of an exon present in the mRNA of the gene. The primer sequences are listed in Table 2-1. The parameters of the PCR were: the reaction mixtures are incubated at 48°C for 30 min followed by 95°C for 15 min to activate the Taq polymerase and amplification of 35 cycles of 95°C for 15 s, and 60°C for 60 s. Reactions without reverse transcriptase were run as negative controls to rule out any residual genomic DNA amplifications. After PCR, melting curves were acquired by stepwise increase of the temperature from 55 to 95°C to ensure that a single product was amplified in the reaction. GAPDH mRNA levels will be measured as an internal control. For each of 3-4 samples per condition, the PCR reactions were performed in duplicate.

Chromatin Immunoprecipitation (ChIP) Assay

ChIP analysis was performed according to the following protocol (Figure 2-2) (45). HepG2 cells (plated 15 X 10^6 cells/ dish X 3 dishes/condition) were cultured in MEM and MEM+HisOH or MEM+TG for the time indicated in each figure. Cross-linking of proteins to the DNA was performed adding formaldehyde to a 1% final concentration and then the cells were incubated for 10 min with shaking at room temperature. Crosslinking was stopped by adding a 2M glycine stock to a 0.125M final concentration and incubation for 5 min. Incubations of 10 min each with nuclei swelling buffer (5mM PIPES, 85mM KCl, 0.5% NP 40) and SDS lysis

buffer (1% SDS, 10 mM EDTA, 50 mM Tris-HCl, pH 8.0) preceded sonication (four bursts of 42 seconds at power 16 with 2.5 minutes cooling on ice between the bursts) that was used to shear the chromatin to ~ 500 bp fragments. Chromatin fragmentation was checked by running a input samples on a 1% agarose gel. Immunoprecipitation consisted of two steps. 1) Incubation of extract from 10 x 10^6 cells in 1 ml ChIP dilution buffer with 2 to 4 μg of antibody was performed overnight at 4°C. A rabbit anti-chicken IgG (a non-specific antibody) was used as a negative control. 2) Then incubation with 60 μl (50% slurry) Protein A/G sepharose beads with the cell extract was performed for 2 h at 4°C to capture and precipitate the pre-formed immune complexes. Immune complexes attached to the beads were pelleted by centrifugation for 1 min at 960 x g. Reverse cross-linking was used to release the DNA fragments precipitated and was performed by adding 5M NaCl followed by incubation at 65°C for 5 h. RNase A 1 μl (1 μg/μl) and proteinase K 1 μl (20 μg/μl) digestion preceded the purification of DNA using QIAquick PCR purification kit (Qiagen). qRT-PCR was performed to amplify the DNA regions of interest. The qRT-PCR was performed using the DNA Engine Opticon 3 system and SYBR Green I detection. The qRT-PCR cycle parameters included: incubation of reaction mixtures with a total volume of 25 μl (5 μl DNA template, (1.25 μl of 5 μM forward primer, 1.25 μl of 5 μM reverse primer, 12.5 μl SYBR Green mastermix and 5 μl nuclease-free water) at 95 °C for 15 min to activate the polymerase, followed by amplification at 95°C for 15 s and 60°C (SNAT2 enhancer and BiP/GRP78 primers), 62°C (SNAT2 promoter primers), or 61.4°C (ASNS promoter primers) for 60 s for 35 cycles. After PCR, melting curves were acquired by stepwise increase in the temperature from 55 to 95°C to ensure that a single product was amplified in the reaction. The relative values of the qRT-PCR samples were obtained by referring them to a standard curve prepared by serial dilutions of input DNA (1/4, 1/16, 1/32, 1/64, 1/128, 1/256, 1/512). The qRT-

PCR reaction for the standards and samples were performed in duplicate for each of 3-5 experiments. The data were analyzed as the ratio of the sample to the input DNA values.

Whole Cell Extract Protein Isolation

Cultured cells in 60 mm dish were washed with ice-cold PBS (after the media was aspirated) and lysed in 500 μl lysis buffer. The composition of 10 ml lysis buffer included: A) 9.3 ml sample dilution buffer (SDB) [5 ml of stacking gel buffer from 100ml stock solution prepared adding 5.98 g Tris-base in 90 ml dH_2O followed by adjustment of ph at 6.6; 20% sodium dodecyl sulfate (SDS), 1 ml; 100% glycerol, 4ml; bromphenol blue dye (stock 1.5mg/ml), 0.4 ml. and dH_2O, 8.6 ml]; B) β merchaptoethanol, 500 μl; C) protease inhibitor, one tablet (Roche, Complete mini tablet); D) Phosphatase inhibitor cocktail I and II (Sigma), 100μl each. The cell lysis was performed on ice to prevent protein degradation by proteases. Samples were stored at -80°C.

Immunoblotting

Protein abundance of the main factors involved in the UPR and AAR pathways was assayed by Western blotting using whole cell protein extracts. Protein content was quantified by a modified Lowry assay(120) and samples containing 30 μg of protein were separated on a 10% polyacrylamide gel. After electrotransfer to a Bio-Rad nitrocellulose membrane, the membrane was stained with Fast Green to check for equal loading and then incubated with 5-10% blocking solution [5-10% (w/v) Carnation non-fat dry milk and Tris-buffered saline/Tween (30 mM Tris base (pH 7.6), 200 mM NaCl and 0.1% Tween-20)] for 1 h at room temperature with mixing. Immunoblotting was performed using the appropriate antibodies against the protein of interest at an antibody concentration of 0.2–2 μg/ml in 5-10% dry milk blocking solution for 2 h at room temperature or overnight at 4°C with mixing. Then, the membrane was washed five times for 5

min each in 2-5% blocking solution on a shaker followed by incubation with a peroxidase-conjugated secondary antibody at the appropiate dilution (1:20000) in 2-5% dry milk blocking solution at the appropriate dilution for 1 h at room temperature with mixing. The membrane was then washed five times for 5 min each in 2-5% dry milk blocking solution and two times for 5 min in TBS/T (30 mM Tris base pH 7.6, 200 mM NaCl and 0.1% Tween-20). The bound secondary antibody was detected using an Enhanced Chemiluminescence kit (Amersham Biosciences, Piscataway, NJ, U.S.A.) and exposing the membrane to a Biomax® MR film. To provide a demonstration of equal loading, membranes were re-probed with a specific actin antibody (Sigma) at 1:5000 dilution.

Statistical analysis

The statiscal analysis of the data was performed using the *t tes*t (Excel). A P value less than 0.05 denotes statistical significance and is indicated in the figures by an asterisk.

DNase I Hypersensitivity Assay

DNase I Treatment

Cultured HepG2 cells were plated and either incubated in MEM only or treated with 2 mM HisOH or 300 nM TG for 8 h. After aspirating the media, washing with PBS and trypsinizing the cells were collected and counted. For each tested DNase I concentration, 20 X 10^6 cells were used. The total number of cells needed per condition was calculated by multiplying the number of DNase I concentrations to be tested by 20 X 10^6 cells. For example, 0, 50, 80 and 110 U of DNase I represent four different concentrations and in this case the total number of cells used equaled 80 X 10^6 cells. The cells and the 5 ml MEM medium used to stop trypsinization were transferred to 50 ml conical tubes. After the centrifugation at 200 x g at 4°C for 5 min, the medium was aspirated and tapping the tube gently to dissolve the pellet. A wash step with 10 ml solution A (containing 150mM sucrose, 80 mM KCl, 35 mM HEPES, 5 mM K_2HPO_4, 5 mM

$MgCl_2$, 0.5 mM $CaCl_2$) per each tube was performed followed by centrifugation at 200 x g in 4°C for 5 min to pellet the cells. Aspiration of the liquid phase of solution A was followed by tapping to dissolve the pellet. To each of the 50 ml tubes was added 1.8 ml of solution B (containing 150 mM sucrose, 80 mM KCl, 35 mM HEPES, 5 mM K_2HPO_4, 5 mM $MgCl_2$, 2 mM $CaCl_2$) which was mixed gently with the cells; the entire volume with the cells equaled 2.2 ml. Four aliquots of 500 µl per 50 ml tube/condition were transferred in 15 ml tubes and put on ice. In the mean time, in 1.7 ml tubes a 500 µl solution was prepared containing the amount of DNase I (Worthington) taken from the stock concentration of 1 mg/ml (1 µg/ul equal to 2 Units/µl) needed (0, 25, 40 and 55 µg) and solution B containing the cell membrane permeabilizer NP 40 (0.4%). The DNase I stock solution was prepared by dissolving it in 50% glycerol and 10 mM Tris ph 7.4; aliquots were stored at -20°C. In the 15 ml tube containing cells in solution B, 500 µl DNaseI-NP 40 containing solution was added and the reaction was allowed to occur for strictly 2 min at 37°C. The reaction was stopped by adding 3 ml of lysis buffer (for its composition see genomic DNA isolation description below). The lysis was continued overnight and the next day the genomic DNA isolation proceeded.

Genomic DNA Extraction From Tissue Cultured Cells

Cells treated with DNase I were lysed overnight using a lysis buffer containing 9.75 ml of DNA extraction buffer (50mM Tris pH 8.5, 25 mM EDTA, 150 mM NaCl), 0.5% sodium dodecyl sulfate (SDS) and 300 µg/ml proteinase K. The following day, DNA isolation proceeded by adding an equal volume of phenol/chloroform (4 ml) and incubating for 1 h with gentle mixing in the shaking platform. After the incubation, the 15 ml tubes were centrifugated at 2800 x g for 10 min and the aqueous phase was transferred to a new 15 ml tube. An incubation with 4 ml of chloroform only for 30 min was used to capture any residual phenol in the sample. After

the centrifugation, the aqueous phase was transferred to a new 15 ml tube and samples were treated with 5 µl (1µg/µl) RNase (Ambion) at 37°C for 1 h. The phenol/cloroform followed by chloroform incubations were repeated with the same parameters as those described above. To precipitate the DNA, 40 µl/ml of 5 M NaCl was added (for 4 ml was added 160 µl of NaCl) and two volumes of 100% ethanol. The reaction was incubated overnight at 4°C. The next day the tubes were gently rotated (to avoid shearing of genomic DNA) to precipitate completely the DNA. Samples were centrifuged at 2800 x g for 20 min at 4°C. After the supernatant was discarded from each tube, the bottom-attached pellet of DNA was allowed to dissolve in 500 µl Tris-EDTA (TE) 10 mM Tris, 1 mM EDTA [pH 8.0] buffer and stored at 4°C for further use in the Southern blotting procedure described below.

Indirect End-labeling

Probe design

The probe-designing step is the most critical one of the entire DNase I/MNase hypersensitivity analysis. After identifying the DNA repeats in the human SNAT2 gene region of interest using a software program available on-line at the address www.repeatmasker.org, the probe was designed against a non-repeat DNA segment. Also, using a software program available on-line at the address http://tools.neb.com/NEBcutter2, the DNA fragment of interest was analyzed for enzyme restriction sites. The human SNAT2 gene from nt –2135 to +5624 (including the promoter, the C/EBP-ATF site and a downstream region) was between two restriction sites of the *Mfe*I enzyme. The probe was designed around the 3' *Mfe*I cutting site in the body of the gene. Primers listed in Table 2-2 were designed to amplify a 541 sequence (this fragment was cloned in the pCR 2.1-TOPO shown in Figure 2-3) that contained the 3' *Mfe*I

restriction site. Both the probe and the genomic DNA were digested with the *Mfe*I enzyme to ensure that proper end-alignment of these two DNA sequences was achieved.

Polymerase chain reaction and cloning procedures

The plasmid pCR 2.1-TOPO was used during the cloning procedure of the SNAT2 probe used in the DNase I hypersensitivity assay. Prior to cloning, polymerase chain reaction (PCR) using primers designed to amplify the 541 nt SNAT2 fragment of interest were used. The PCR reaction composition included: DNA template, 5µl of HepG2 genomic DNA; 1.5 µl of 5 µM concentration forward primer, 1.5 µl of 5 µM concentration reverse primer, 20 µl of 2.5X Eppendorf HotMasterMix (HotMaster Taq DNA polymerase (50u/ml), 2.5X HotMaster Taq buffer pH 8.5 with $Mg(OAc)_2$, 500 µM of each dNTP and stabilizers) and 22 µl of H_20 in a total reaction volume of 50 µl. The PCR cycle parameters included: a DNA denaturing step for 5 min at 95°C followed by 30 cycles of amplification for 30 sec at 95°C and 59°C for 30 sec. For verification of the correct size of the PCR product, 2 µl of the latter, 2 µl of genomic DNA and 1 µl 2-log DNA (New England Biolabs, MA) were separated in a 1% agarose gel followed by ethidium bromide staining. The PCR product of the right size (541 bp) was excised and purified using a QIAquick gel extraction kit (Qiagen). The manufacturers protocol was followed and no deviations were made. Following gel extraction of the PCR product, a ligation reaction of the latter in the pCR 2.1-TOPO plasmid was performed. The ligation reaction was done in a total volume of 6 µl containing 4 µl of DNA product extracted, 1 µl of plasmid and 1 µl buffer containing the ligase. The ligation reaction, after mixing gently, was incubated for 10 min at room temperature. Transformation of Escherichia Coli (chemically competent) cells followed the ligation reaction. Cells (25 µl) were thawed on ice and incubated with 2.5 µl of the ligation reaction for 15 min. After the incubation, the cells were heat-shocked for 45 sec at 42°C and

transferred to ice immediately for 5 minutes. To maximize the transformation efficiency, the SOC rich medium (250 µl) from Sigma was added and the tubes were put in the horizontal shaking platform at 200 rpm at 37°C for 1 h. At the end of the incubation period, 30 µl of each transformation was spread on a Luria Broth (LB) ampicillin plate with 40 µl of X-gal. Plates were put in the incubator at 37°C overnight. The next day the white/light blue colonies were picked and the bacterial cultures were prepared to grow overnight. Grown bacterial cultures were collected the next day and processed following the manufacturer's instruction protocol for miniprep preparation using the QIAprep Spin Miniprep kit. The DNA concentration of minipreps was measured by spectrophotometer. The DNA was verified for the correct insert inside the plasmid by digestion with the enzyme *EcoR*I (three cutting sites, two in the plasmid and one in the insert) and *Mfe*I (one cutting site in the insert). The digestion reaction composition was: DNA template, 1.5 µl; *EcoR*I buffer, 1.5 µl; *EcoR*I enzyme, 0.3 µl and 11.7 µl H_20 in total volume of reaction of 15 µl. For the *Mfe*I digestion reaction, 0.6 µl of enzyme was used in total reaction volume of 15 µl. The reactions were incubated at 37°C for 1 h. The products of the digestion reaction were verified in a 1% agarose gel with ethidium bromide staining. To obtain the SNAT2 fragment of interest from this cloning procedure, a double digestion was performed. First with the *Mfe*I, which cut the insert once, followed with BstX1 enzyme digestion that cut the vector once. The digestion reaction included 36.9 µl DNA, 10 µl of NEB 2 buffer, 5 µl of *Mfe*I enzyme and 48.1 µl of nuclease-free water in a 100 µl final reaction volume. The reaction was incubated at 37°C for 3 h. For the BstX1 digestion reaction, the parameters were the same as the MfeI reaction, except for the usage of the BstX1 enzyme and the temperature of incubation at 55 °C. Following the digestion reaction, the human SNAT2 insert of 411 bp was captured in 1% low

melting point agarose gel. The fragment was excised and stored at 4°C for further use as a probe after radiolabelling in the DNase I hypersensitivity assay (for the Southern blot analysis).

Probe radiolabeling reaction

The already prepared SNAT2 DNA probe was used in the reaction of random priming and radiolabelling. First, 10 µl of DNA probe in 23 µl nuclease-free H_2O was denatured at 95°C for 10 min. Added in a sequential order were 2 µl of dATP, dGTP and dTTP at 20 µM final concetration, 5 µl of 10X label buffer (New England Biolabs, MA), 5 µl (50 µCi) of ^{32}P labeled dCTP (PerkinElmer) and 1 µl DNA polymerase I – Klenow (New England Biolabs, MA). The reaction was incubated for 1 h at room temperature on an assigned bench for working with radioactive materials. Meantime, a Sephadex column was prepared (Sephadex from a stock of 10 mg/100ml and 1 ml seringe). After 1 h incubation, the radiolabelling reaction was transferred to the Sephadex column, placed inside a 15 ml tube, and centrifuged for 4 min at maximum speed. The recovered radioactive probe was used in the hybridization procedure.

Southern blotting

Genomic DNA digestion: After the isolation of the genomic DNA and the OD determined by spectrophotometer analysis, an amount in excess of 50 µg DNA was used for *Mfe*I digestion reaction. For example, in a total reaction volume of 110 µl there was 60 µl genomic DNA, 10 µl of *Mfe*I enzyme, 11 µl of 10x NEBuffer 4 and 29 µl of nuclease-free water.

Gel electrophoresis: The DNA concentration of the samples was measured prior to loading in the gel and an amount equal to 15 µg per lane was loaded into the 0.8% ultra pure agarose gel. The gel was run overnight at 45 volts constant voltage. The next day, the gel was stained with ethidium bromide and a picture was taken with a ruler next to the 1 kb DNA ladder. The ruler is used later to determine the size and localization of the parental band and

hypersensitive sites if the DNA ladder is invisible, meaning non-reactive with the radiolabelled probe.

Denaturing and neutralization: Immediately after running the gel was denatured for 30 min in a horizontal shaker using denaturing buffer (1.5 M NaCl, 0.5 N NaOH and ddH_2O) followed by neutralization (two incubations each of 15 min with horizontal shaking) with neutralizing buffer (1 M Tris, 1.5 M NaCl and ddH_2O at pH 8.0). *Transfer*. After a quick rinse with water, the gel was set in the transfer sandwich composed of starting from the bottom: 1.5L 10X SSC buffer (from 20X SSC stock containing 3M NaCl, 0.3 M sodium citrate and ddH_2O at pH 7.0) in a glass baking dish, a piece of glass, two layers of filter paper in contact with the 10X SSC buffer, two short filter papers, the gel itself, positively-charged nylon transfer membrane (GE Healthcare, catalog # RPN203B), two short filter papers and three layers of paper towel. The latter were used to absorb the SSC buffer through the membrane by a capillarity phenomenon, and by doing so, allowed the DNA to transfer from the gel to the positively-charged membrane. The transfer was allowed to proceed overnight. The next day, the membrane was quickly rinsed with 5X SSC buffer to eliminate any residual agarose gel fragments and was incubated at 80°C for 1.5 h to strengthen the binding of the already weakly bound DNA to the membrane. This membrane was further used for hybridization.

Hybridization: After incubation for 2 h with 15 ml of pre-hybridization buffer (bovine serum albumin, BSA 1g/100ml, 7% SDS, phosphate buffer at pH 7.3 containing Na_2HPO_4 and H_3PO_4, and water), the buffer was discarded and hybridization with 10 ml of hybridization buffer (composition was the same as the pre-hybridization buffer) containing the recovered radioactive probe was performed overnight at 65°C with rotation in the proper incubator assigned for use of radioactive-containing samples. Then the membrane was washed with 65°C pre-heated washing

buffer (1% SDS, phosphate buffer at pH 7.3 containing Na_2HPO_4 and H_3PO_4 and water) for three times followed by three 10 min incubations with washing buffer, rotating at 65°C. After the washes, the membrane was exposed overnight to a storage phosphor screen and the image was captured by using a phosphorimaging scanner. To obtain the film autoradiographs, the blots were exposed to Biomax® MR film for a period of time varying from 8 to 14 days.

Nucleosome Positioning

The determination of translational nucleosome positioning was performed following the same strategy and procedures as for the DNase I hypersensitivity assay, with the following differences. Cells were treated with the micrococcal nuclease (MNase) (Sigma) enzyme. The MNase concentrations used to treat HepG2 cells permeabilized with 0.4 % NP40 were 0, 1, 5, 50 and 100 units. The incubation time was 2 minutes and the reaction was allowed to proceed at room temperature. This enzyme, during short time digestion, cuts in the linker regions of the DNA, between the nucleosomes, allowing one to map the position of nucleosomes in the region scanned. A 211 bp probe was designed (localized between –2320 nt and –2109 nt) and the restriction enzyme *EcoR*I was used to generate a parental band of 4.39 kb from nt –2320 to nt +2070. The Southern blotting procedure was performed identically with the one described above for the DNase I hypersensitivity assay.

Short Interfering RNA (siRNA) Transfection

The human ATF3, XBP1, ATF6α and ATF6β (CREBL1) siGENOME SMARTpool (Dharmacon# M-008663-01-0005, M-009552-02-0005; M-009917-00-0005; M-008805-00-0005), siControl Non-Targeting siRNA (# D-001210-02), and DharmaFECT 4 transfection reagent were purchased from Dharmacon, Inc. (Lafayette, CO). HepG2 cells were seeded in 6-well plates at a density of 4×10^5 cells per well in MEM and grown for 16 h. Transfection was performed according to Dharmacon's instructions using 3 µl of DharmaFECT-4 and 100 nM per

well final siRNA concentration. HepG2 cells were treated with transfection reagent for 24 h then rinsed with PBS, given fresh MEM+10%FBS, and cultured for another 24 h. The medium was then removed and replaced with control MEM+10%FBS or MEM +Tg for the time indicated in each figure. Total RNA and whole cell extracts were isolated at 8 h and analyzed by RT-PCR and immunoblotting.

Table 2-1. Sequence of primers used in reverse transcriptase PCR analysis.
H=human. M=mouse. TA=transcription activity. Ex=exon. In=intron. FP=forward primer. RP=reverse primer. RT-PCR= reverse transcriptase PCR.

GENE	Species	Assay (RT-PCR)	Position of amplicon	Annealing T °C	Sequence
SNAT2	H	TA	Ex4-In4	63	FP 5' - GCAGTGGAATCCTTGGGCTTTC - 3'
					RP 5' - CCCTGCATGGCAGACTCACTACTTA - 3'
SNAT2	H	mRNA	Ex10	60	FP 5'- CAGGTACAAGAGCTGTTGGCTGTGT- 3'
					RP 5'- GTGTCCTGTGGAAGCTGCTTTGA - 3'
SNAT2	M	TA	Ex13-In 13	60	FP 5′- GTCACCCTCACGGTCCCAGTAGTTA - 3'
					RP 5′-GCATACCCATAGCTGTCGCAGAAGT - 3′
ASNS	H	TA	In12-Ex13	60	FP 5'- CCTGCCATTTTAAGCCATTTTGC - 3'
					RP 5'-TGGGCTGCATTTGCCATCATT - 3'
ASNS	H	mRNA	Ex7	60	FP 5'- GCAGCTGAAAGAAGCCCAAGT - 3'
					RP 5'-TGTCTTCCATGCCAATTGCA-3'
BiP/ GRP78	H	TA	Ex2-In2	60	FP 5′-AGGACATCAAGTTCTTGCCGTTCA - 3′
					RP 5′- CACCACCCACCCGTTCTCTAACT - 3′
ATF6α	H	mRNA	Ex9	60	FP 5'- GGAACAGGATTCCAGGAGAATGAACCCTAGTG - 3'
					RP 5'-GATGTGTCCTGTGCCTCTTTAGCAGAAAATCC-3'
ATF6β CRBL1	H	mRNA	Ex10	61	FP 5'-CTGAAGCGGCAGCAGCGAATGATCAAG-3'
					RP 5'-CGAGCCTCCAGTCCCTGCAGATACTCTTTC-3'
XBP1	H	mRNA	Ex2	60	FP 5'- CAGAGTAGCAGCTCAGACTGCCAGAGATCG-3'
					RP 5'-GCTGTTCCAGCTCACTCATTCGAGCC-3'
ATF4	H	mRNA	Ex3	60	FP 5′-TGAAGGAGTTCGACTTGGATGCC-3′
					RP 5′-CAGAAGGTCATCTGGCATGGTTTC-3'
GAPDH	H	mRNA	Ex8 – Ex9	60	FP 5′-TTGGTATCGTGGAAGGACTC - 3′
					RP 5′- ACAGTCTTCTGGGTGGCAGT - 3′

Table 2-2. Sequence of primers used in ChIP analysis, DNase I and micrococcal nuclease assays
H=human. M=mouse. Ex=exon. in=intron. FP=forward primer. RP=reverse primer.

GENE	Species	Position of amplicon	Annealing T °C	Sequence
SNAT2	H	Ex 1 Promoter	62	FP 5′-GCCGCCTTAGAACGCCTTTC-3′
				RP 5′-TCCGCCGTGTCAAGGGAA-3′
SNAT2	H	In 1 C/EBP-ATF	60	FP 5′-GGGAAGACGAGTTGGGAACATTTG-3′
				RP 5′-CCCTCCTATGTCCGGAAAGAAAAC-3′
SNAT2	M	Promoter	60	FP 5′-GGAGCCCAGGTGCTGTTGATACA-3′
				RP 5′-GCTTCCCGAGCGCGAGTTATA-3′
SNAT2	M	C/EBP-ATF	60	FP 5′-ATCGGGTCTTGTGCCTCGAAA-3′
				RP 5′-ATACCGAGGGGCGATTGATTGT-3′
ASNS	H	Promoter	61.4	FP 5′-TGGTTGGTCCTCGCAGGCAT-3′
				RP 5′-CGCTTATACCGACCTGGCTCCT-3′
BiP/GRP78	H	Promoter	60	FP 5’- CACCAATCGGCGGCCTCCACG -3’
				RP 5’- GCGTCGACCTCACCGTCGCCTAC-3’
ChOP	H	ERSE and C/EBP- ATF	60	FP 5′-AAGCCTCGTGACCCAAAGC-3′
				RP 5′-GTCGCTCCCTCTCGCTAG-3′
SNAT2	H	*Mfe*I restriction site	60	FP 5’-CCTGAGAAATGATGCAAGTTTTTACTGCCAGCC-3’
				RP 5’-GCATGTGTCACCATTCTGTGCTCCACAATGAG-3’
SNAT2	H	*EcoR*I restriction site	60	FP 5’-CCACTGAATTCATCACTATCCACCACTTGGTCC-3’
				RP 5’-CCTGATGTGCTCTGAGCAATTGCTGTTATGC-3’

Table 2-3. Catalog numbers of the antibodies used in ChIP and western blot analysis Sc=Santa Cruz.

Antibody	Catalog number/Company
ATF4 [CREB-2 (cAMP-response-element-binding	sc-200
ATF4 rabbit antiserum	Cocalico Biologicals (Reamstown, PA)
ATF3	sc-188
C/EBPβ	sc-150; sc-7962
RNA Pol II (polymerase II)	sc-899
TFIID (TBP)	sc-204
TFIIB	sc-274
TFIIE-α	sc-237
Normal rabbit IgG	sc-2027
Acetylated histone H3	06–599 Upstate Biotechnology (Millipore)
Acetylated histone H4	06-866 Upstate Biotechnology (Millipore)
H3	ab1791 Abcam
HDAC1	sc-6298
HDAC2	sc-6296
HDAC3	sc-11417
HDAC4	sc-11418
HDAC5	sc-11419
HDAC6	sc-11420
HDAC7	sc-11421
N-CoR	sc-8994
p300	sc-584
PCAF	sc-8999
SNF5/Ini1	sc-9751
ERK	sc- 94
p-ERK	sc-7383
eIF2 alpha	9722 Cell signaling technology
P-eIF2 alpha	9721 Cell signaling technology
Cdk8	sc-5612
MED1	sc-5334
MED23	sc-12454
Actin	A2066 Sigma-Aldrich

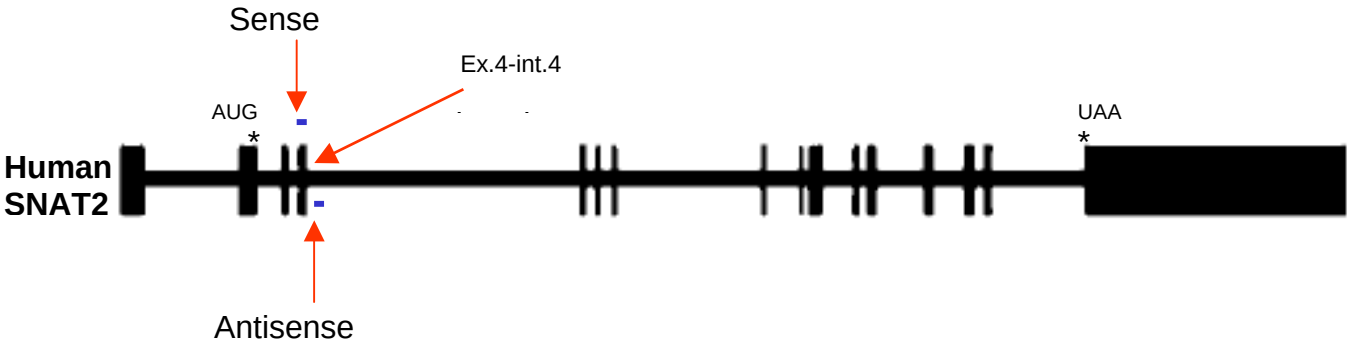

Figure 2-1. Position of transcription activity primers for the human *SNAT2* gene

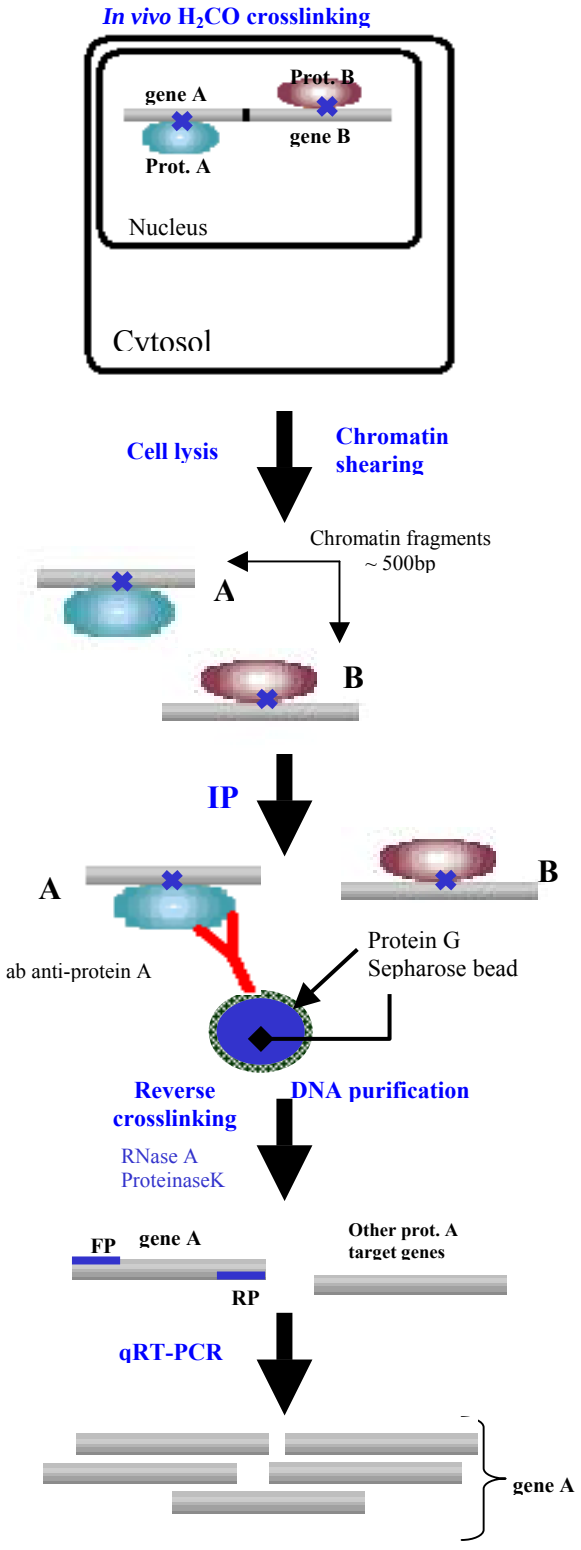

Figure 2-2. The ChIP protocol. After *in vivo* crosslinking chromatin is sheared. Immune complexes are captured using incubation with protein G beads. Washes and reverse crosslinking are followed by DNA purification and amplification of the gene of interest (gene A in the diagram) using specific primers.

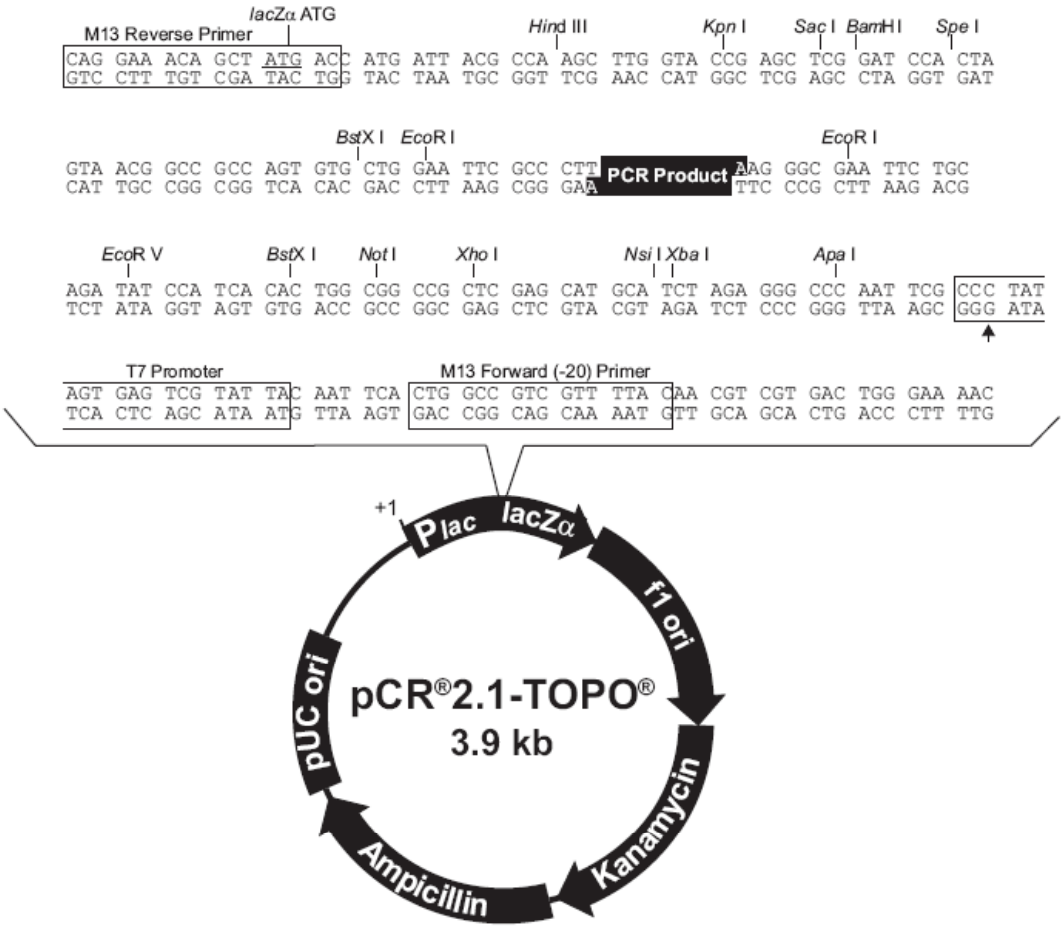

Figure 2-3. Map of pCR®2.1-TOPO® and the sequence surrounding the TOPO® cloning site (Invitrogen).

CHAPTER 3
DESPITE INCREASED ATF4 BINDING AT THE C/EBP-ATF COMPOSITE SITE AFTER ACTIVATION OF THE UNFOLDED PROTEIN RESPONSE, SYSTEM A TRANSPORTER 2 (*SNAT2*) TRANSCRIPTION ACTIVITY IS REPRESSED IN HEPG2 CELLS

Introduction

A wide variety of stress signals activate one or more of a set of eukaryotic initiation factor 2 alpha (eIF2α) kinases (70). Phosphorylation of the translational initiation factor eIF2α at serine 51 by these kinases provokes a suppression of global protein synthesis and a paradoxical increase in the translation of selected mRNAs containing short upstream opening reading frames, including that of activating transcription factor 4 (ATF4) (57,121). One of the eIF2α kinases is double-stranded RNA-activated protein kinase-like endoplasmic reticulum kinase (PERK), which is activated by ER stress conditions, such as perturbation of calcium homeostasis, glucose deprivation, or other causes of misfolded protein accumulation in the ER lumen. Experimentally, the drugs tunicamycin (Tm), an inhibitor of N-glycosylation, or thapsigargin (Tg), an ER Ca^{++}-ATPase blocker, can also be used to induce the UPR (68). PERK is one component of an adaptive response known as the unfolded protein response (UPR), which is comprised of three signal transduction pathways mediated by the ER membrane-resident stress sensors PERK, IRE1 and ATF6 (64,67-69,122) . In contrast to the UPR, amino acid deprivation leads to an increase in uncharged tRNA, which binds to and activates the eIF2α kinase GCN2 (42,43). This cascade of events is called the amino acid response (AAR) pathway.

Activation of either PERK or GCN2 leads to the induction of specific target genes, as a result of increased ATF4 synthesis (1). Amino acid deficiency in yeast results in an increase in GCN4 (the yeast counterpart to ATF4) translation affecting the transcription of hundreds of genes, which has led Hinnebusch to characterize it as a " master regulator" (60,61). Array analysis in yeast and mouse revealed over-lapping targets for GCN4 and ATF4, including genes

involved in amino acid transport and metabolism (123). ATF4 is a member of the ATF subfamily of the basic leucine zipper (bZIP) factor super family (124). ATF members are known to heterodimerize within the ATF group as well as with other bZIP transcription factors, including members of the C/EBP family. However, ATF4 also interacts with non-bZIP proteins including, general transcription factors, RPB3 subunit of RNA polymerase II, ribosomal S6 kinase 2 (RSK2), and runt-related transcription factor 2 (RUNX2) (125-127). The interactions of ATF4 with its partners appear to be both stress specific and tissue specific, and its up-regulation represents a major component of the adaptive AAR and UPR stress responses. ATF4-dependent activation of transcription is mediated through binding to a C/EBP-ATF composite genomic element that is made up of half sites for the C/EBP and ATF families respectively (128). Among the target genes up-regulated by ATF4 is System A sodium-dependent neutral amino acid transporter 2 (*SNAT2*). Both the expression of the *SNAT2* gene and its transport activity are up-regulated during amino acid deprivation, hypertonic stress or hormonal stimulation (48,94,129). *SNAT2* activity in the liver is induced by glucagon, and its role in supplying alanine and other gluconeogenic amino acids is likely to contribute to the excessive glucose biosynthesis in insulin-dependent diabetes (130). In addition, System A transport is elevated during the cell cycle and is constitutively high in nearly all transformed cells and tissues (131). Its adaptive regulation by substrate supply and hormones, as well as its increased expression in transformed cells and its role in diabetes makes *SNAT2* a potentially attractive therapeutic target.

Another ATF4-regulated gene is asparagine synthetase (*ASNS*). The two *cis*-acting elements, Nutrient Sensing Response Elements-1, 2 (NSRE-1, NSRE-2), in the proximal promoter of human *ASNS* mediate the transcriptional activation of the gene by either the AAR or

the UPR pathway (112,132). The NSRE-1 sequence is a C/EBP-ATF composite site that binds ATF4 following activation of either the AAR or the UPR (45,59,112). In contrast, the ATF4-responsive enhancer element in the *SNAT2* gene is composed of a single 9 bp intronic sequence (5′-TGATGCAAT-3′) that is also a C/EBP-ATF composite site, but differs in sequence by 2 bp from the *ASNS* NSRE-1 (5′-TGATGAAAC-3′) (114). Although ATF4 binding to the *SNAT2* C/EBP-ATF site has been documented during AAR activation (46), whether or not there is ATF4 binding to *SNAT2* during UPR activation has not been investigated. It is interesting to note that despite the increased ATF4 synthesis known to occur during the UPR and the presence of an ATF4-responsive C/EBP-ATF composite site within the *SNAT2* gene, the cellular SNAT2 mRNA content and transport activity are not induced in response to UPR activation (101).

The present study was designed to explore the differences in the mechanisms for transcriptional control of the *SNAT2* gene during UPR and AAR activation (133) . Three questions were addressed. 1) Does ATF4 bind to the *SNAT2* C/EBP-ATF composite site during the UPR? 2) Is ATF4 binding to the C/EBP-ATF site the determinant event that induces *SNAT2* gene transcription? 3) Are other components of the general transcriptional machinery assembled on the *SNAT2* gene during the UPR? The experiments revealed that *SNAT2* transcriptional activity remains at the basal level in the presence of ER stress despite increased synthesis of ATF4 and its subsequent enhanced binding to the *SNAT2* C/EBP-ATF composite site. Chromatin immunoprecipitation (ChIP) analysis revealed no increase in histone H3 acetylation or general transcription factor (GTF) recruitment to the *SNAT2* promoter following activation of the UPR pathway. Simultaneous activation of both pathways indicated that the UPR generates a suppressive signal that blocks the AAR-induced *SNAT2* transcription activity downstream of ATF4 binding.

Results

Transcriptional Activity of *SNAT2* Gene Is Induced during AAR Activation, But Not during UPR Activation

Despite the prediction that ER stress will activate C/EBP-ATF containing genes via ATF4 action, previous studies have reported that the steady state mRNA content for SNAT2 is increased after amino acid deprivation, but not after treatment of HepG2 human hepatoma cells to induce ER stress (101). To extend those observations, we monitored the effect of Tg treatment on *SNAT2* transcription activity in several cell types (Fig. 3-1). The basal rate of *SNAT2* transcription between cell types was quite variable (Fig. 3-1A). Interestingly, the UPR insensitivity of the *SNAT2* gene was cell specific (Fig. 3-1B, 3-1C). Human kidney cells (293) and breast cancer cells (MDA) both exhibited increased *SNAT2* transcription activity, whereas normal human fibroblasts, mouse embryonic fibroblasts (MEF), and mouse fetal liver cells (BNL-CL2) did not respond to ER stress. For the HepG2 human hepatoma cells and the mouse BNL-CL2 cells, the SNAT2 responsiveness to amino acid limitation was tested and in both cell types transcription was induced as expected (Fig. 3-1C). These observations are consistent with the proposal that the UPR plays different roles in different cell types (1). To further investigate the mechanism of the UPR insensitivity, the time course for *SNAT2* transcription activity during UPR or AAR activation was measured in HepG2 hepatoma cells (Fig. 3-2, top panel). The results revealed that the activity of the *SNAT2* gene during AAR activation by HisOH started to increase at 2 h, peaked at 8 h with a four-fold increase, and then declined at the 12 h time point. In contrast, after activation of the UPR by Tg, the *SNAT2* transcriptional activity transiently fluctuated upward at 4 h, but by 8 h had returned to the basal level observed in the control MEM condition. The MEM values at 2 and 4 h also rose modestly (Fig. 3-2, top panel). As a positive control for the UPR, *BiP/GRP78*, a known UPR-activated gene (134,135), was monitored. In

contrast to previous reports that have relied on the steady state mRNA content to assess *BiP/GRP78* expression, I measured the actual transcription activity of the gene, which was enhanced at all time points at 2 h and beyond, with a maximum of nearly 8-fold at 8 h (Fig. 3-2, bottom panel). This result is in clear contrast to the short, transient rise observed for *SNAT2* during the UPR. As reported previously (136), *BiP/GRP78* expression was not responsive to amino acid deprivation.

Protein Abundance of C/EBP-ATF Binding Proteins Is Elevated by Both Amino Acid Deprivation and ER Stress

A temporal sequence of events occurs in response to amino acid limitation during which target gene activation, induced by ATF4 binding, is followed by a subsequent period of transcriptional suppression. The decline in transcription parallels an increased *de novo* synthesis of ATF3 and C/EBPβ and their subsequent recruitment to the target gene (45,116). Changes in the protein levels of these three transcription factors were assayed after either AAR or UPR activation in HepG2 cells (Fig. 3-3). An increase in the ATF4 protein level during either the AAR or UPR occurred within 1 h and the maximum expression level at 4-12 h was similar for both stress conditions. Likewise, both stress pathways also induced the expression of ATF3 as well as the C/EBPβ-LAP* and C/EBPβ-LAP isoforms beginning at 4 h and continuing through the 12 h time period tested (Fig. 3-3). The truncated C/EBPβ–LIP isoform was also induced, but the level of induction was lower than that for LAP* or LAP (Fig. 3-3).

Protein Binding at the *SNAT2* C/EBP-ATF Enhancer Site

Chromatin immunoprecipitation analysis (ChIP) of ATF4, ATF3, and C/EBPβ binding to the human *SNAT2* C/EBP-ATF site revealed an increase in ATF4 binding within 2 h that reached a maximum between 4-8 h that was approximately equal in magnitude regardless of whether the AAR or the UPR stress signaling pathway had been activated (Fig. 3-4B). ATF4 association

with the human *SNAT2* gene approximately paralleled the AAR-induced transcription activity illustrated in Fig. 3-2. Consistent with the proposal that C/EBPβ expression is itself regulated by ATF4 (137) and that C/EBPβ action at an AARE temporally follows that of ATF4 (45), the ChIP analysis revealed a minimal increase in C/EBPβ binding at 2 h and a significant increase at 4 and 8 h (Fig. 3-4B). However, C/EBPβ binding to the *SNAT2* gene exhibited a similar time course in response to activation of either the AAR or the UPR pathway. In contrast, the time course of ATF3 recruitment to the human *SNAT2* gene was slightly different in response to the two stress-activated pathways. Tg treatment led to an increased association of ATF3 with the *SNAT2* C/EBP-ATF site at 4 h and 8 h, but the level of ATF3 binding was not increased during the initial 4 h after amino acid limitation, and the degree of association was still less than the Tg value at 8 h (Fig. 3-4B). Given that the *SNAT2* gene in the mouse BNL-CL2 fetal hepatocytes also showed insensitivity to ER stress, the ATF4 recruitment to the SNAT2 C/EBP-ATF site in those cells was monitored (Fig. 3-4C). The results showed that, like HepG2 cells, ATF4 binding was enhanced following Tg treatment despite no increase in SNAT2 transcription activity (Fig. 3-1C). This result in the immortalized fetal cell line demonstrates that the lack of an induction following UPR activation is not unique to the transformed HepG2 cells.

Neither Histone H3 Hyperacetylation Nor Assembly of the Transcription Pre-initiation Complex Occurs at the *SNAT2* Gene in Response to the UPR

Increased transcription from the *SNAT2* gene following amino acid limitation is associated with increased histone acetylation and increased recruitment of the general transcription machinery (46). To determine if ATF4 binding was sufficient to induce changes in chromatin structure at the *SNAT2* gene, histone H3 and H4 acetylation at the *SNAT2* promoter and the intronic C/EBP-ATF site was analyzed at 8 h following activation of the AAR or UPR pathways (Fig. 3-5). Increased H3 acetylation was observed at both the promoter and the C/EBP-ATF site

following AAR activation, but, relative to the MEM control values, there was little or no change in Tg-treated cells. Investigation of the histone H4 acetylation status of the *SNAT2* gene revealed no significant difference upon activation of either the AAR or UPR pathway (Fig. 3-5). As a positive control, analysis of the chromatin status of the *ASNS* gene illustrated a significant increase in H3 and H4 acetylation during both UPR and AAR activation, consistent with previously published work (45). The ChIP assay was also employed to explore the recruitment to the SNAT2 promoter of several general transcription factors (GTFs) associated with the pre-initiation complex (Fig. 3-6). At 1 h after activation of the AAR pathway, the association of RNA POL II, TBP, TFIIB, and TFIIE with the SNAT2 promoter remained at basal levels, whereas by 8 h the recruitment for each of these factors increased by 2- to 3-fold. In marked contrast, upon activation of the UPR, there was no enhanced recruitment of these GTFs to the promoter, even at 8 h. As a positive control, the binding of ATF4 at the *SNAT2* C/EBP-ATF site was shown to increase following induction of both pathways (Fig. 3-6). The background value for the ChIP analysis was measured using a non-specific IgG (n/s IgG). Furthermore, to illustrate the degree of non-specific binding for each of the GTF antibodies tested and their specificity for the promoter, primers for a downstream sequence within the SNAT2 gene (exon 10) were used (Fig. 3-6).

UPR-dependent Activation of Transcription From a Plasmid-based SNAT2-driven Reporter Gene

The lack of SNAT2-associated histone modification and recruitment of the GTFs in response to the UPR suggested that changes in chromatin structure may be a critical factor in triggering enhanced transcription via the C/EBP-ATF composite sequence. The less organized chromatin structure of a plasmid may allow for increased *SNAT2* transcription during UPR. To further test this possibility, the transcriptional response of a Firefly luciferase reporter gene,

driven by a *SNAT2* genomic fragment containing the promoter and the C/EBP-ATF site (nt -512/+770), was monitored during either AAR or UPR activation (Fig. 3-7). Consistent with the known function of the *SNAT2* C/EBP-ATF sequence as an amino acid responsive enhancer, activation of the AAR resulted in a 25-fold induction of luciferase activity. Unexpectedly, in contrast to the lack of a response by the endogenous *SNAT2* gene, UPR activation by medium lacking glucose, containing tunicamycin (Tm), or containing Tg led to an induction of SNAT2-driven transcription (Fig. 3-7). The contribution of the C/EBP-ATF site was investigated by transfection of a SNAT2/luciferase reporter construct containing mutations within the C/EBP-ATF sequence. Surprisingly, mutation of the C/EBP-ATF site, previously thought only to function as an AARE, abolished the transcriptional response to both amino acid limitation and ER stress.

Role of ATF3 in the Regulation of *SNAT2* Transcription

The data of Fig. 3-3 showed that the recruitment of ATF3 to the *SNAT2* C/EBP-ATF site was different following activation of the AAR and the UPR. Particularly at 4 h, ATF3 binding was enhanced by the UPR, but not by the AAR. Given the proposal that ATF3 serves as a repressor of ATF4 action at C/EBP-ATF sites (45,128,138), this difference in ATF3 binding a 4 h may explain the lack of Tg-induced transcription subsequent to this time period (Fig. 3-2). To test the hypothesis that a UPR-driven recruitment of ATF3 is responsible for the SNAT2 insensitivity to this pathway, HepG2 cells were transfected with an siRNA against ATF3 and then tested for *SNAT2* transcription activity (Fig. 3-8A). Immunoblot analysis of ATF3 protein content after siRNA treatment documented an effective inhibition of expression under both basal and induced conditions (Fig. 3-8B). In the absence of ATF3 protein expression, activation of the UPR pathway still did not result in an increase in *SNAT2* transcription (Fig. 3-8A). Similar results were obtained when ATF3 wild type and deficient mouse embryonic fibroblasts were

used to monitor *SNAT2* expression, that is, *SNAT2* transcription was not activated by ER stress in either cell population (data not shown). Thus, using two independent systems, the results indicate that ATF3 is not a necessary component of the *SNAT2* UPR-insensitivity. The trend toward higher SNAT2 transcription activity in the siATF3-treated cells is consistent with the proposal that ATF3 is a repressor of this and other C/EBP-ATF regulated genes (45,138).

Activation of the UPR Pathway Blocks the Activation of the *SNAT2* Gene by Amino Acid Limitation

The lack of activation of *SNAT2* transcription by the UPR could result from either the lack of generating a positive secondary signal to the gene that complements ATF4 action or from production of a negative signal to repress the gene despite ATF4 binding. To distinguish between these two possibilities, HepG2 cells were treated to induce the AAR (MEM + HisOH or MEM lacking histidine) independently or in combination with Tg (Fig. 3-9). As expected, the AAR alone activated *SNAT2* transcription, whereas the UPR did not. However, activating both pathways simultaneously resulted in almost a complete blockade of the AAR induction (Fig. 3-9A, left panel). To insure that this effect of Tg was not a direct interaction with the HisOH itself, histidine-free MEM was used instead of HisOH to trigger the AAR pathway. Cells were subjected to histidine deprivation without or with simultaneous Tg treatment, and once again, the increased *SNAT2* transcription resulting from activation of the AAR pathway was blocked by simultaneous activation of the UPR pathway (Fig. 3-9A, right panel). To demonstrate that the response was specific for the *SNAT2* gene, the same samples were used to monitor the transcription activity from the *ASNS* gene (Fig. 3-9B). *ASNS* contains an ATF4-responsive C/EBP-ATF element (NSRE-1), which, in conjunction with a second element (NSRE-2), mediates activation of *ASNS* transcription in response to either the AAR or the UPR pathway (112). Consistent with its responsiveness to the UPR, the induction of *ASNS* transcription by the

AAR was not blocked by simultaneous treatment with Tg; regardless of whether HisOH (Fig. 3-9B, left panel) or histidine-free medium (Fig. 3-9B, right panel) was used to trigger the AAR. As an aside, it should be noted that the simultaneous activation of the AAR and UPR pathways produced no change, or a slight decline, in transcription activity of *ASNS* relative to the AAR pathway alone (Fig. 3-9B). This observation is consistent with the proposal that both of these pathways activate this gene through the common set of genomic elements, NSRE-1 and NSRE-2 (112). The antagonism of the AAR pathway by Tg for the *SNAT2* gene suggests that the lack of increased transcription following the UPR pathway arises from an UPR-dependent repressive activity, rather than simply a lack of an activating signal. Immunoblot analysis for ATF4 protein content did not reveal any difference between activation of the AAR alone or in combination with the UPR, suggesting that the action of the UPR was downstream of ATF4 translational control (Fig. 3-9C). Furthermore, ChIP analysis demonstrated that ATF4 binding at the SNAT2 C/EBP-ATF site occurred during concomitant activation of AAR and UPR pathways (Fig. 3-9D).

Knockdown of the XBP1 and ATF6 Expression Does Not Result in Activation of the *SNAT2* Gene by ER Stress

Although an ERSE or UPRE element has not been described for the *SNAT2* gene, the role of the UPR effectors XBP1, ATF6α, and ATF6β was investigated to rule out the possibility that these transcription factors may contribute to the repression of *SNAT2* transcription during ER stress. Thuerauf et al. (76) used an siRNA knockdown strategy against ATF6α or ATF6β in HeLa cells to test their role in transcription regulation of ER stress target gene *BiP*. It was shown in that study that ATF6α acts as a transcriptional activator, whereas ATF6β functions as a transcriptional repressor of *BiP/GRP78*, although other investigators question whether or not ATF6β serves in this capacity (77). Yamamoto et al (91) have demonstrated in IRE1$\alpha^{-/-}$ MEFs

that transcriptional up-regulation of *BiP* during ER stress is not affected by the absence of the Ire1-XBP1 arm of the UPR.

To investigate whether or not the XBP1 and ATF6 arms of the UPR contribute to *SNAT2* repression by ER stress, HepG2 cells were transfected with siRNA sequences against XBP1, ATF6α, or ATF6β (Fig. 3-10). The mRNA analysis for these factors demonstrated that the siRNA transfection was effective in lowering their expression (Fig. 3-10C), and as a control it was demonstrated that ATF6α knockdown did result in a suppression of UPR-dependent activation of *BiP/GRP78* transcription activity (Fig. 3-10B). The results show that suppression of XBP1, ATF6α, or ATF6β expression did not alter the UPR-dependent repression of *SNAT2* transcription. Collectively, these data indicate that the UPR effectors ATF6α, ATF6β, and XBP1 do not mediate the repressive effect of the UPR on *SNAT2* transcription.

Conclusions

The data obtained for HepG2 human hepatoma cells in the present report led to the following novel observations, some of which are presented graphically in Fig. 3-11. 1) The responsiveness of the *SNAT2* gene to activation by the UPR pathway is cell specific. 2) In HepG2 human hepatoma cells and mouse BNL-CL2 fetal hepatocytes *SNAT2* transcriptional activity remains near basal levels despite a readily detected increase in ATF4 recruitment and binding to the C/EBP-ATF site within the *SNAT2* gene that equals that observed during the AAR. 3) The lack of increased *SNAT2* transcription by the UPR results from an active repression of the gene rather than merely an absence of an activating signal. 4) The mechanism of this repression is unknown, but it appears to occur at a step downstream of ATF4 binding, it is not triggered by the ATF6 or XBP1 arms of the UPR, and it can override the activation by the AAR pathway. 5) The results demonstrate that the *SNAT2* C/EBP-ATF composite site,

previously considered to function exclusively as an AARE, can mediate a UPR-initiated induction of transcription outside the context of intact chromatin (i.e., a plasmid) in HepG2 hepatoma cells.

With regard to the genomic elements that mediate transcriptional activation by the AAR and UPR stress pathways, there are three classes of genes. 1) Those genes that are only induced by one or the other pathway via a specific genomic element (e.g., BiP/GRP78, containing an endoplasmic reticulum stress element (ERSE), but insensitive to the AAR). 2) Those genes, such as CHOP, that are induced by both pathways, but that contain two different genomic elements that exhibit distinct AARE and ERSE activities. 3) The *ASNS* gene, which thus far is a unique case in that it is activated by both pathways through a common bipartite site consisting of NSRE-1, a C/EBP-ATF composite site, and NSRE-2 (45,112,113). Consistent with these distinctions, promoter deletion analysis by Jousse et al. (139) demonstrated that amino acid depletion and ER stress act via independent elements to activate the CHOP gene. However, there are also data indicating that the ERSE (nt –93 to –75) and AARE (C/EBP-ATF sequence at nt -310 to -302) sites both contribute to the CHOP induction in response to ER stress (90,140,141). In this regard, the results of Yoshida et al. (74) are noteworthy. Those authors showed that a *CHOP* promoter construct (nt –870/+17) containing wild type ERSE-I and ERSE-II exhibited a 3-fold increase in transcription in response to UPR activation. However, even after mutating both ERSE sites, the construct yielded about a 2-fold increase, albeit the absolute values of luciferase activity were lower (see Fig. 4, Yoshida et al.). These data can be interpreted to suggest that the *CHOP* C/EBP-ATF site at nt –310/-302 may still allow this promoter fragment to respond to the UPR. The Yoshida et al. (74) result for *CHOP* would be

analogous to and consist with the present result for UPR activation of *SNAT2* in the context of a plasmid.

ATF4 has been shown to activate the transcription from many stress-sensitive genes that contain a C/EBP-ATF composite site (47). The C/EBP-ATF composite site within the intron of the *SNAT2* gene functions as an AARE, mediating ATF4-dependent activation of the gene following amino acid deprivation (46). However, given that ER stress also induces ATF4 synthesis, the question of whether or not ATF4 bound to the *SNAT2* C/EBP-ATF composite site during ER stress remained unanswered. The answer to this outstanding issue is mechanistically important because it is known that SNAT2 mRNA content and transport activity are not increased proportionally to the increase in ATF4 protein following ER stress in HepG2 cells (101). The present ChIP data demonstrate clearly that ATF4 protein, increased in abundance following UPR activation, is bound to the *SNAT2* C/EBP-ATF site at a level equal to or greater than that observed after activation of the AAR pathway in both HepG2 human hepatoma cells and mouse BNL-CL2 immortalized fetal hepatocytes.

Induction of *SNAT2* transcription during amino acid deprivation is controlled by the sequential binding and interplay of ATF4, ATF3, and C/EBPβ at the *SNAT2* C/EBP-ATF site (46). Previous results had illustrated that the binding of these three factors at an AARE parallels their *de novo* synthesis (45), and that this programmed sequence of factor synthesis and recruitment occurs in a qualitatively similar manner for each of six different C/EBP-ATF containing genes tested (116). ATF4 binding is at least a component of the transcriptional trigger because the time course of ATF4 recruitment closely parallels histone acetylation, GTF recruitment, including Pol II, and the actual transcription activity (45). Conversely, increased ATF3 and C/EBPβ binding to the C/EBP-ATF site occurs later (after 6-8 h) and corresponds

with the repression phase of transcription (45,116). Remarkably, the ChIP data in the present study show that the binding of all three of these factors at the *SNAT2* C/EBP-ATF site occurs during ER stress, indicating that the subsequent recruitment of ATF3 and C/EBPβ may be triggered by bound ATF4, but it is not dependent on histone acetylation, assembly of the general transcriptional machinery, or on enhanced transcription from the gene. With one exception, the temporal and quantitative binding of ATF4, ATF3 and C/EBPβ following UPR activation is nearly identical to that for the AAR activation. Increased ATF3 binding during ER stress occurred at an earlier time (4 h) than during amino acid limitation (8 h), and that UPR-associated ATF3 binding was followed by a complete repression of a transient rise in *SNAT2* transcription. However, knockdown of ATF3 with siRNA did not reverse the UPR repression of the *SNAT2* gene, indicating that ATF3 is not a critical mediator of that action.

The absence of sustained induced transcription activity from the *SNAT2* gene following activation of the UPR pathway could have been the consequence of two different mechanisms. It was possible that increased transcription requires not only ATF4 binding to the C/EBP-ATF composite site, but also a second activating signal. If this hypothesis were true, it would be that amino acid deprivation initiates this secondary signal, whereas ER stress does not. Conversely, it was possible that the UPR pathway triggers a repressive signal for the *SNAT2* gene, which overrides the ATF4 binding and prevents an induction of transcription activity. Support for the latter proposal came from results demonstrating that the induction of *SNAT2* transcription by amino acid deprivation was blocked by the concurrent activation of the UPR pathway. The nature of this signal remains to be elucidated, but, as discussed below, the evidence presented here links the signal to chromatin structure. Furthermore, knockdown of the ATF6 and XBP1

arms of the UPR did not relieve the *SNAT2* repression suggesting that neither of these transcription factors mediates the repression, either directly or indirectly.

To further explore the mechanistic basis for the lack of *SNAT2* activation during ER stress, histone acetylation and recruitment of general transcription factors (GTFs) was investigated. Our ChIP data revealed that there is an increase in histone H3 acetylation at the *SNAT2* promoter and the C/EBP-ATF region following AAR activation, but not following UPR activation. Likewise, while the GTF proteins that make up the preinitiation complex (PIC) are present on the *SNAT2* promoter following amino acid limitation, they are not recruited following UPR activation. These data also document that histone modification and assembly of the PIC at the *SNAT2* promoter is an event that occurs subsequent to ATF4 binding. ATF4 has been shown to interact directly with several GTFs including TBP, TFIIB, and TFIIF (125) and the RPB3 subunit of RNA polymerase II (127). Indeed, co-expression of RPB3 with ATF4 enhances its transcriptional activation capabilities (127), so it is possible that ATF4 plays a direct role in the GTF recruitment. Our results suggest that the recruitment of chromatin modifying complexes containing HAT activity may not occur. Why the bound ATF4 does not trigger histone modification and GTF recruitment to the *SNAT2* gene when the initial stimulus was ER stress is not clear.

Another important observation of the present study was that, in contrast to the endogenous *SNAT2* gene, transcription from a SNAT2-driven luciferase reporter was induced upon UPR activation. The lack of higher-order chromatin structure of a plasmid may confer the UPR sensitivity to the *SNAT2* gene. Furthermore, mutations of the *SNAT2* C/EBP-ATF composite site abolished the transcriptional induction by several different UPR activators, confirming that the response was dependent on the integrity of this intronic enhancer element. In

addition to potential differences in chromatin structure, it is possible that there is a recruitment of a repressor/co-repressor to the *SNAT2* gene in response to the UPR that does not occur following activation of the AAR. Another explanation for selective regulation of the *SNAT2* gene may be a relocalization within the nucleus. For example, the recruitment of the *SNAT2* promoter to a transcription factory during AAR activation, but not in the presence of ER stress, could also explain the difference in response between the two pathways. An example of such a relocation mechanism and of the association of a gene with a transcription factory is described for the murine β-globin locus during erythroid maturation (6,7). If such a mechanism exists for SNAT2, UPR activation may block this relocalization. Regardless of the mechanism, the present results suggest a link between *SNAT2* activation by ATF4 and chromatin structure. Thus, the specificity of the *SNAT2* C/EBP-ATF composite site to distinguish between the AAR and UPR signals depends on the context of the chromatin environment. It is interesting to speculate that ATF4 is a pioneer factor that binds to the C/EBP-ATF site in a nucleating event without the prerequisite of extensive chromatin modification, but then a second, chromatin-associated event becomes critical in triggering transcriptional activation. The *SNAT2* gene provides an interesting model to investigate these and other mechanisms associated with transcriptional control in response to cellular stress and the associated signaling pathways.

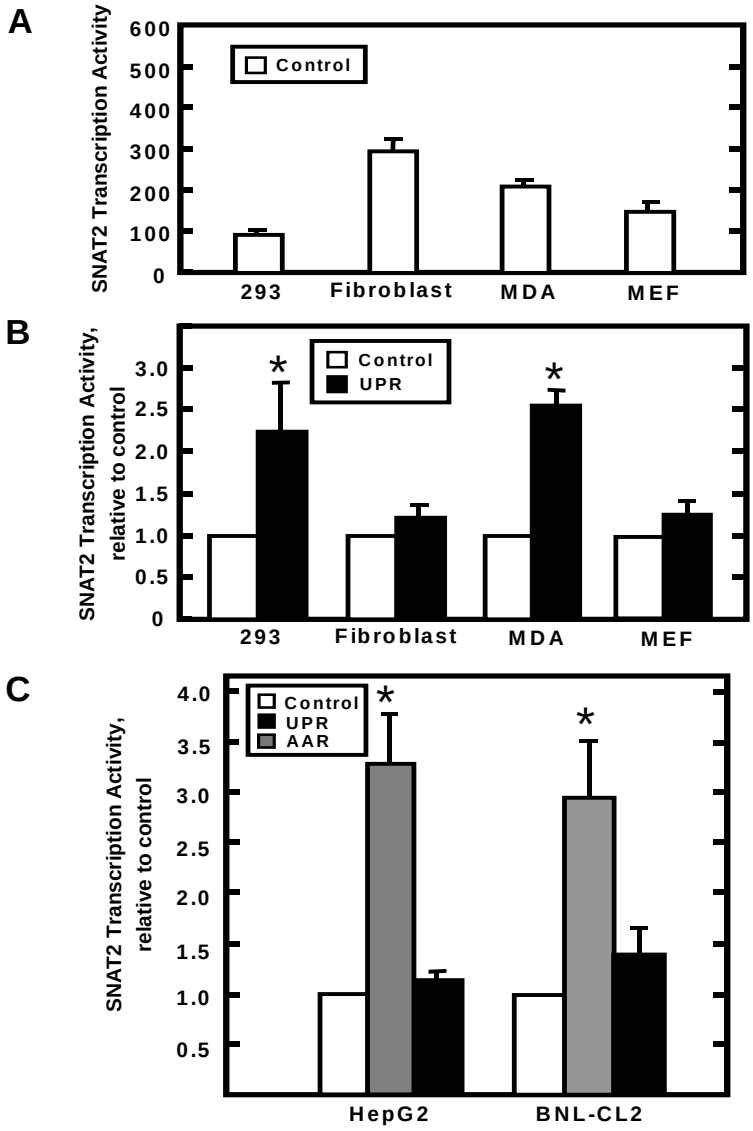

Figure 3-1. Transcriptional activity of the *SNAT2* gene in different cell lines during UPR or AAR. Panel A shows the transcription activity of the *SNAT2* gene in several human and mouse cell lines in the "control" or basal state (cultured in MEM). The transcription activity was assayed by measuring the SNAT2 hnRNA using primers spanning the human exon 4–intron 4 junction and for mouse, spanning the exon 13–intron 13 junction. Panel B shows the fold-change, relative to the control value shown in Panel A, in *SNAT2* transcription activity after Tg treatment for 8 h to induce the UPR. Values are expressed as means ± standard error of the means (S.E.M.). Panel C shows the *SNAT2* transcriptional activity for two cell lines, HepG2 human hepatoma cells and BNL-CL2 mouse immortalized fetal hepatocytes that do not activate the *SNAT2* gene in response to the UPR, but do respond to amino acid limitation (AAR). The asterisk denotes a value significantly different from the control at $p < 0.05$. The labels are: "HepG2", human hepatoma cells; "293", human kidney; "fibroblast", immortalized normal human fibroblast; "MDA-MB-231", human breast cancer; "MEF", mouse embryonic fibroblast; "BNL-CL2", mouse fetal hepatocytes. Data in panel A and B are courtesy of Jixiu Shan.

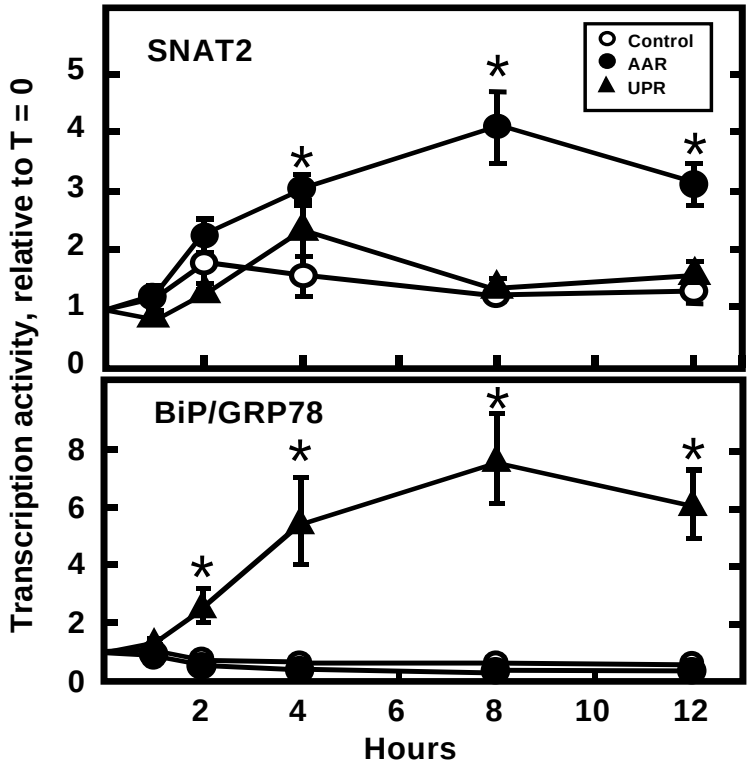

Figure 3-2. Transcription activity of the *SNAT2* and *BiP* genes in HepG2 human hepatoma cells during activation of the UPR or AAR pathways. HepG2 cells were incubated for 0–12 h in MEM (Control), MEM + HisOH (AAR), or MEM + Tg (UPR). At the time points indicated, total RNA was isolated and analyzed by qRT-PCR. The transcription activity was assayed by measuring the *SNAT2* hnRNA using primers spanning the exon 4intron 4 junction and the *BiP* primers spanned the exon 2–intron 2 junction. The results are expressed as fold-change relative to the control value at time zero (T=0). The PCR reactions were performed in duplicate for each sample, and samples were collected from three independent experiments. Values are expressed as means ± standard error of the means (S.E.M.). Where not shown, the error bars are within the symbol. The asterisk denotes a value significantly different from the control at $p < 0.05$.

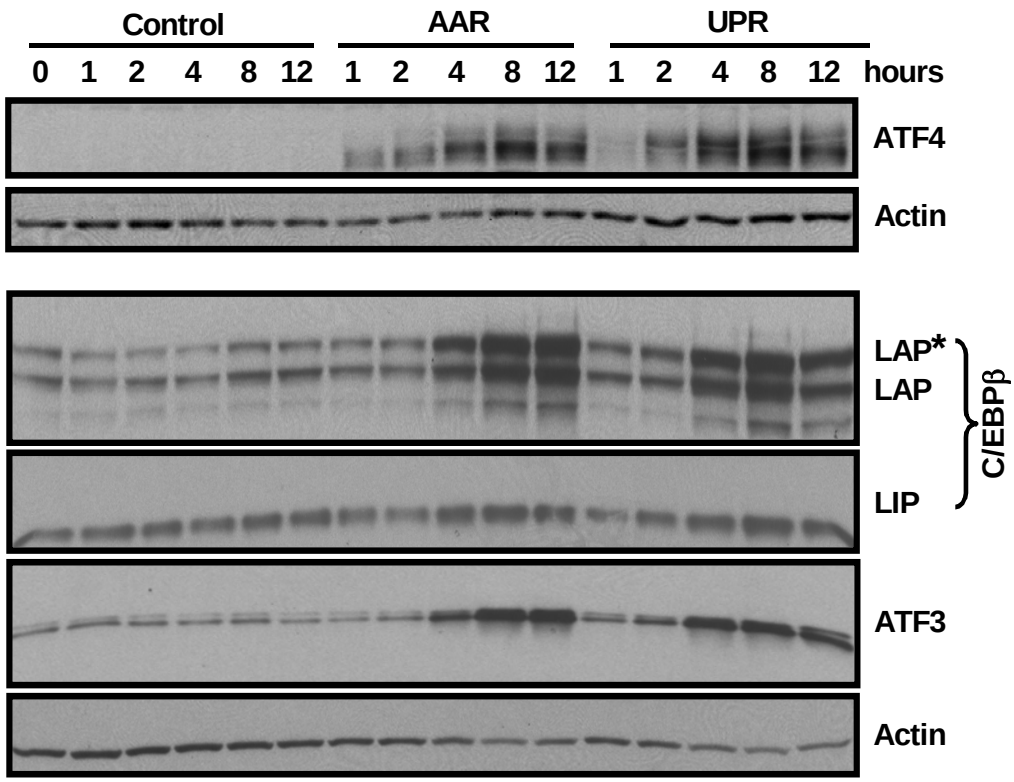

Figure 3-3. Immunoblot analysis of ATF4, ATF3, and C/EBPβ protein expression during amino acid deprivation or ER stress. Whole cell lysates of HepG2 cells incubated for 0–12 h in MEM (Control), MEM + HisOH (AAR), or MEM + Tg (UPR) were collected and subjected to immunoblot analysis. After transfer to a nitrocellulose membrane, the blot was probed with antibodies against ATF4, ATF3, C/EBPβ (showing the LAP*, LAP, and LIP isoforms), or actin. The blots shown are representative of several experiments performed to ensure qualitative reproducibility.

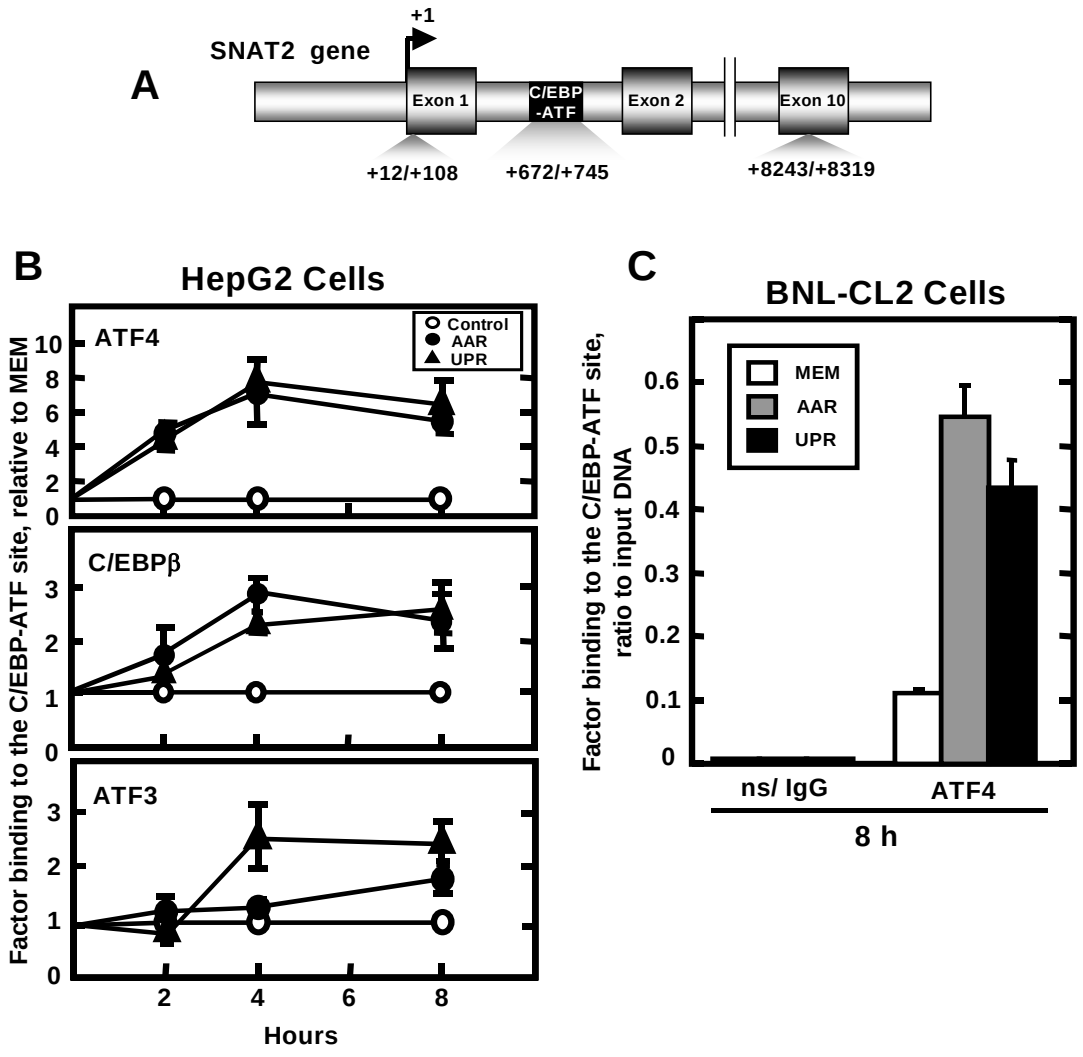

Figure 3-4. Binding of ATF4, ATF3, and C/EBPβ proteins to the *SNAT2* C/EBP-ATF composite site following activation of either the AAR and UPR pathways. (A) Scheme of human SNAT2 gene showing the qRT-PCR primer positions for ChIP analysis. (B) ChIP analysis was performed on HepG2 cells incubated for 2, 4, or 8 h in MEM (Control), MEM + HisOH (AAR), or MEM + Tg (UPR). (C) ChIP analysis was performed on mouse BNL-CL2 immortalized fetal hepatocytes incubated for 8 h in MEM (Control), MEM + HisOH (AAR), or MEM + Tg (UPR). The antibodies used in the assay were against ATF4, C/EBPβ, or ATF3. As a negative control, rabbit anti-chicken IgG was tested and the values were always less than 5% of those with the transcription factor antibodies (for example, see Panel C). Primers specific for the *SNAT2* intronic C/EBP-ATF region were used for amplification during qRT-PCR. The data are presented as the fold change relative the MEM values (Panel B) or the ratio to the input DNA (Panel C). Each time point was calculated from analysis in duplicate for samples from at least three independent experiments and represents the mean ± S.E.M.

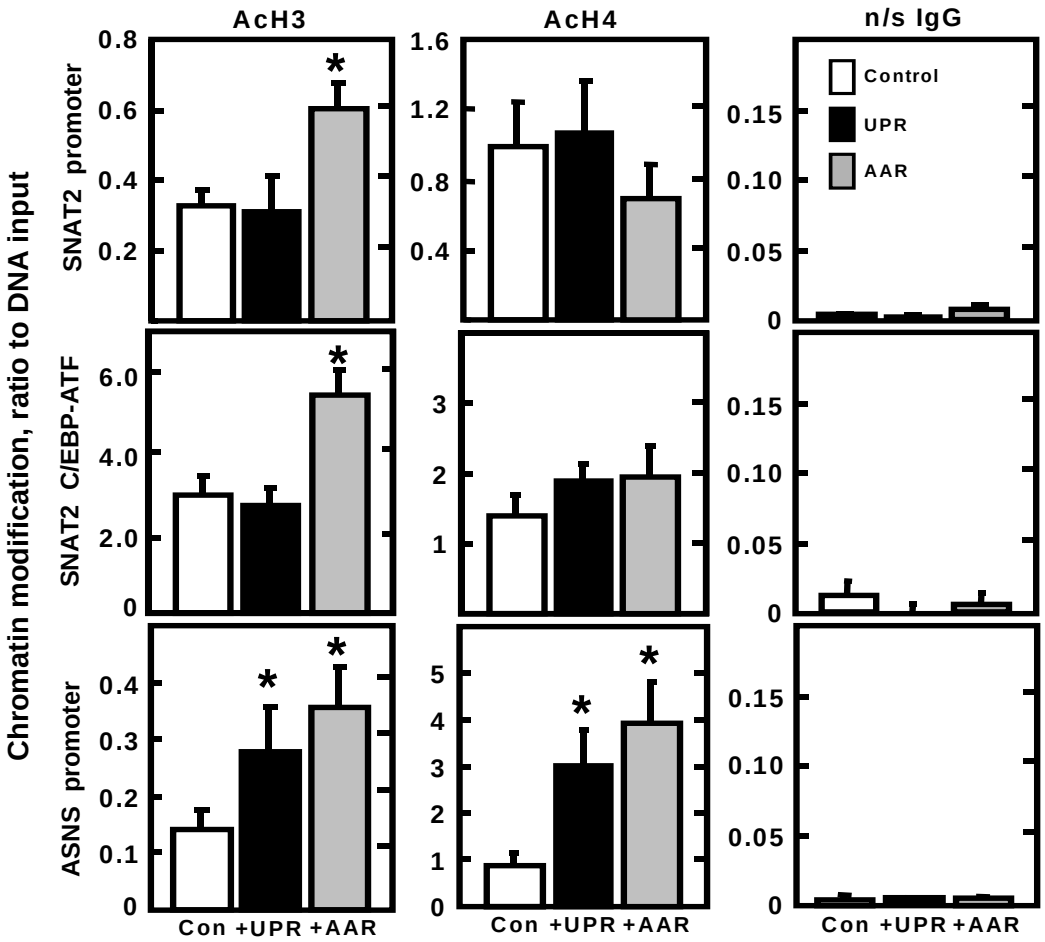

Figure 3-5. Endoplasmic reticulum stress does not provoke an increase in acetylation of histone H3 at the *SNAT2* promoter or at the C/EBP-ATF site. ChIP analysis was performed on HepG2 cells incubated for 8 h in MEM (Control), MEM + HisOH (AAR), or MEM + Tg (UPR). Antibodies against acetylated histone H3, acetylated H4, or non-specific IgG were used in the assay. Primers specific for the SNAT2 promoter or the SNAT2 C/EBP-ATF region, as shown in Fig. 4A, and the ASNS promoter regions were used for amplification during qRT-PCR. The data are presented as the ratio to input DNA. The values for each time point are calculated from duplicate assays for at least three independent experiments and are represented as the mean ± S.E.M. The asterisks denote a value that is statistically different ($p < 0.05$) from the MEM control.

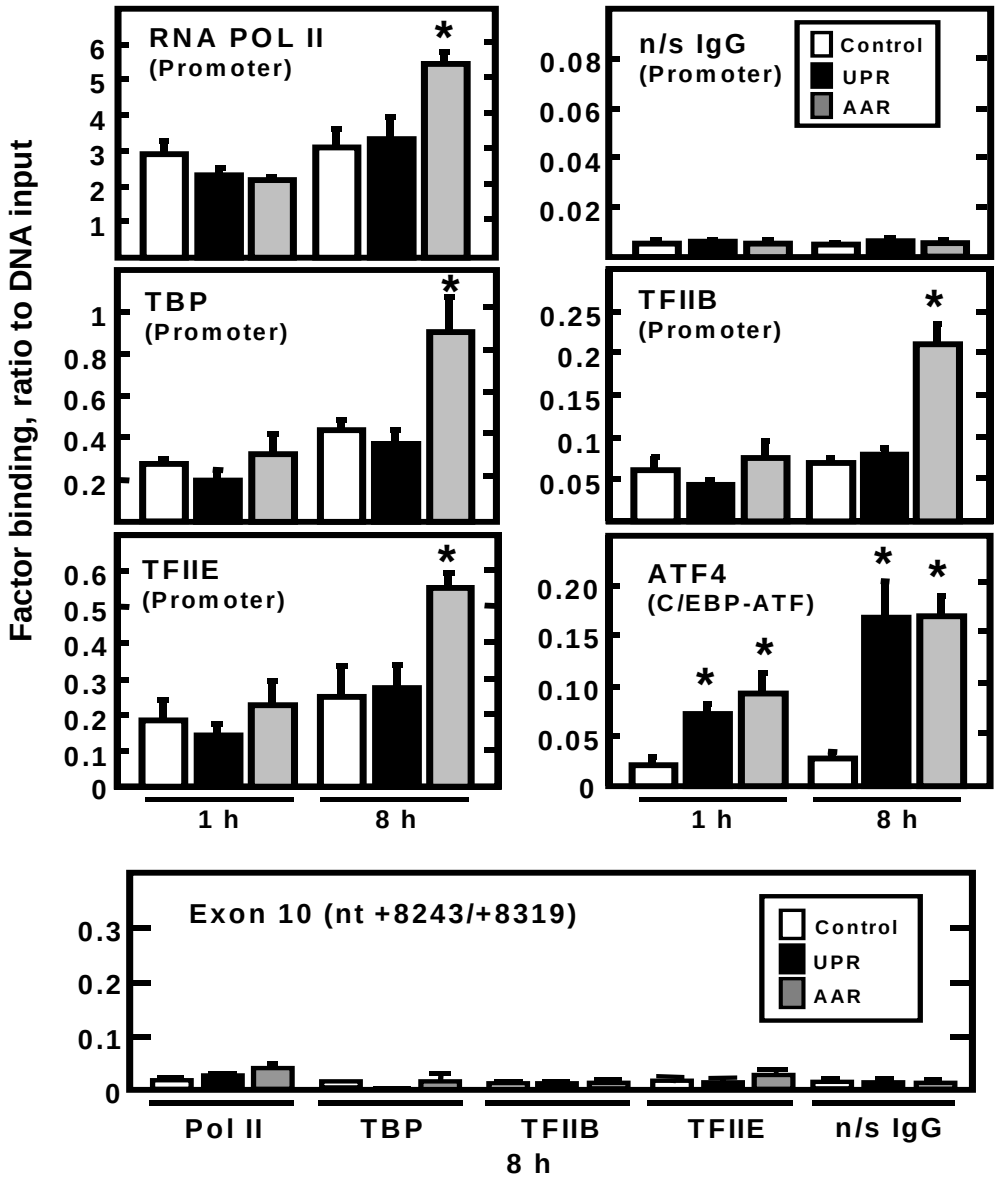

Figure 3-6. Preinitiation complex is not assembled on the *SNAT2* promoter during UPR activation. ChIP analysis was performed on HepG2 cells incubated for 1 h or 8 h in MEM (white bars), MEM + Tg (UPR, black bars), or MEM + HisOH (AAR, gray bars). Antibodies against RNA Pol II, TBP, TFIIB, TFIIE, ATF4 and non-specific IgG were used. Primers specific for the *SNAT2* promoter (RNA Pol II, TBP, TFIIB, and TFIIE) or the C/EBP-ATF (ATF4), as shown in Fig. 4A, were used for amplification during qRT-PCR. As an additional negative control for each antibody, PCR was performed with primers corresponding to the *SNAT2* exon 10, a downstream region of the gene (bottom panel). The data are presented as the ratio to input DNA and the values for each time point are calculated from duplicate assays for at least three independent experiments. The data shown represent the mean ± S.E.M and an asterisk denotes values that are statistically different ($p < 0.05$) from the MEM control.

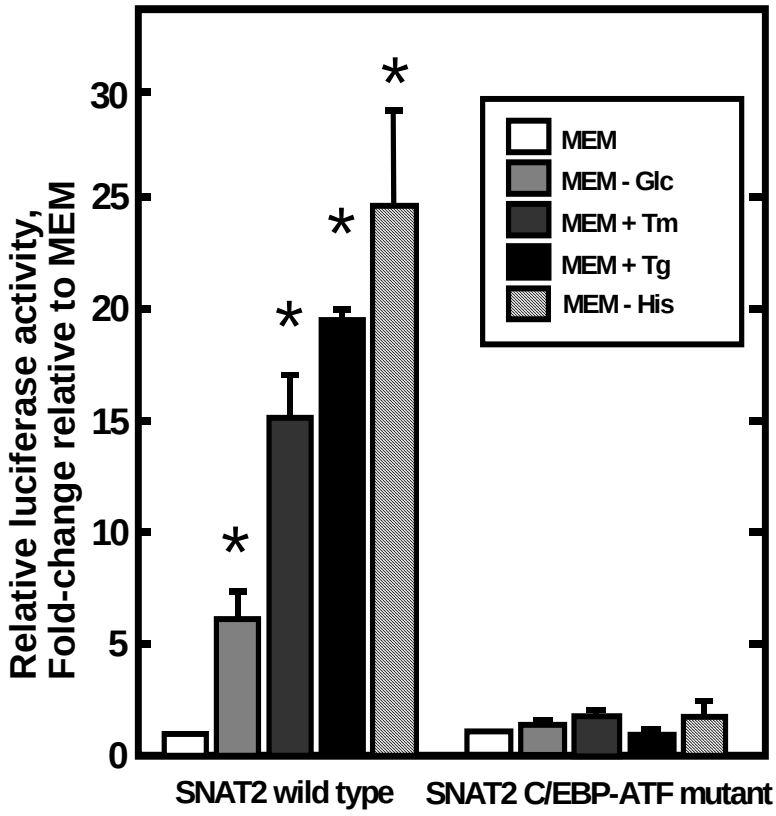

Figure 3-7. Endoplasmic reticulum stress induces *SNAT2* transcription from a reporter plasmid through the C/EBP-ATF composite site. HepG2 cells were transfected with a Firefly luciferase reporter gene driven by a *SNAT2* genomic fragment (nt -512/+770), containing both the promoter and the wild type or mutated C/EBP-ATF enhancer sequence (nt +709/+717). The cells were co-transfected with a SV40-driven Renilla luciferase as a transfection control. Induction of the AAR pathway was achieved by incubation for 10 h in histidine-free MEM, whereas the UPR was activated by a 10 h incubation in MEM lacking glucose (-Glc), MEM + 300 nM thapsigargin (Tg), or MEM + 5 μg/ml tunicamycin (Tm). The data are the averages ± standard deviations for 4-6 individual assays and all differences marked with an asterisk are statistically significant at $p < 0.01$. Data courtesy of Stela Palii.

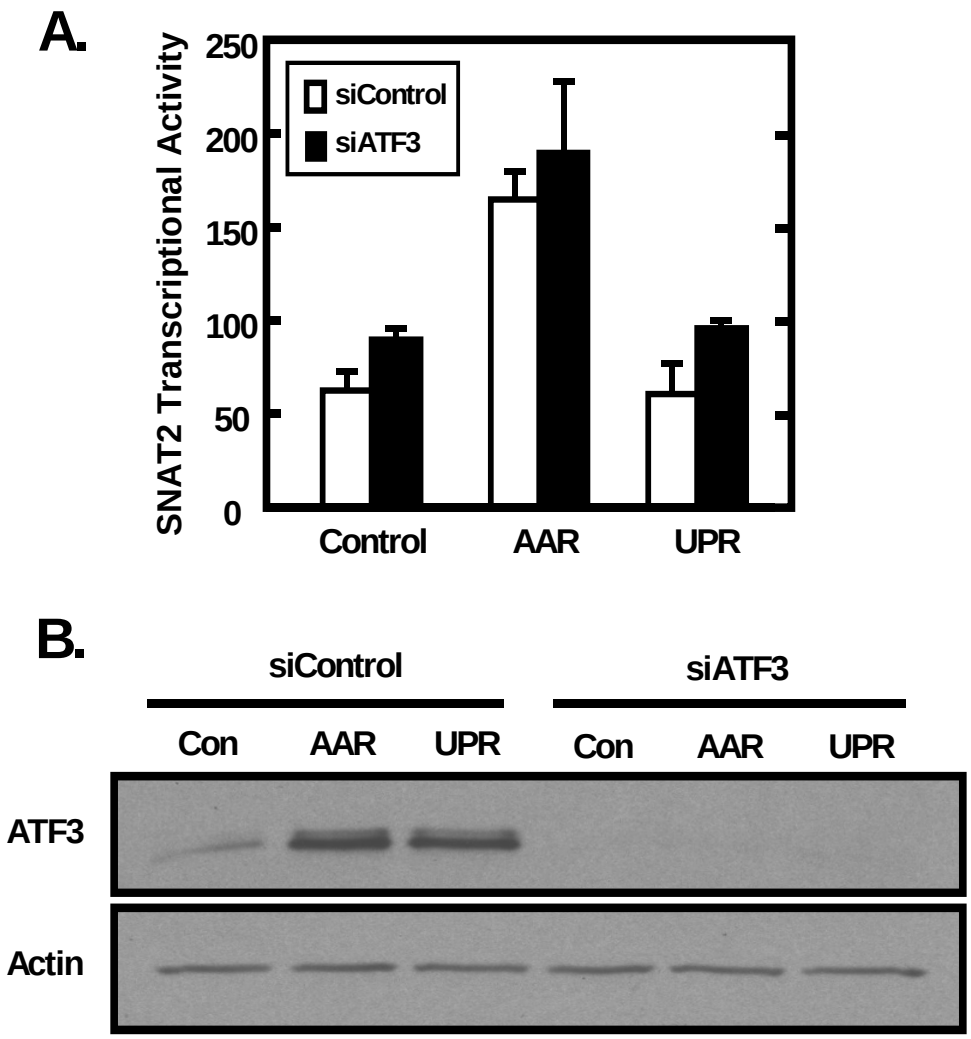

Figure 3-8. Knockdown of ATF3 does not reverse the insensitivity of the *SNAT2* gene to the UPR. HepG2 cells were transfected with either a control siRNA (siControl) or an siRNA against ATF3, as described in the Materials and Methods. The cells were then incubated for 8 h in either MEM (Control), MEM + HisOH (AAR), or MEM + Tg (UPR) prior to isolation of RNA for analysis of SNAT2 transcription activity (A). The PCR reactions were performed in duplicate for each sample, and samples were collected from three independent experiments. Values are expressed as means ± S.E.M. Isolation of whole cell extracts was performed for immunoblot analysis of ATF3 protein content and for actin as a loading control (B). The immunoblot results shown are representative of multiple experiments.

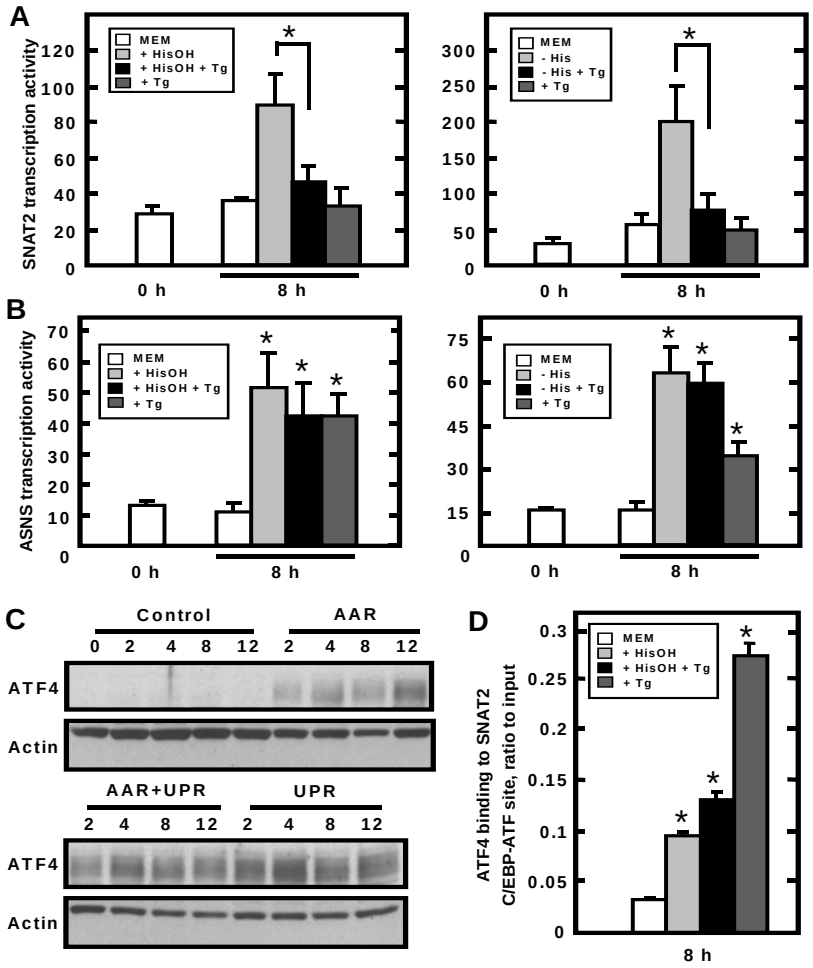

Figure 3-9. Activation of the UPR pathway antagonizes the induction of the *SNAT2* gene by the AAR pathway. HepG2 cells were incubated in control MEM or in the indicated conditions to activate either separately or concomitantly the AAR and UPR. To obtain the data in (A) (SNAT2) and (B) (ASNS), the AAR pathway was activated by two different treatments, either MEM containing HisOH (left hand side) or MEM lacking histidine (right hand side). At 0 h and 8 h, total RNA was isolated and analyzed by qRT–PCR. The transcription activity was assayed by measuring the SNAT2 (A) and ASNS (B) hnRNA using primers spanning the exon 4–intron 4 and the intron12–exon13 junctions, respectively. The PCR reactions were performed in duplicate for each sample, and samples were collected from three independent experiments. Values are expressed as means ± S.E.M. (C) Illustrates an immunoblot analysis of ATF4 protein abundance in whole cell lysates prepared from HepG2 cells incubated in the indicated condition for 0-12 h (AAR = MEM - His; UPR = MEM + Tg). After the transfer, the blot was probed with an ATF4 antibody followed by an actin antibody, as described in the Materials and Methods section. (D) ChIP analysis of ATF4 binding to the SNAT2 C/EBP-ATF site was performed on HepG2 cells treated for 8 h with the indicated AAR or UPR pathway activators. Samples were collected from three independent experiments. Values are expressed as means ± S.E.M. For Panel A, the asterisk denotes that the value for the simultaneous treatment is significantly different ($p < 0.05$) from that for the HisOH treatment alone. For Panels B and D, the asterisk denotes a value statistically different ($p < 0.05$) from the MEM control.

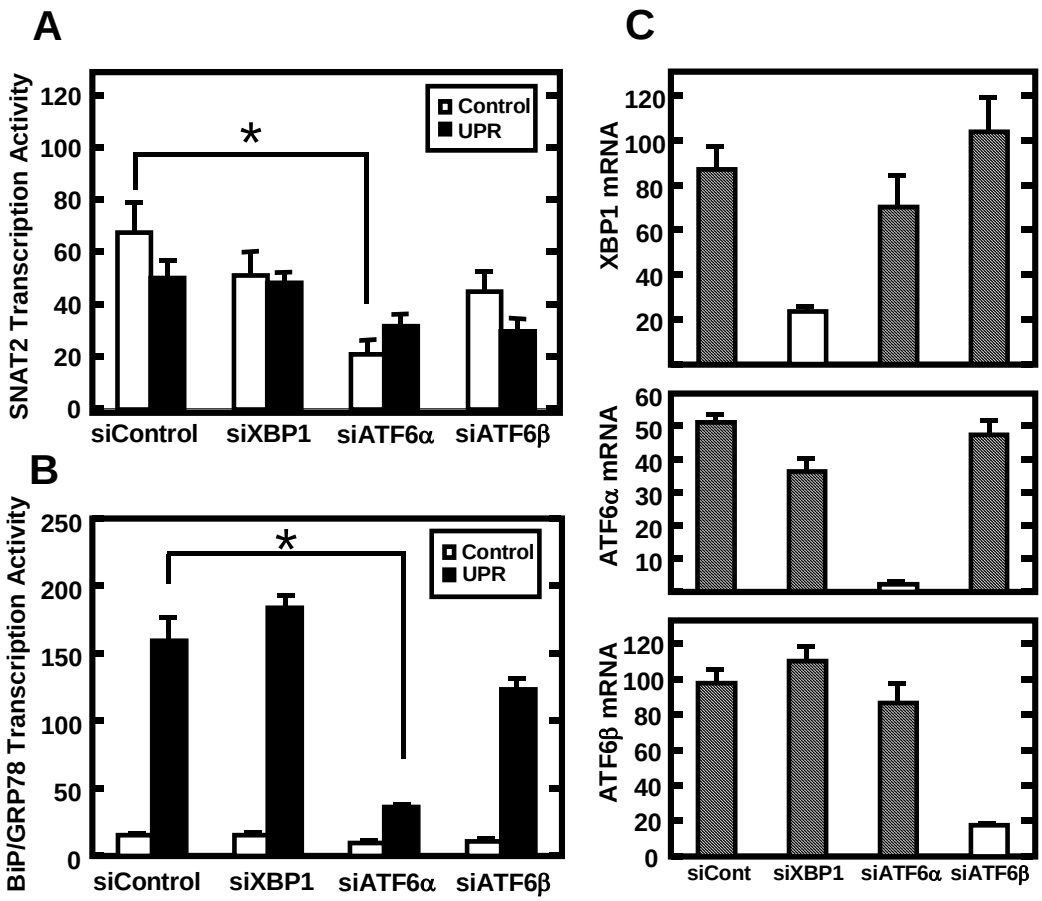

Figure 3-10. Knockdown of the expression of XBP1, ATF6α or ATF6β does not increase *SNAT2* transcription activity during UPR activation. HepG2 cells were transfected with either a control siRNA (*siControl*) or an siRNA specific for XBP1, ATF6α or ATF6β for 24 h followed by incubation in complete MEM for 24 h. The cells were then incubated for 8 h in MEM or MEM + Tg. Total RNA was isolated and transcription activity of *SNAT2* (A), *BiP*/*GRP78* (B) and steady state mRNA (C) of XBP1, ATF6α and ATF6β were assayed. The qPCR reactions were performed in duplicate for each sample, and samples were collected from three independent experiments. Values are expressed as means ± S.E.M. An asterisk indicates a statistically significant difference ($p < 0.05$) relative to the respective siControl value.

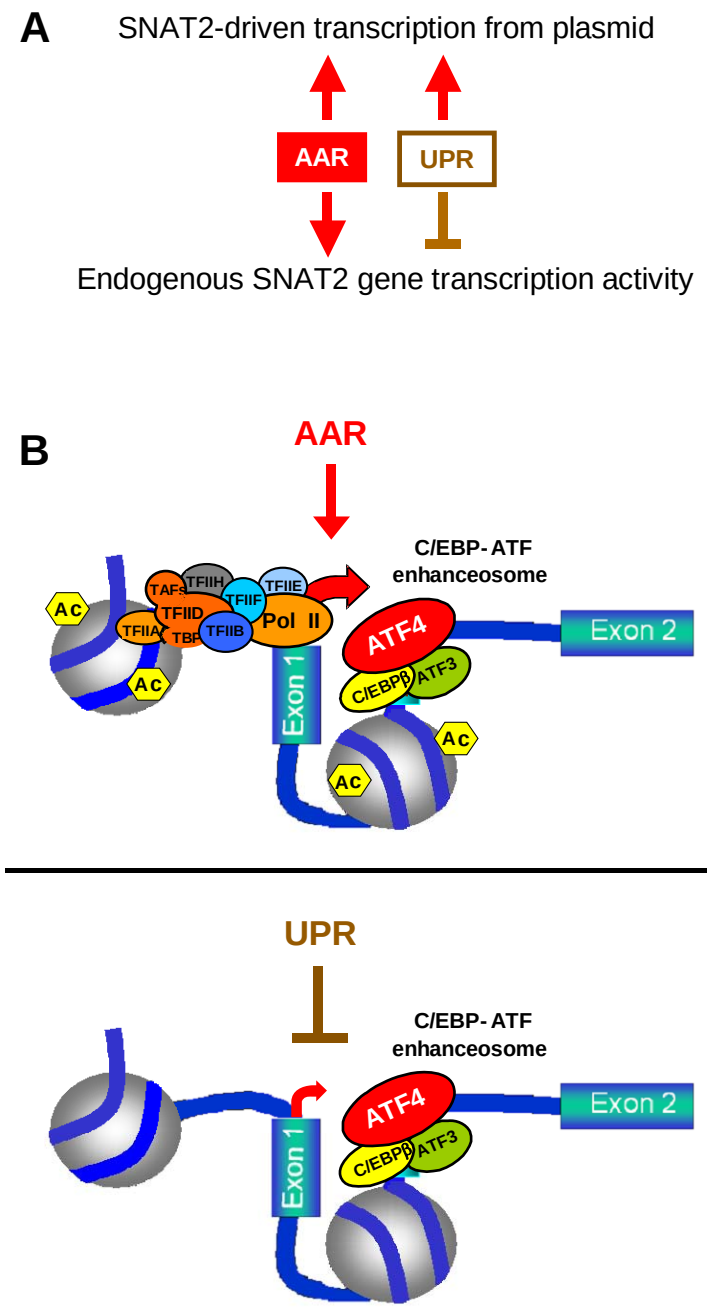

Figure 3-11. Working model for the differential regulation of the *SNAT2* gene in HepG2 cells during activation of the AAR or UPR pathways. (A) *SNAT2*-driven transcription is induced by either AAR or UPR from a plasmid-based luciferase reporter that contains the *SNAT2* promoter and C/EBP-ATF site. In contrast, *SNAT2* transcription from the endogenous gene is induced only by the AAR, but not by the UPR pathway. (B) The AAR pathway triggers assembly of the ATF4-enhanceosome, increased H3 hyperacetylation, and PIC formation, events that lead to enhanced *SNAT2* transcription activity. Conversely, despite the assembly of the ATF4-enhanceosome, the UPR represses *SNAT2* transcription

CHAPTER 4
HUMAN *SNAT2* GENE CHROMATIN CONFORMATION

Introduction

Chromatin Modifications

Chromatin conformation has been shown for many genes to be the determinant factor in promoting transcription. Histone modifications and chromatin remodeling complexes influence the state of chromatin conformation. Packaging of eukaryotic DNA into nucleosomes makes it less accessible to the transcription machinery (33). Therefore, depending on the environment around a particular gene, modification of chromatin structure may be a pre-requisite for transcription from that gene. Chromatin modifications can be initiated by covalent modifications of histone tails through acetylation, phosphorylation, methylation, ubiquitination, sumoylation, ADP-ribosylation and glycosylation (8). There is evidence that these post-translational modifications can occur not only on the histone tails, but in the histone body as well (8). Certain covalent modifications of histone tails are associated with activation and others with repression of transcription, and are considered markers of chromatin influence on gene expression (142). *Histone acetylation* is one of the most studied chromatin modifications. Acetylation of lysines in histones neutralizes the positive electric charge, which contributes to the interaction of histones with the negatively charged DNA backbone, causing chromatin relaxation, while deacetylation shifts the balance back to condensing the chromatin and silencing gene expression. Acetylation of amino groups of conserved lysine residues (AcH3 K4, K9, K14, K18, K23, K27; AcH4 K5, K8, K12, K16) present in histone tails is linked to transcriptional activation, whereas deacetylation of these residues is linked to transcriptional repression. Mammalian histone acetyltranferases (HATs) such as GCN5, PCAF, TAF1, ATF2, p300, CBP and mammalian histone deacetylases (HDACs - homologs of yeast RPD3, Hda1 and Sir2) are the enzymes

responsible for the histone acetylation and deacetylation, respectively. *Histone methylation* occurs predominantly on specific lysine or arginine residues on histone H3 and H4. Amino groups of histone lysines can be mono-, di-, or trimethylated in vivo. The lysine-specific SET domain, containing histone methyl transferase (HMT) activity, is responsible for the methylation of H3 K4, K9, K27, K36 and H4K20. The methylation of H3K9 is a marker of the initiation and maintenance of heterochromatin, whereas H3K4me2 and H3K4me3 have been linked to transcriptionally active genes (143). Histone demethylation of mono- and dimethylated K4 residues, but not trimethylated K4 residues, is done by LSD1. The recently discovered human demethylase JMJD2A demethylates histone H3 dimethylated or trimethylated at lysine 9 and lysine 36 (144,145). The exploration of histone modifications at the SNAT2 gene during activation of either AAR or UPR represented a major part of the efforts of this study in understanding the differential transcriptional response of the SNAT2 gene to the activation of these two pathways.

DNase I Hypersensitive Sites

The investigation of cis-regulatory elements of a certain gene can be performed by exposing DNA from NP-40 permeabilzed cells to short DNaseI digestion. The pattern of cleavage and the cleavage sites reflect the open/accessible chromatin conformation around these regulatory elements that bind the respective transcription factors. Exploring the DNA regulatory elements and chromatin conformation of the SNAT2 gene represents particular interest given the wide range of stimuli that SNAT2 is responsive to, such as amino acid starvation, hormone stimulation, cell volume changes and hypertonicity (48,94,109,129). Also, this method addresses the question of chromatin conformation in basal conditions when compared with that in the presence of stress.

Results

H3K4 Trimethylation (H3K4Me3) Profile of the *SNAT2* and *ASNS* Genes During Amino Acid Limitation or ER Stress

Recent reports have established that H3K4Me3 modification of nucleosomes in a set of promoters in vivo represents an anchor for the TFIID complex (through TAF3 plant homeodomain (PHD) finger) and consequently, contributes to PIC assembly and increased transcription (143). The presence of this marker of transcription activation was investigated by ChIP analysis for SNAT2 and ASNS genes during either AAR or UPR activation. The data presented in Fig. 4-1 showed that high H3K4 trimethylation levels were present during basal conditions for both genes and no significant differences were observed upon stress for the ASNS promoter and SNAT2 C/EBP-ATF site. The only statistically significant difference was achieved during the decrease of H3K4Me3 at the SNAT2 promoter upon UPR activation.

There Is Histone H3 Depletion at the *SNAT2* and *ASNS* Promoters upon UPR or AAR Activation

Total histone H3 protein levels are indicative of the presence or depletion of nucleosomes in a particular gene region. How the H3 levels of SNAT2 and ASNS are affected by stress, represented another important question. This analysis was particularly interesting because the findings would be novel and contribute to the understanding of transcriptional regulation of both SNAT2 and ASNS genes. The results shown in Fig. 4-2 demonstrated that levels of H3 present during unstimulated conditions decreased significantly at both the SNAT2 and the ASNS promoter upon stress, regardless if that was amino acid limitation or ER stress. Histone H3 levels at the SNAT2 C/EBP-ATF remained unchanged.

The HDAC Inhibitor Trichostatin A (TSA) Blocks the AAR Induced *SNAT2* Transcription

The data presented in previous chapters indicated that chromatin plays a critical role in SNAT2 transcription activation. Histone deacetylases are chromatin modifiers that remove the

acetyl groups on histone tails (other proteins (TFs) can be HDAC substrates as well) leading to tight packaging of chromatin making it less accessible to TFs. HDACs repress transcription by behaving as co-repressor molecules. To further explore the chromatin and HDACs contribution, the HDAC inhibitor TSA was used. In these experiments, a pretreatment of cells for 15 h with TSA was followed by AAR or UPR activation. TSA treatment led to inhibition of SNAT2 transcription activity and mRNA (Fig. 4-3, panel A) during AAR but it did not affect SNAT2 transcription during UPR. To prove that TSA affects specifically SNAT2 gene transcription and to rule out any effects on the AAR or PERK/eIF2α/ATF4 signaling cascades, ASNS mRNA levels were measured and immunoblotting of whole cell extracts was performed. The induction of the ASNS transcription (an AAR and UPR target gene) during either AAR or UPR was not affected as demonstrated by the ASNS mRNA levels (Fig. 4-3, panel B). The Western blot data presented in Panel C shows that the p-eIF2α and ATF4 induction by AAR or UPR was not affected by TSA treatment, indicating that the signaling cascades investigated are intact in the presence of TSA.

HDACs 1, 2, and 3 Occupy the Human *SNAT2* and *ASNS* Promoters Under Basal Conditions

To further explore the involvement of HDACs in the SNAT2 and ASNS transcription, their recruitment on the promoter regions was subject of investigation**.** ChIP analysis with antibodies against HDAC1,2,3,5 revealed that HDACs 1, 2, and 3, but not HDAC5 occupy the SNAT2 (Fig. 4-4) and ASNS (Figure 4-5) promoters during unstimulated conditions. AAR and UPR activation led to a depletion of these particular HDACs on SNAT2 and ASNS promoters most of which were statistically significant, as indicated by the asterisk (Fig. 4-4 and 4-5). The binding of ATF4 at the ASNS promoter region (where the C/EBP-ATF site is located) was elevated as expected during both AAR and UPR activation in these experiments, indicating that

the drug treatments (HisOH and TG) triggered the respective pathways and that the ATF4 enhanceosome at the ASNS C/EBP-ATF site was recruited. The HDAC5 was not part of the ASNS or SNAT2 promoter complex in either basal or stressed conditions as denoted by the values that equal those of a non-specific antibody (Fig. 4-4 and 4-5).

The p300 and PCAF Recruitment on the *SNAT2, BiP, ASNS* and *CHOP* Genes during AAR or UPR Activation

The role of co-activators has been widely investigated in the activation of transcription from the promoters of various genes (146). Is a co-activator a component of the complex that is formed at the target genes SNAT2, BiP, ASNS and CHOP? The recruitment of p300 and PCAF, two well-known co-activators, was investigated by ChIP (Fig. 4-6). The results showed that for the SNAT2 gene, although there was some level (above non-specific IgG background) of p300 detected, the binding was not enhanced during stress. For the specific UPR target gene BiP, there was some degree of p300 recruitment during ER stress, but not during amino acid limitation. A similar situation as the BiP promoter was observed at the ASNS promoter, although this gene is sensitive to both pathways (Fig. 4-6). CHOP is another gene that responds to both pathways, it contains a C/EBP-ATF site and an ERSE. p300 recruitment to the CHOP C/EBP-ATF was detected during both AAR and UPR activation (Fig. 4-6). No PCAF recruitment was detected on any of the target genes tested. There are two possible explanations: first, there is no PCAF recruitment to these genes; and second, the antibody used was not efficient in immunoprecipitating the PCAF protein.

There Are Six DNase I Hypersensitive Sites on the *SNAT2* Gene Region Scanned Between –2135 and +5624

Another experimental approach that is adopted to provide insight into chromatin conformation is the DNase I hypersensitivity assay. To understand and explore the differential transcriptional response of the SNAT2 gene to the AAR versus UPR, DNaseI hypersensitive

sites were measured. The Southern blot presented in Fig. 4-7 shows that there are six hypersensitive sites on the SNAT2 gene region scanned, nt –2135 and +5624. These DNaseI hypersensitive sites were present both under basal and stress triggered conditions. The sites were labeled as HS1-6 and were constitutive sites. Some of the sites presented higher intensity in their respective bands on the blot and were considered strong hypersensitive sites: HS1, 3 and 5. Other sites showed less sensitivity to the DNaseI digestion and were considered weaker hypersensitive sites: HS2, 4 and 6. As mentioned above the appearance of these six DNase I hypersensitive sites was not dependent on the presence or absence of stress with one exception. HS2 site, present during basal or UPR activation, decreased in intensity during HisOH triggered AAR pathway activation.

Conclusions

This chapter of addresses the role of chromatin in the differential transcriptional response of SNAT2 to the activation of AAR and UPR pathways. The study of SNAT2 gene chromatin conformation involved an array of assays. ChIP was employed to assay histone acetylation, histone methylation, total H3, p300 and PCAF recruitment. Determination of transcription activity was done in the presence or absence of the HDAC inhibitor TSA. DNaseI hypersensitivity assay was used to identify cis-regulatory elements and to evaluate the status of the chromatin conformation.

In addition to the differences in acetylation of histones H3 at the SNAT2 promoter and C/EBP-ATF site during AAR and UPR activation, there were some notable differences in the H3K4me3 and total H3 profile (Fig. 4-1 and 4-2). The basal levels of H3K4me3 were high for both genes tested (SNAT2 and ASNS) and there was a significant decrease of H3K4me3 during UPR activation at the SNAT2 promoter. Given that H3K4me3 is a hallmark of transcription activation which serves as an anchor for the TFIID protein complex and PIC assembly, this

decrease provides a possible explanation for the lack of PIC assembly at the SNAT2 promoter during ER stress. Another implication of this finding would be the involvement of a H3K4 histone demethylase, such as JARID1B (Plu-1)(147). Another interesting result was the total H3 pattern, which showed that the promoters of SNAT2 and ASNS undergo histone depletion upon activation of the AAR or UPR pathways. This is consistent with the current thinking that during induction of transcription most genes have nucleosomes displaced or removed to allow PIC assembly and transcriptional activation.

The possible recruitment of co-activators p300 and PCAF (Fig. 4-6) was investigated. Although the binding levels of p300 assayed by ChIP were overall low, those levels were above the non-specific IgG background. PCAF was not detected at any of the genes tested. For the SNAT2 gene, p300 present at basal conditions did not exhibit enhanced recruitment during AAR activation, those levels actually decreased. The degree of enhanced recruitment of p300 that was observed for ASNS and BiP during UPR, and CHOP during AAR and UPR indicated that this co-activator might be part of the transcriptional activation complex of these genes during stress.

The exploration of how chromatin and chromatin modifiers influence SNAT2 transcription was followed by experiments that involved the HDAC inhibitor TSA (Fig. 4-3). The intriguing finding that the AAR-induced SNAT2 transcription is inhibited in the presence of TSA indicates the necessity of an HDAC action on either histones or a transcription factor, action that is inhibited by TSA. The other observation was that the presence of TSA did not affect the SNAT2 transcription during UPR. Given that HDACs behave as repressors or are part of bigger repressor complexes, the HDAC recruitment was pursued by ChIP analysis (Fig. 4-4 and 4-5). The results of these experiments led to the novel observation that HDACs 1-3 are constitutively bound to the SNAT2 and ASNS promoters and their binding decreases upon activation of the AAR or UPR

pathways. The removal or the loss of HDACs during a period of increased transcription would be consistent with their co-repressor role. HDACs are responsible for the deacetylation of chromatin and consequent inaccessibility of the gene locus to transcription factors. Although a specific HAT for the SNAT2 and ASNS genes has not been identified (except for the TAF1/TAF250 recruitment as part of the TFIID complex), the HDAC depletion during stress is very likely to be followed by recruitment of a HAT that would account for the increase in acetylation during AAR activation.

The investigation of chromatin structure using the DNase I hypersensitivity assay was the next step in addressing the contribution of chromatin to the transcriptional response of the SNAT2 gene. The data revealed the striking observation that there are six DNase I hypersensitive sites in the SNAT2 gene between nt –2135 and +5624. DNase I hypersensitive sites correspond to DNA cis-regulatory elements, consistent with the mapping of HS1 to the SNAT2 promoter region and HS3 to the SNAT2 C/EBP-ATF site. The HS1-6 were constitutive sites that were maintained and did not change during either AAR or UPR activation with one exception. Although the HS2 site was present in the MEM control condition and during TG-induced ER stress, HS2 intensity decreased during HisOH triggered AAR pathway. The behavior of this site would be consistent with that of a boundary element or silencer. The HS2 was mapped between the two strong hypersensitive sites HS1 and HS3 that correspond to the SNAT2 promoter and C/EBP-ATF site, respectively. This possible boundary or silencer element might bind TFs that are repressors of trascription, impeding the interaction between the promoter and the enhancer during conditions that the gene is not actively transcribing (i.e. basal or ER stress), whereas during AAR, when the SNAT2 gene transcription rates are high, this site is in a closed chromatin conformation, not accessible to repressors. The open chromatin conformation

indicated by the existence of the six constitutive DNase I hypersensitive sites in the SNAT2 gene and the HepG2 cell type used is noteworthy. Being a hepatoma cell line, the basal levels of System A transport activity (SNAT2) are known to be up-regulated in transformed cells (94), and the observation that SNAT2 transcription levels are relatively high and that there is an open chromatin conformation suits this profile.

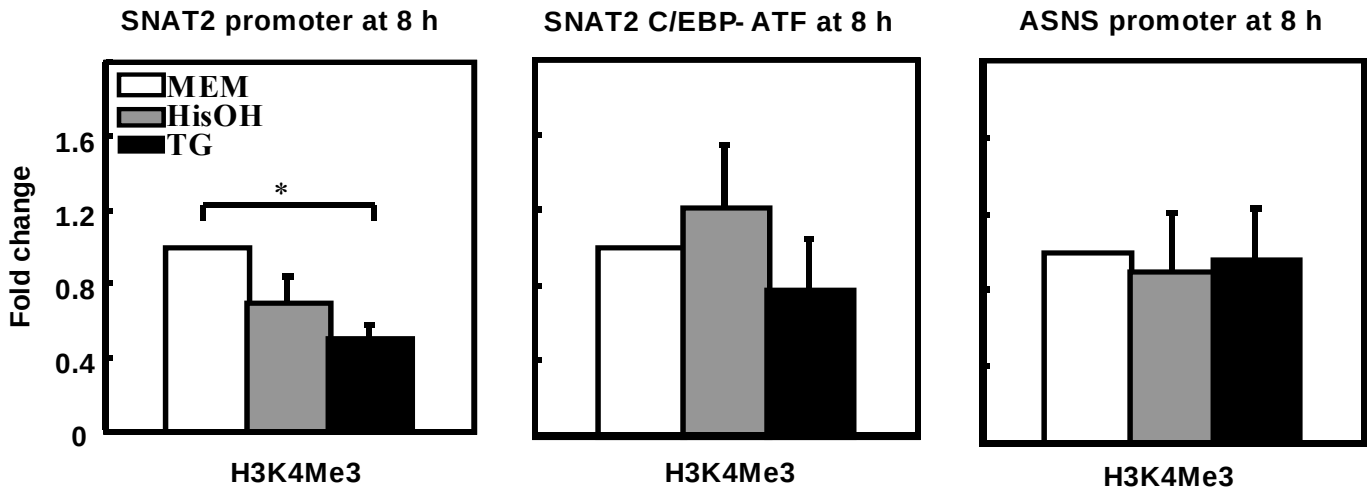

Figure 4-1. Profile of H3K4 trimethylation of the *SNAT2* promoter, C/EBP-ATF site and *ASNS* promoter by ChIP analysis. HepG2 cells treated with 2 mM HisOH or 300 nM TG for 8 h were used for the ChIP assays. An antibody specific for H3K4Me3 was used during the IP step. Primers that amplified the human promoters of ASNS and SNAT2 and the SNAT2 enhancer were used in the for the qPCR. The data are presented as fold change relative to the MEM control, which was set to one. The qPCR reactions were run in duplicate and the data were collected from at least three independent experiments. The values represent the mean±SEM. An asteriks denotes statistical significance, $p<0.05$.

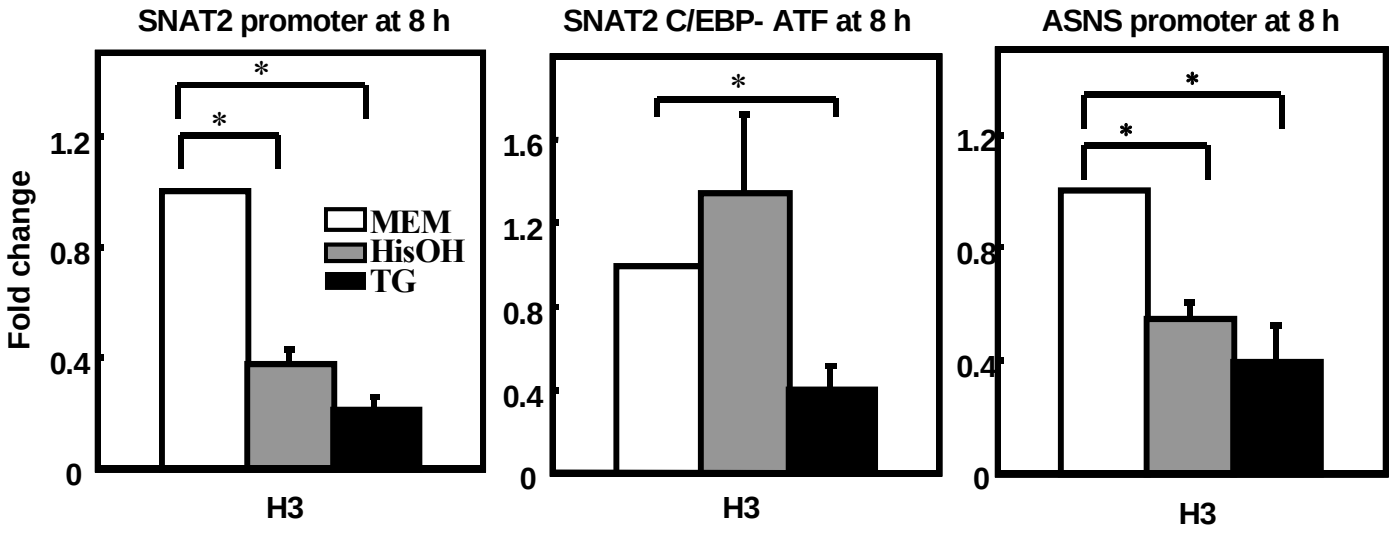

Figure 4-2. Total histone H3 ChIP analysis at the *SNAT2* promoter, C/EBP-ATF site and ASNSpromoter. After treatment of HepG2 cells with 2 mM HisOH or 300 nM TG for 8 h ChIP analysis was performed. An antibody specific for total histone H3 was used during the IP step. The data are shown as fold change relative to the MEM control, which was set to one. The qPCR reactions were done in duplicate and the data were collected from at least three independent experiments. The values represent the mean±SEM. An asteriks denotes statistical significance, $p<0.05$.

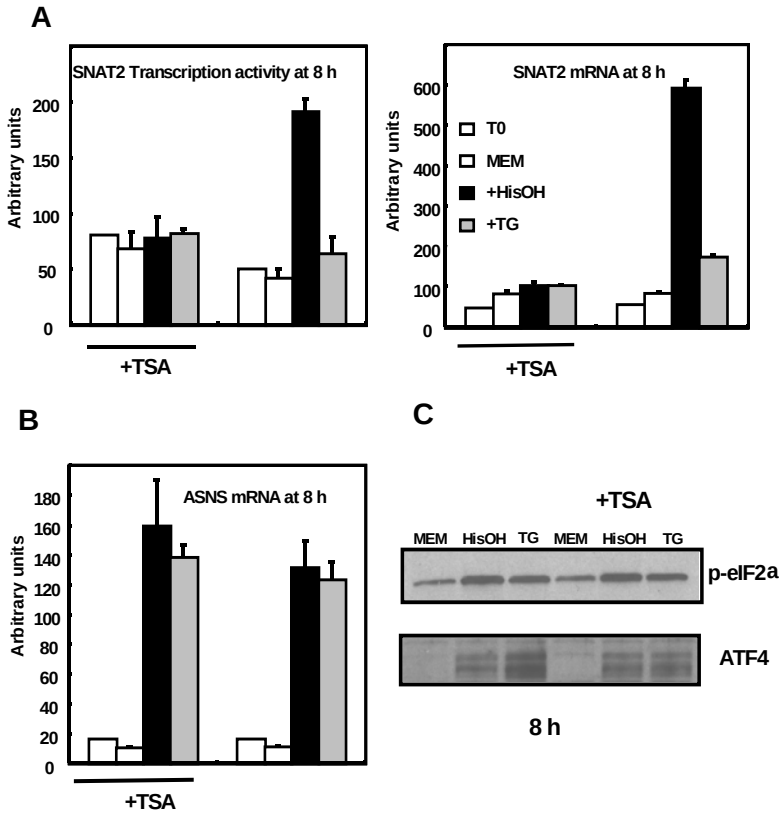

Figure 4-3. Effect of HDAC inhibitor- Trichostatin A (TSA) on the *SNAT2* and *ASNS* transcription. A pretreatment for 15 h with 100ng/ml TSA of HepG2 cells preceded the 8 h incubations with HisOH or TG. Total RNA or whole cell extracts were isolated. The SNAT2 transcription activity (panel A) and steady state mRNA levels for SNAT2 and ASNS (Panel A and B) were determined. The qRT-PCR reactions were done in dublicate and the data were collected from three independent experiments. The immunoblot analysis was performed using specific antibodies against the p-eIF2a and ATF4 (Panel C).

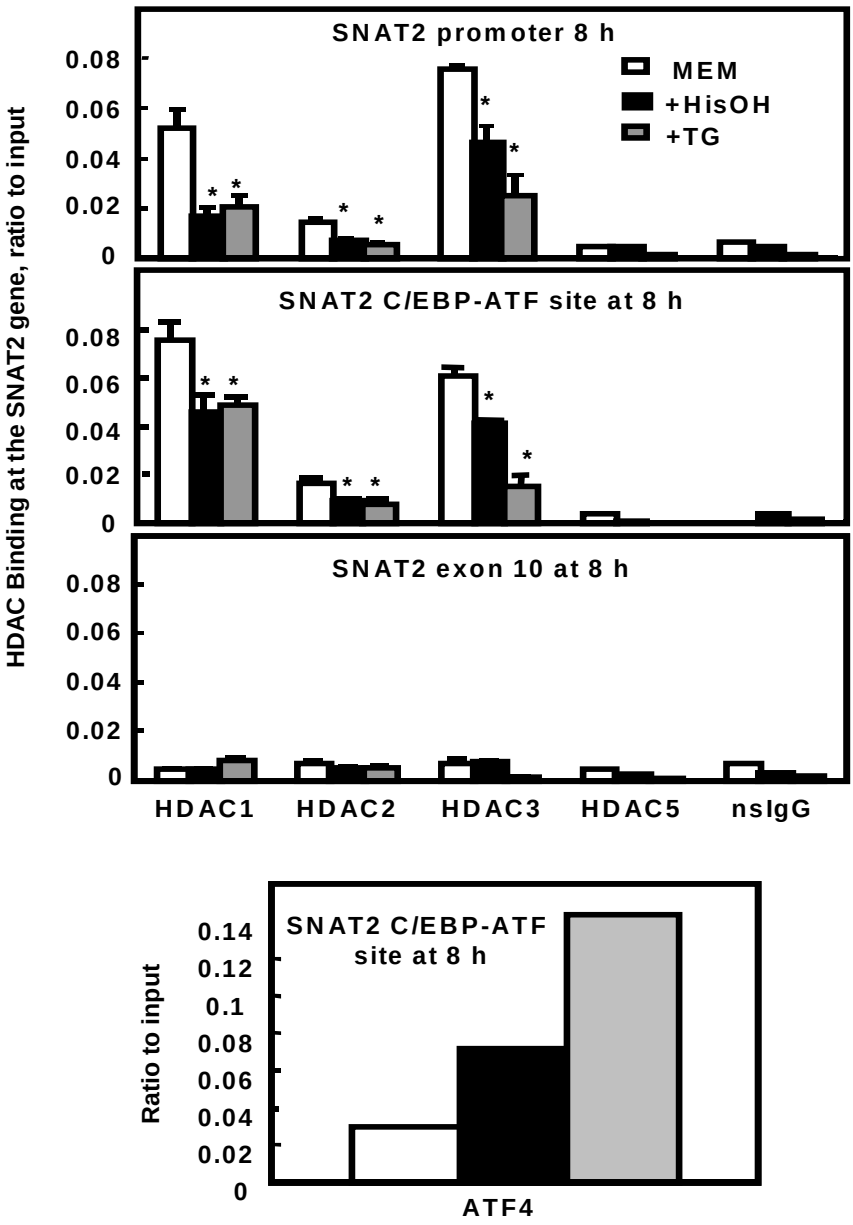

Figure 4-4. Occupancy of the *SNAT2* promoter and C/EBP-ATF site by HDACs. ChIP analysis was performed on HepG2 cells treated with either HisOH or TG for 8 h. Specific antibodies against HDACs 1, 2, 3, 5 and ATF4 were used in the IP step. A non specific IgG (ns/IgG) antibody was used to establish the background values for the antibodies. Primers that amplified SNAT2 promoter or C/EBP-ATF site were used during the final qPCR. The reactions were run in dublicate and the data for HDAC1, 2 and 3 were collected from at least three different experiments whereas those for ATF4 and HDAC5 represent the mean of values from two independent experiments. An asterisk denotes statistical significance $p<0.05$.

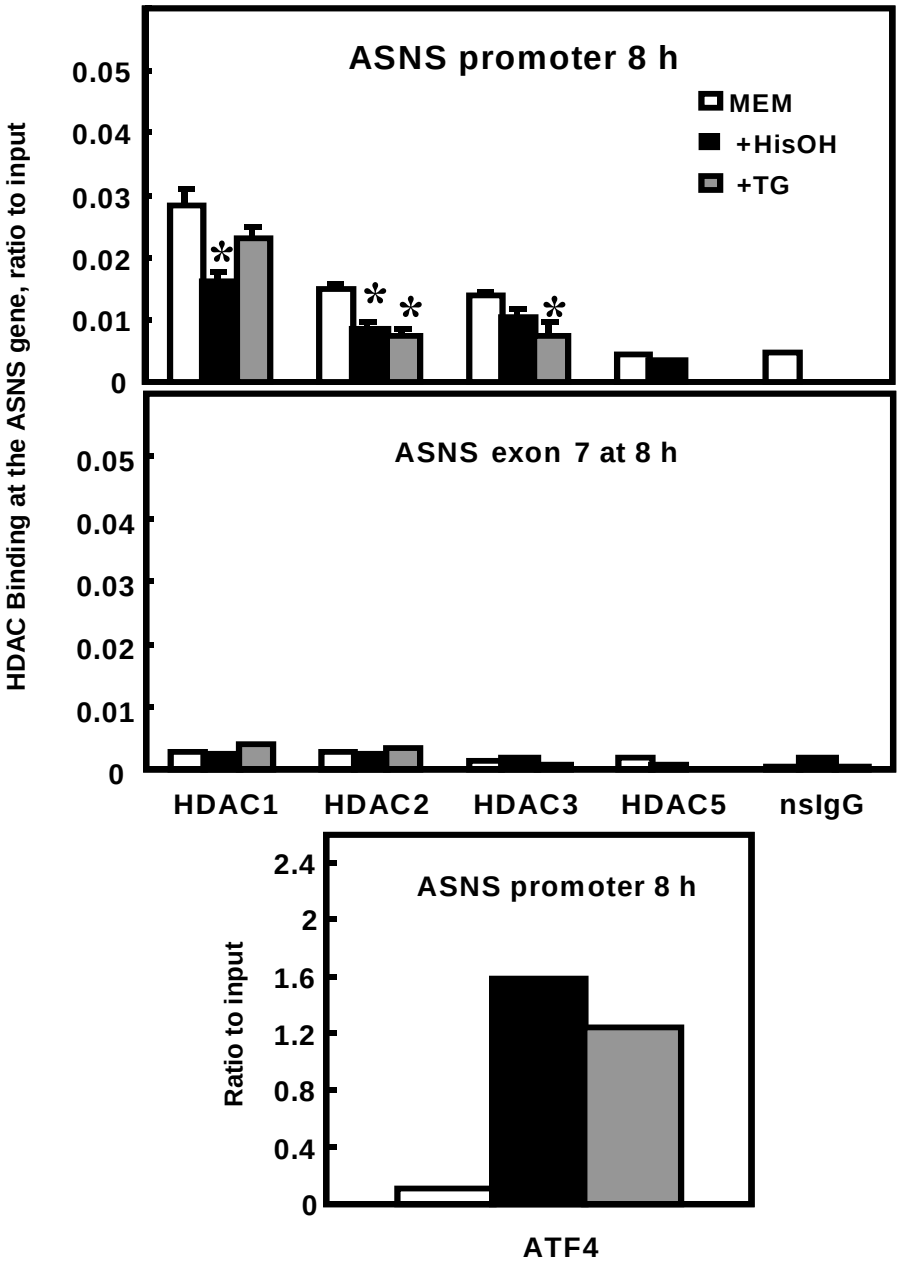

Figure 4-5. Occupancy of the *ASNS* promoter by HDACs. ChIP analysis was performed on HepG2 cells treated with either HisOH or TG for 8 h. Specific antibodies against HDACs 1, 2, 3, 5 and ATF4 were used in the IP step. A non specific IgG (ns/IgG) antibody was used to establish the background values for the antibodies. Primers that amplified ASNS promoter were used during the final qPCR. The reactions were run in dublicate and the data for HDAC1, 2 and 3 were collected from at least three different experiments whereas those for ATF4 and HDAC5 represent the mean of values from two independent experiments. An asterisk denotes statistical significance $p<0.05$.

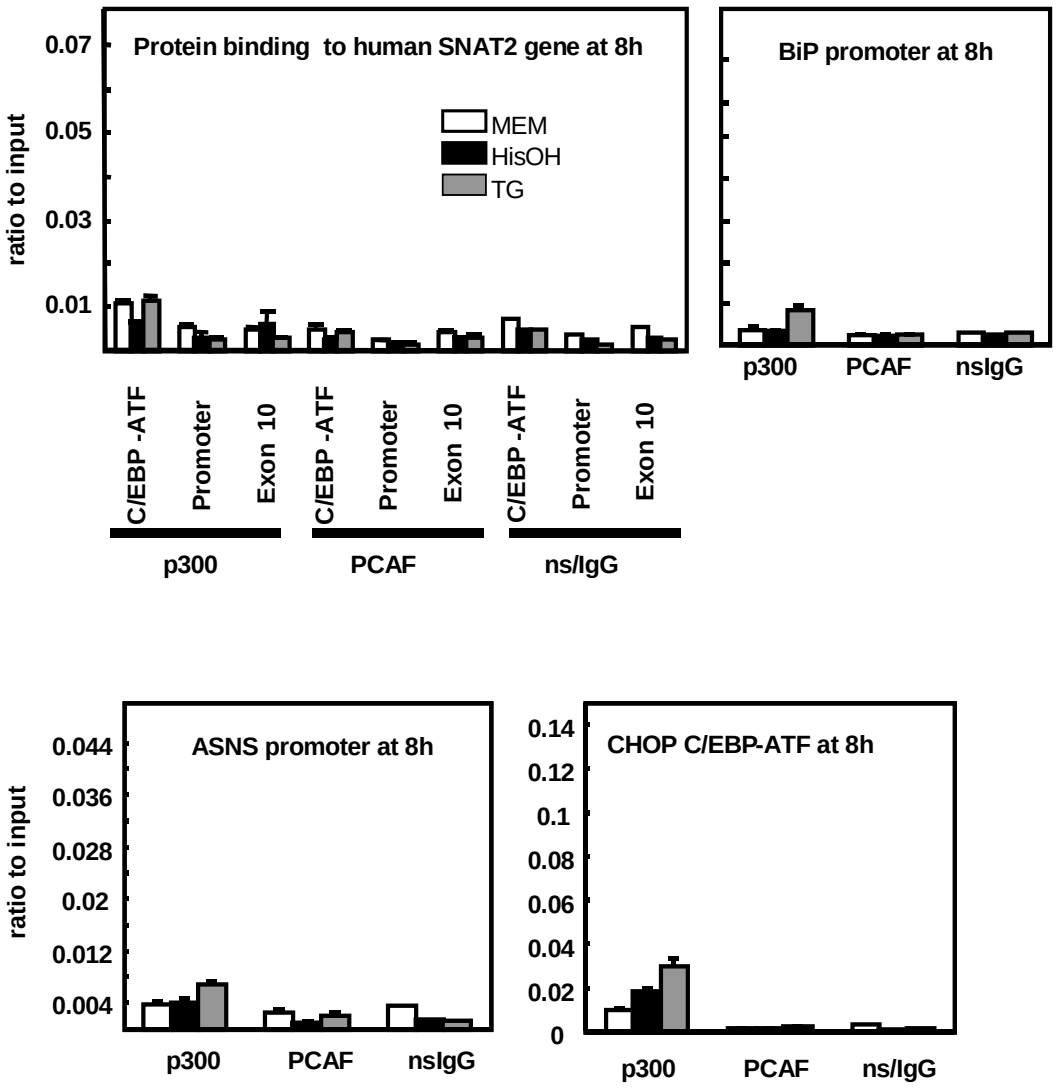

Figure 4-6. Coactivator recruitment at the *SNAT2, BiP, ASNS* and *CHOP* genes. Cells treated with HisOH to activate the AAR or TG to trigger the UPR were used to perform ChIP assays with antibodies against p300, PCAF and a nonspecific IgG (ns/IgG). Primers that amplified human SNAT2 (C/EBP-ATF, promoter, exon10), BiP promoter, ASNS promoter or CHOP C/EBP-ATF were used in the ChIP assays. The qPCR reactions were run in duplicate and the data were collected from at least three independent experiments.

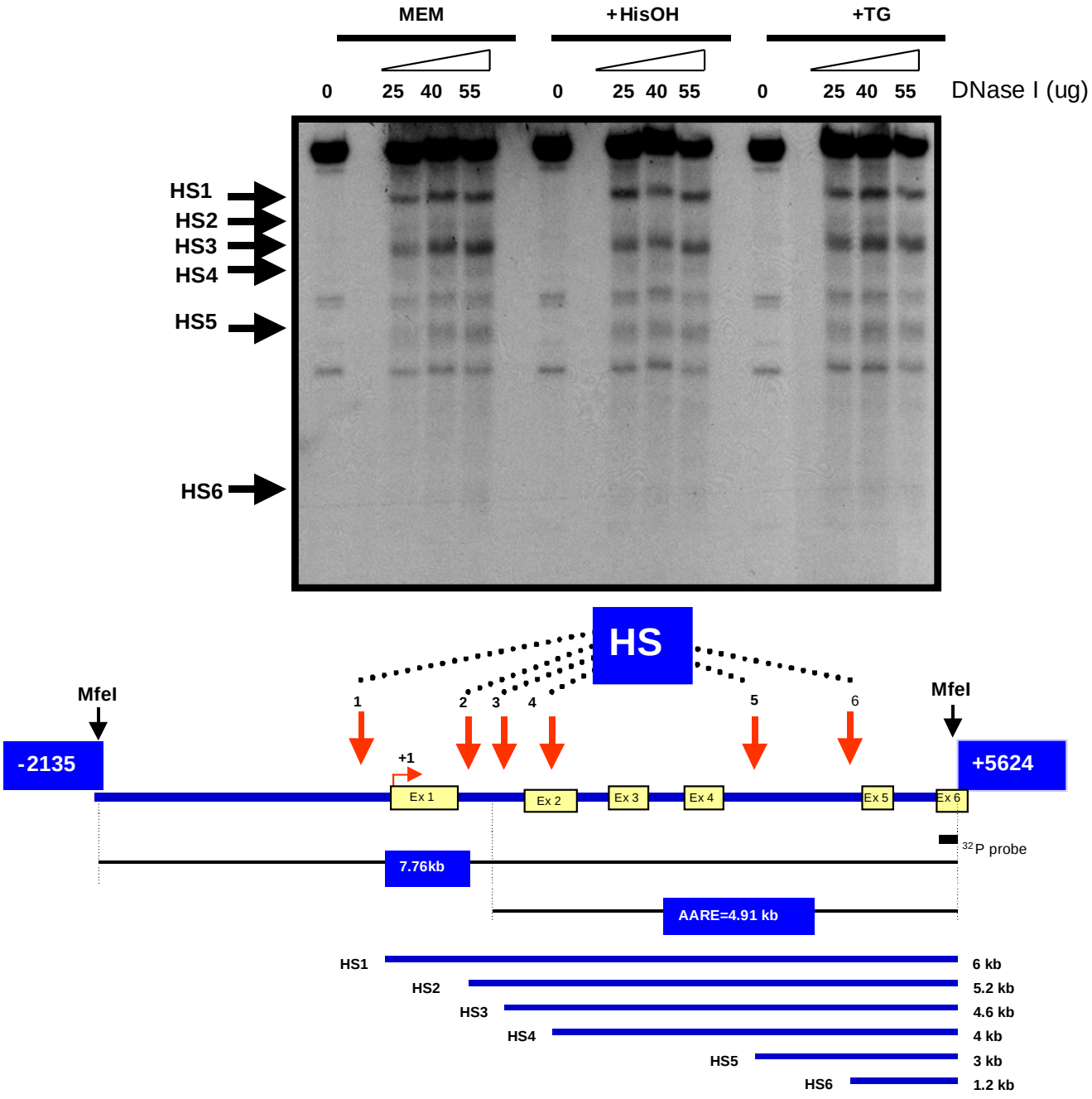

Figure 4-7. Treatment with DNase I and indirect end-labelling. HepG2 cells were incubated for 8 h in MEM, MEM+HisOH or MEM+TG after which were DNase I treated at the concentrations indicated. After DNAse I and *Mfe*I digestion, 15 mg of DNA were loaded in each lane. The detailed protocol is available in the materials and methods section. The diagram at the bottom indicates the position of the radiolabeled probe, the cutting positions of the *Mfe*I restriction enzyme, the length of the parental band (7.76kb) and of other fragments assigned as hypersensitive sites 1-6 . The positions of hypersensitive sites are indicated by black arrows at the margin of the blot and red arrows in the diagram. The blot shown is representative of multiple experiments.

CHAPTER 5
TRANSCRIPTIONAL INDUCTION OF THE HUMAN ASPARAGINE SYNTHETASE GENE DURING THE UNFOLDED PROTEIN RESPONSE DOES NOT REQUIRE THE ATF6 AND IRE1/XBP1 ARMS OF THE PATHWAY

Introduction

Endoplasmic reticulum (ER) stress represents an imbalance between ER protein load and ER processing capacity (67). Cellular stresses that lead to perturbation in calcium homeostasis, abnormal protein glycosylation, glucose deprivation, or expression of mutant membrane and secretory proteins lead to the accumulation of unfolded proteins in the ER lumen (66). As a consequence, three signal transduction cascades are triggered that are collectively referred to as the unfolded protein response (UPR). These signaling pathways include both translational and transcriptional control mechanisms that reduce protein synthesis, increase the ER folding capacity by up-regulating the transcription of chaperones, activate ER-associated protein degradation (ERAD), and ultimately, provoke cell death (64,69,148). Upon accumulation of malfolded proteins, the ER lumenal chaperone immunoglobulin heavy chain binding protein (BiP), also known as glucose-regulated protein 78 (GRP78), dissociates from the lumenal domains of three ER resident trans-membrane sensors and binds to the unfolded proteins. The ER-stress sensors, inositol-requiring kinase 1 (IRE1), double-stranded RNA-activated protein kinase (PKR)-like endoplasmic reticulum kinase (PERK), and activating transcription factor 6 (ATF6) are all activated after dissociation from BiP/GRP78 through either dimerization and *trans*-autophosphorylation (IRE1 and PERK) or translocation to the Golgi complex followed by proteolysis to a functional form (ATF6) (67). Active IRE1 is an endonuclease that contributes to the splicing of the XBP1 precursor mRNA, which then permits synthesis of XBP1 protein (149). IRE1/XBP-1 and ATF6 mediate transcriptional regulation of chaperones that assist folding in the ER as well as protein degradation mechanisms (86), metabolism (150), and apoptosis (140,141).

XBP1 or ATF6 bind to genomic elements, called ER stress response elements, (ERSE-I, CCAAT-N_9-CCACG or ERSE-II, ATTGG-N_1-CCACG) in the presence of a constitutively bound nuclear factor Y (NF-Y), which is a CCAAT/binding factor (74,134). XBP1 also binds to another UPR-mediating genomic element called the mammalian UPRE (mUPRE, TGACGTGG/A) (151).

Translational control during UPR activation is exercised through the PERK/eIF2α/ATF4 branch. ER stress activates PERK, an eukaryotic initiation factor 2α (eIF2α) kinase that phosphorylates eIF2α at serine 51 (68). An increase of p-eIF2α leads to a transient suppression of general translation, but increased translation of the mRNA for the transcription factor ATF4 as a consequence of a ribosome scanning mechanism and two short upstream opening reading frames in the ATF4 mRNA (57,121). Repression of general translation by p-eIF2α alleviates the protein load of the ER, while the increased translation of ATF4 leads to transcriptional induction of ATF4-responsive genes involved in the ER stress response (70,124).

In contrast to ER stress, the cellular stress of protein limitation or amino acid limitation leads to the activation of a signaling cascade called the Amino Acid Response (AAR) pathway. A limiting amount of an amino acid that is essential for that particular cell type leads to the accumulation of uncharged tRNA that binds to and activates a ribosome-associated protein called general control non-derepressible 2 (GCN2) (54). GCN2 is a eIF2α kinase that phosphorylates serine 51 (43,152). As described above for PERK, phosphorylation of eIF2α at serine 51 leads to increased ATF4 synthesis and downstream transcriptional activation. Among the many ATF4 target genes is asparagine synthetase (*ASNS*), for which transcription is increased in response to activation of both the UPR and AAR pathways. Mutagenesis and transient transfection of the *ASNS* promoter region has suggested that the two *cis*-acting elements, Nutrient Sensing

Response Elements-1, 2 (NSRE-1, NSRE-2) mediate the transcriptional induction by both AAR and UPR pathway activation (112). NSRE-1 and NSRE-2 function together as an enhancer element, and are referred to as the nutrient sensing response unit (NSRU) (113). The NSRE-1 sequence 5'-TGATGAAAC-3' is a C/EBP-ATF composite site(113,153), and these sequences have been shown to bind heterodimers of the C/EBP and ATF bZIP subfamilies, including C/EBPβ and ATF4 (59,154,155). Electrophoresis mobility shift analysis documented that ATF4 binds to the *ASNS* NSRE-1 site *in vitro* (59). However, those previous studies did not document ATF4 binding to the NSRE-1 site *in vivo*, nor were the ATF6 and XBP1 arms of the UPR tested for their potential role in *ASNS* regulation. The question of whether the IRE1/XBP1 and ATF6 arms of the UPR impact *ASNS* transcription is an important one because the ATF half-site sequence of the C/EBP-ATF site (TGATG) has similarity to the 5′ portion of the mUPRE (TGACG).

This study characterizes the transcriptional control of the *ASNS* gene during UPR activation in human HepG2 hepatoma cells (156). Extensive ChIP analysis of the C/EBP-ATF site in the *ASNS* proximal promoter during UPR activation revealed the time-dependent binding of the transcription factors ATF4, ATF3, and C/EBPβ providing further evidence that the NSRU genomic element mediates the transcriptional response during both the AAR and UPR. Data obtained from the concomitant activation of the AAR and UPR indicated that these two pathways share a common step in the regulation of the *ASNS* gene. The siRNA-mediated knock-down of XBP1, ATF6α, and ATF6β expression documented that these UPR arms do not have a critical contribution to the *ASNS* induction following ER stress. Collectively, the results demonstrate that the PERK-mediated arm of the UPR is the sole signaling cascade responsible

for *ASNS* transcriptional induction and that, along with the ERSE and mUPRE sequences, the NSRU is an ER stress responsive genomic element.

Results

ASNS Transcriptional Activity and Steady State mRNA Levels Are Up-Regulated during ER Stress

The response of the *ASNS* gene during UPR activation was investigated by analyzing the transcription activity and steady state mRNA levels after treatment of HepG2 cells with the ER calcium ATPase blocker thapsigargin (Tg) or the N-glycosylation inhibitor tunicamycin (Tu) (Fig. 5-1), both known and widely used UPR activators (64). *ASNS* transcription activity during Tg treatment of HepG2 cells was analyzed by specific primers that amplify the *ASNS* intron 12 – exon 13 junction to measure the short-lived hnRNA levels (45). The results revealed an increase in *ASNS* transcription activity starting within 1 h, peaking between 2 to 4 h, and then declining slightly at 8 h and 12 h (Fig. 5-1). Consistent with the transcription activity, steady state ASNS mRNA levels lagged behind reaching a plateau at 8-12 h. Similar results were obtained using Tu to initiate ER stress, although the time course was slightly delayed relative to Tg, presumably because of the difference in the mechanisms by which they trigger ER stress.

Transcription Factor Recruitment to the *ASNS* Promoter during the UPR

During amino acid limitation, *ASNS* transcription is controlled by ATF4, ATF3 and C/EBPβ by a self-regulating mechanism involving an initial period of activation by ATF4 and subsequently, suppression of transcription by ATF3 and C/EBPβ (45). Whether these same transcription factors mediate the *ASNS* transcription control during ER stress has not yet been established. Given that transcriptional activation of UPR target genes is mediated by three signaling cascades PERK/eIF2α/ATF4, ATF6, and IRE1/XBP1, investigating which of them contributes to the control of the *ASNS* gene represents an important question. ChIP analysis of

the *ASNS* promoter, shown in Fig. 5-2, revealed a time course of binding for RNA Pol II and ATF4 that paralleled the *ASNS* transcription activity (Fig. 5-1 and dashed line in top panel of Fig. 5-2). Upon UPR activation by Tg, RNA Pol II binding increased within 1 h, peaked at about 2 h, and then declined but remained elevated even at 12 h. The binding of ATF4 also occurred within 1 h of Tg treatment, peaked between 2 and 4 h, and slowly decreased at later time points (Fig. 5-2). Following amino acid deprivation, ATF4 induction of C/EBPβ and ATF3 expression leads to a feedback mechanism by which these two factors are subsequently recruited to the NSRU and suppress the ATF4-enhanced *ASNS* transcription (45). To determine if a similar mechanism was operational during the UPR, ChIP analysis of C/EBPβ and ATF3 was performed after Tg treatment (Fig. 5-2). Delayed relative to the RNA Pol II and ATF4 binding, increased C/EBPβ binding began at 4 h and steadily increased at 8 h and 12 h. Likewise, relatively little ATF3 binding occurred at the early time points of 1-4 h, but increased recruitment was observed at 8 h and 12 h, at a time when the transcription activity was declining (Fig. 5-1).

The preinitiation complex is comprised of general transcription factors (GTFs) that are responsible for the recruitment and correct positioning of RNA Pol II to the promoter (157). Assembly of the PIC at the *ASNS* promoter during ER stress was investigated by ChIP analysis of representative GTFs in Tg-treated HepG2 cells (Fig. 5-3). The data at 1 h showed enhanced recruitment for each of the factors tested, RNA Pol II, TBP, TFIIB and TFIIE, and the abundance was even greater at 8 h, consistent with the increased transcription activity (Fig. 5-1). The background binding for the TBP, TFIIB, and TFIIE was established by measuring association of these factors with the coding region (exon 7) of the ASNS gene (Fig. 5-3).

UPR Activation Does Not Trigger Increased Recruitment of Mediator Subunits to the *ASNS* Promoter

Mediator is large protein complex that has been proposed to be necessary for most, if not all, Pol II-mediated transcription (158,159). However, several studies have shown that in *Saccharomyces cerevisiae* (160,161) and *Schizosaccharomyces pombe* (162) Mediator recruitment does not always correlate with transcription activity or the recruitment of the GTF complex. Fan et al. (160) have suggested that Mediator might be selectively associated with genes that are activated by environmental stress or sub-optimal growth conditions. Given that the ChIP data indicated an increase in recruitment of GTFs to the *ASNS* promoter region following UPR activation, the question of Mediator recruitment was also addressed. The RNA Pol II data (Fig. 5-4, Panel A) are shown to demonstrate additional recruitment of the pre-initiation complex to the *ASNS* promoter during ER stress. *ASNS* (Fig.5-1, left hand panels) and *BiP/GRP78* (Fig. 5-4, Panel C) transcription activity is presented to demonstrate increased transcription from the promoters of these genes following UPR activation. The ChIP results shown in Fig. 5-4, indicated that despite the fact that some of the basal values obtained were above the background established by the non-specific IgG antibody, during ER stress there is no enhanced recruitment of the MED1, MED23, and CDK8 Mediator subunits to the *ASNS* promoter at 1 h or 8 h (Fig. 5-4, Panel B). In contrast to the *ASNS* promoter, ChIP analysis of the *BiP/GRP78* promoter revealed a trend toward a greater degree of Mediator association after ER stress, occurring at 1 h for MED1 and CdK8, and at 8 h for all three subunits tested (Fig. 5-4, Panel D). However, only the MED1 values at 8 h reached statistical significance.

Concurrent Activation of the AAR and UPR Pathways Does Not Have an Additive Effect on Induction of *ASNS*

To measure the efficacy of ER stress on ATF4 protein abundance in HepG2 cells, immunoblot analysis was performed after Tg treatment (Fig. 5-5). Consistent with its prompt translational

control and the relatively rapid binding to the *ASNS* promoter (Fig. 5-2), increased ATF4 protein levels were observed within 2 h (Fig. 5-5). ATF4 expression levels further increased at 4 h and 8 h and remained relatively high during the later time points (Fig.5-5).

. In contrast, ASNS protein content showed little or no change up to 4 h after which it increased (Fig. 5-5). This pattern of ASNS protein expression is consistent with the UPR model, which proposes an initial transient period of translational inhibition to lower the ER load, followed by a recovery phase characterized by an increase in protein synthesis to allow for expression of the UPR target proteins (163).

The AAR pathway and the PERK-mediated arm of the UPR both lead to an increase in ATF4 translation, whereas the XBP1 and ATF6 arms of the UPR activate transcription independent of ATF4 action (64). To determine if either of the latter two UPR arms influences *ASNS* protein expression, the simultaneous activation of the AAR and UPR pathways in HepG2 cells was investigated. The concurrent AAR and UPR activation in HepG2 cells revealed an increase in both ATF4 and ASNS protein abundance that was similar to that after induction of either pathway alone (Fig.5-5). This observation provides initial, but not conclusive evidence for the interpretation that the IRE1/XBP1 and ATF6 branches of the UPR do not participate in the induction of *ASNS* transcription. Furthermore, the lack of an additive effect by these two pathways is consistent with the known convergence of the UPR PERK arm and the AAR at the common step of eIF2α phosphorylation and subsequent increased ATF4 translation.

Short Interference RNAs against UPR Effectors XBP1, ATF6α, and ATF6β Have Minimal Effect on *ASNS* Transcription

To further explore whether or not the IRE1/XBP1 and ATF6 branches of the UPR participate in the induction of the *ASNS* gene by ER stress, an siRNA strategy was used to knockdown expression of XBP1, ATF6α, and ATF6β (Fig.5-6). Despite significant reductions

of XBP1, ATF6α, or ATF6β expression (Fig.5-6C), there was no significant effect on the induction by ER stress of either *ASNS* steady state mRNA (Fig.5-6A) or *ASNS* transcription activity (Fig.5-6B). As an aside, it is noteworthy that ER stress of the HepG2 cells induced the ATF6α mRNA levels, whereas it did not affect those for XBP1 and ATF6β.

Conclusions

Although previously published work had established that steady state ASNS mRNA content is induced by ER stress (164), the transcription activity of the endogenous gene, the individual factors responsible, and the possible role of the IRE1/XBP1 and ATF6 arms of the UPR had not been investigated fully. Given that all three arms of the UPR are activated in a coordinated manner and contribute to the overall transcriptional response to ER stress, firmly establishing which signaling cascade or combination of them regulates the induction of *ASNS* was necessary. The present study demonstrates that the PERK/p-eIF2α/ATF4 signaling cascade is the only arm of the UPR that is responsible for *ASNS* transcriptional induction during ER stress of HepG2 human hepatoma cells. Indeed, neither the IRE1/XBP1 nor the ATF6 arms of the UPR appear to influence regulation of the *ASNS* gene. This interpretation is based on two independent approaches. First, activation of both the AAR and UPR pathways simultaneously was not additive with regard to *ASNS* induction. Second, knockdown of the IRE1/XBP1 and ATF6 arms of the UPR pathway did not suppress induction of *ASNS* transcription activity or steady state mRNA. The latter result also indicates that the IRE1/XBP1 and ATF6 arms do not substantially alter *ASNS* mRNA stability either. The present data, obtained by siRNA treatment of human cells, agree with the observation that *ASNS* induction is intact in ATF6 and IRE1 knockout mouse embryonic fibroblasts (165,166). Furthermore, *in vivo* ChIP analysis revealed that the same three transcription factors, ATF4, C/EBPβ, and ATF3, that have been identified as

members of C/EBP-ATF enhanceosome during the ATF4-dependent AAR, are also associated with the *ASNS* NSRU during UPR activation.

Results show that after ER stress there is a parallel time course of increased ATF4 protein abundance and ATF4 binding to the *ASNS* promoter. ChIP assays show RNA Pol II recruitment, which paralleled the increased transcription activity and ATF4 binding, consistent with the role of ATF4 as a potent activator of *ASNS* transcription. In contrast, an increase in C/EBPβ and ATF3 binding was observed at later time points when the *ASNS* transcription activity was declining. Therefore the NSRU enhancer binding proteins involved and the time course of their recruitment to the ASNS promoter region during ER stress is similar to that of *ASNS* transcription regulation during amino acid limitation (45). These observations are consistent with the conclusion that the induction of *ASNS* by the UPR is purely ATF4 driven and does not involve the IRE1/XBP1 or ATF6 arms.

The transcriptional response for most of the ER stress target genes studied to date was shown to be mediated by ER stress responsive elements I or II (ERSE-I or ERSE-II) or the mammalian unfolded response element (mUPRE) (149), shown in Fig.5-7. For example, genes such as *BiP* and *CHOP* contain an ERSE-I, whereas the *Herp* gene contains both an ERSE I and an ERSE-II [39]. The mUPRE is composed of a single contiguous sequence (5´-TGACGTGG/A-3´) that binds XBP1 and is present in genes such as *EDEM* (167), *HRD1* (167), and *C/EBPβ* (168). In contrast, the NSRU within the *ASNS* promoter is composed of two sequences (NSRE-1 and NSRE-2) that are separated by a spacer of 11 nucleotides (Fig.5-7). Single nucleotide mutagenesis of the *ASNS* promoter demonstrated that both components of the NSRU are required to mediate the transcriptional response to either amino acid limitation or ER stress (112). This requirement makes the *ASNS* gene unique thus far, in that no other gene has

been discovered that responds to these two stress pathways through the same genomic elements. In contrast to the *ASNS* gene that requires both NSRE-1 and NSRE-2, the *Cat-1* cationic amino acid transporter gene is induced by amino acid limitation through a sequence identical to NSRE-1 without the presence of an NSRE-2 like sequence (169). Consistent with this lack of an NSRE-2 element, the *Cat-1* NSRE-1 site does not mediate this gene's response to the UPR (169). Like all other known amino acid response elements (AARE), the *ASNS* NSRE-1 (5′-TGATGAAAC-3′) is a C/EBP-ATF composite site. C/EBP-ATF composite sites are sequences that bind heterodimers of ATF and C/EBP bZIP transcription factors (59,154,155). The binding proteins for NSRE-2 (5′-GTTACA-3′) have yet to be determined. Interestingly, although NSRE-2 does not have the ability to mediate the ER stress signal when NSRE-1 is deleted or mutated in the *ASNS* promoter (112), the NSRE-2 sequence can confer ER stress responsiveness to an otherwise unresponsive AARE (170). The *CHOP* gene is induced by both amino acid limitation and ER stress, but the *CHOP* promoter contains both a C/EBP-ATF composite site that acts as an AARE (nt –301 to –310) and a separate ERSE-I (nt –93 to –75) the mediates the UPR (74,139). Ma et al. (140) have presented evidence that the CHOP C/EBP-ATF site and the ERSE are both required for maximal induction during the UPR. Conversely, Jousse et al. (139)showed that a promoter deletion construct retaining the ERSE-I, but lacking the C/EBP-ATF site, exhibited a complete loss of the amino acid response and no reduction of UPR activation. Thus, in this circumstance, the C/EBP-ATF sequence appears to function primarily as an AARE. However, when the *ASNS* NSRE-2 sequence was placed downstream of the *CHOP* C/EBP-ATF sequence, the *CHOP* promoter gained UPR sensitivity (170).

Collectively, the present observations extend our knowledge of genomic targets of the UPR and demonstrate that the *ASNS* NSRU genomic element is unique in that, independent of

the well-known UPR-associated sequences of ERSE-I, ERSE-II, and mUPRE, the NSRU is capable of mediating the transcriptional response to ER stress.

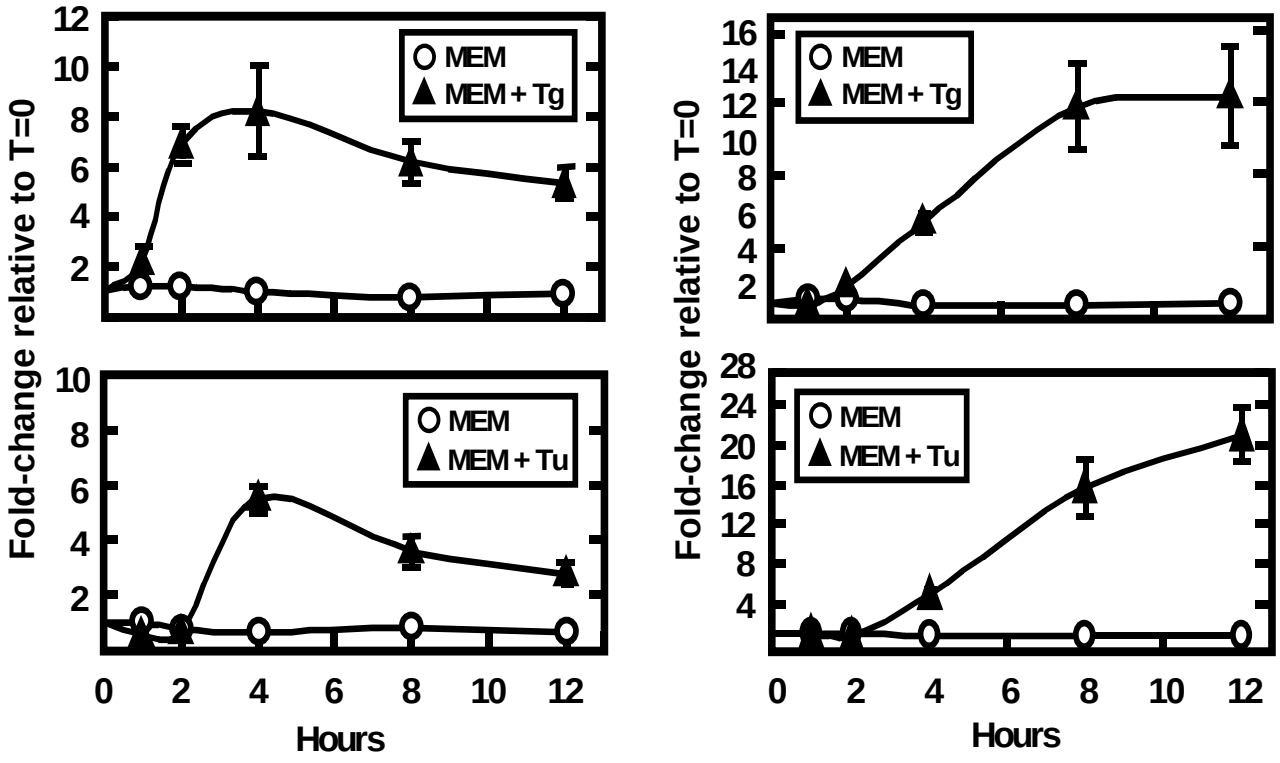

Figure 5-1. Asparagine synthetase transcription activity and steady state mRNA are induced during Tg- or Tu- triggered ER stress. Cultured HepG2 cells, treated for 0-12 h with 300 nM Tg (upper panels) or 5 μg/ml Tu (lower panels), were used to collect total RNA. Specific primers that amplify across the intron 12 - exon 13 junction of the *ASNS* gene were used to measure the hnRNA (ASNS transcription activity) (left panels), whereas primers that amplify a segment of *ASNS* exon 7 were used to assay the steady state mRNA levels (right panels). The data were collected from three independent experiments, the qRT-PCR for each sample was done in duplicate, and the values shown represent the means ± S.E.M. and are plotted as the fold-change relative to T=0.

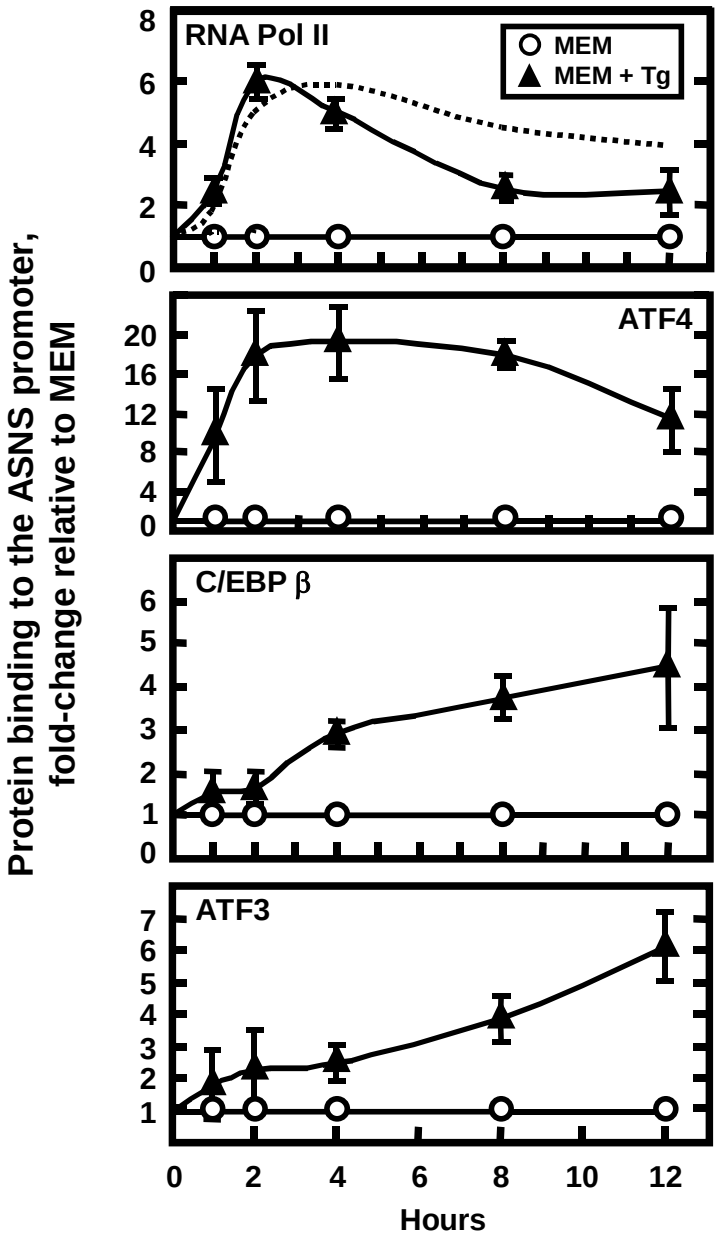

Figure 5-2. Profile of transcription factor binding at the *ASNS* proximal promoter during UPR activation. ChIP analysis was performed on HepG2 cells treated for 0-12 h with Tg to induce ER stress. Antibodies against RNA Pol II, ATF4, ATF3, and C/EBPβ were used for the immunoprecipitation step and primers specific for the *ASNS* promoter region were used for qPCR amplification. Each PCR reaction was run in duplicate and the data were obtained from at least three independent experiments. The data are shown as fold-change relative to the MEM control and represent the mean ± S.E.M. The dashed line in the top panel represents the *ASNS* transcription activity for the Tg-treated cells in Figure 1.

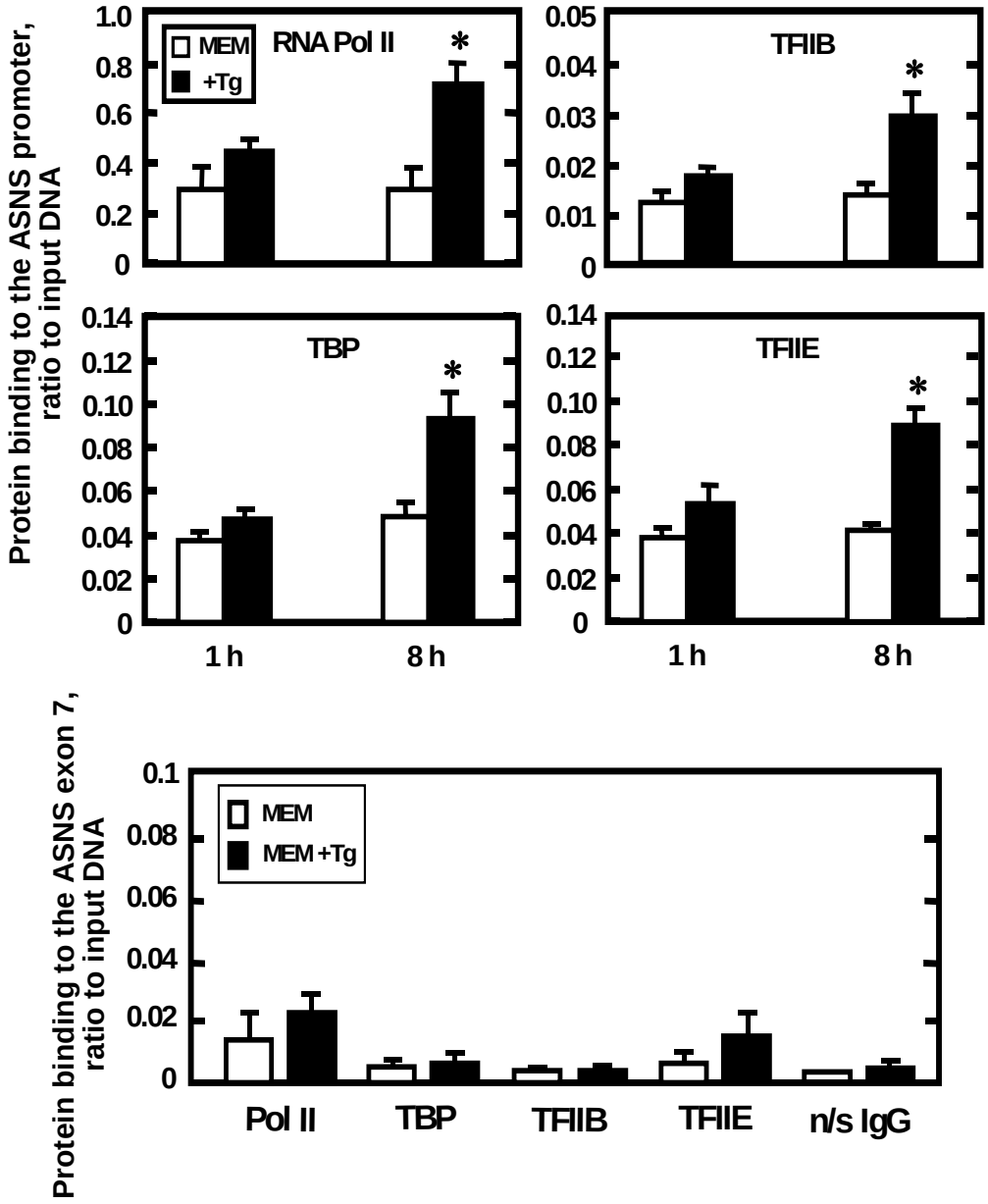

Figure 5-3. Asparagine synthetase promoter occupancy by general transcription factors is increased during ER stress. HepG2 cells treated for 1 h and 8 h with Tg were analyzed by ChIP for binding of RNA Pol II, TBP (TFIID), TFIIB and TFIIE at the *ASNS* promoter. As a negative control, the same 8 h samples were used to amplify a downstream region of the *ASNS* gene (exon 7) to illustrate the background binding. The qPCR reactions for each experiment were performed in duplicate and the data shown, as the ratio to DNA input, were collected from three independent experiments. The values represent the mean ± S.E.M. and the asterisk indicates that the differences are statistically significant to $p < 0.05$.

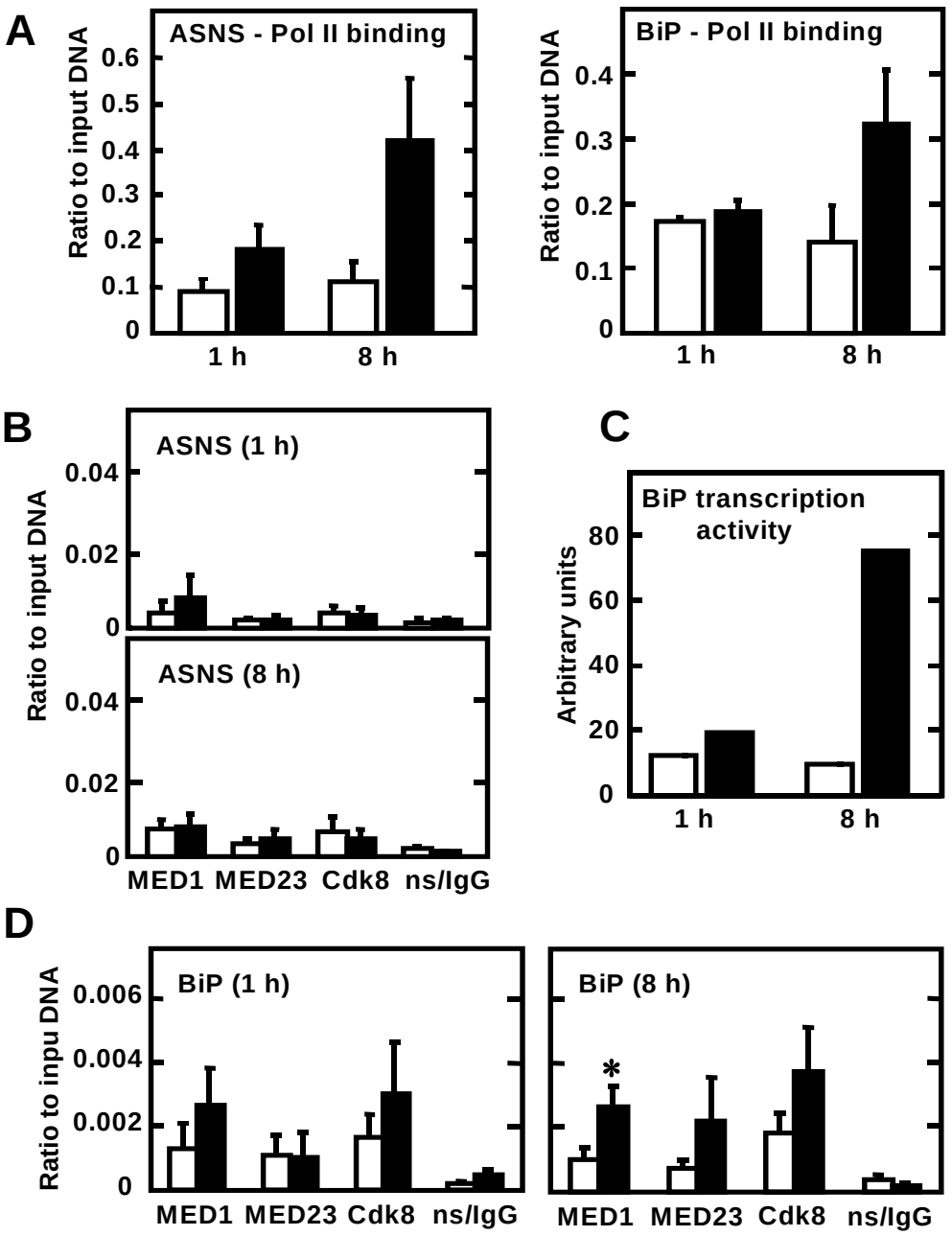

Figure 5-4. Asparagine synthetase transcriptional induction during ER stress does not involve enhanced recruitment of mediator subunits. HepG2 cells incubated in MEM only (white bars) or MEM + Tg (black bars) for 1 h and 8 h were used to perform ChIP analysis using antibodies specific for RNA Pol II (Panel A), the MED1, MED23, or CdK8 Mediator subunits (Panels B and D), or a non-specific rabbit IgG (ns/IgG), as indicated. During the final qRT-PCR step, primers specific for the *ASNS* promoter region or *BiP/ GRP78* were used (Panels A, B, D). The transcriptional activity of *BiP/GRP78* (Panel C) was measured using primers that span the exon 2 - intron 2 junction. The qRT-PCR reactions were performed in duplicate for each sample. The ChIP data were collected from at least three independent experiments and the values represent the mean ± S.E.M. An asterisk indicates statistical significance ($p < 0.05$).

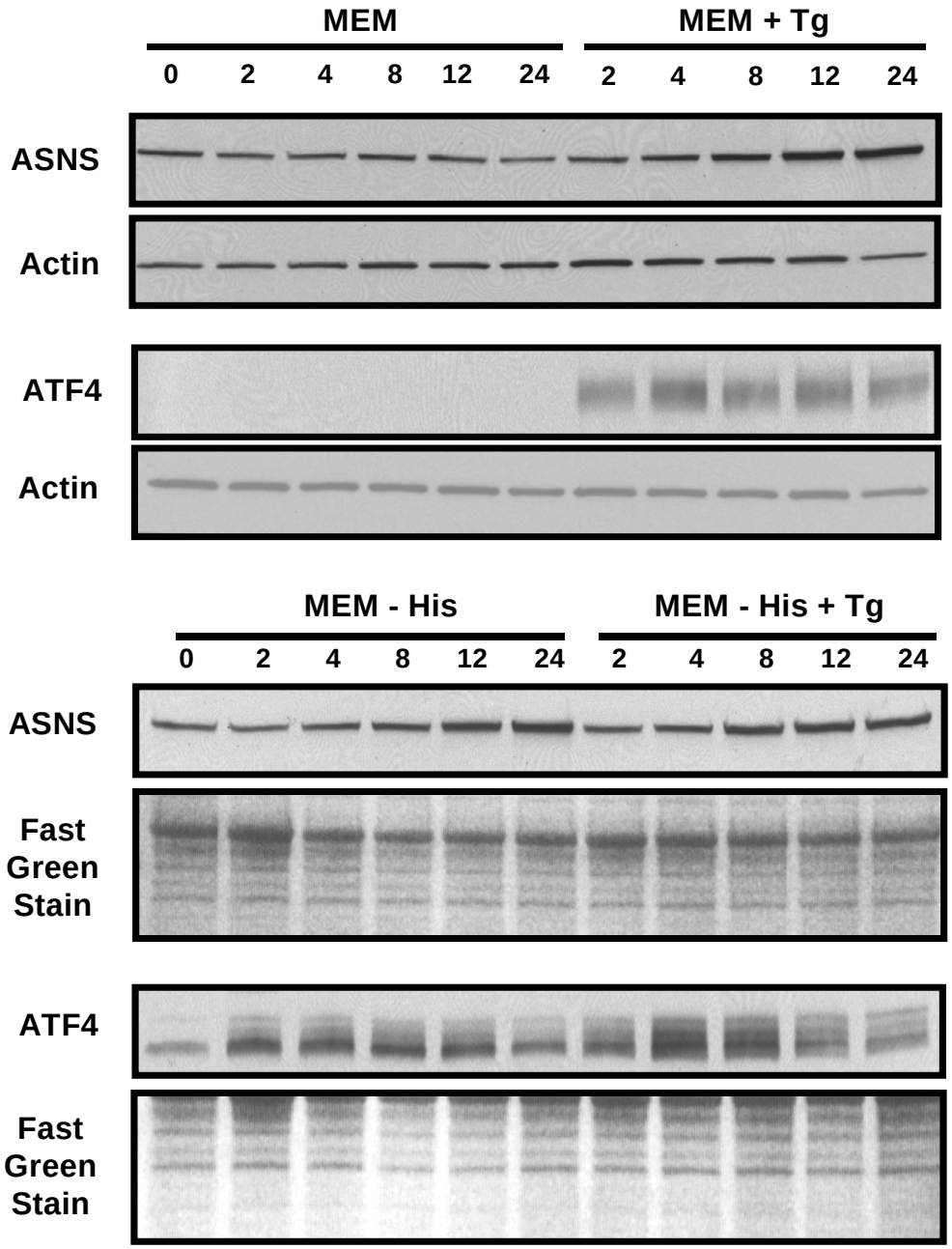

Figure 5-5. Induction of *ASNS* expression is not further enhanced by simultaneous activation of the AAR and UPR pathways. Whole cell lysates were prepared for ASNS and ATF4 immunoblot analysis from HepG2 cells treated for 0-24 h with either Tg, medium lacking amino acid histidine (MEM-His), or the simultaneous treatment with MEM–His and Tg. As measure of equal protein loading, the blots were stained with Fast Green or probed with an actin antibody. Antibodies against ATF4 and ASNS protein were used as described in the Materials and Methods. Each blot shown is representative of multiple experiments.

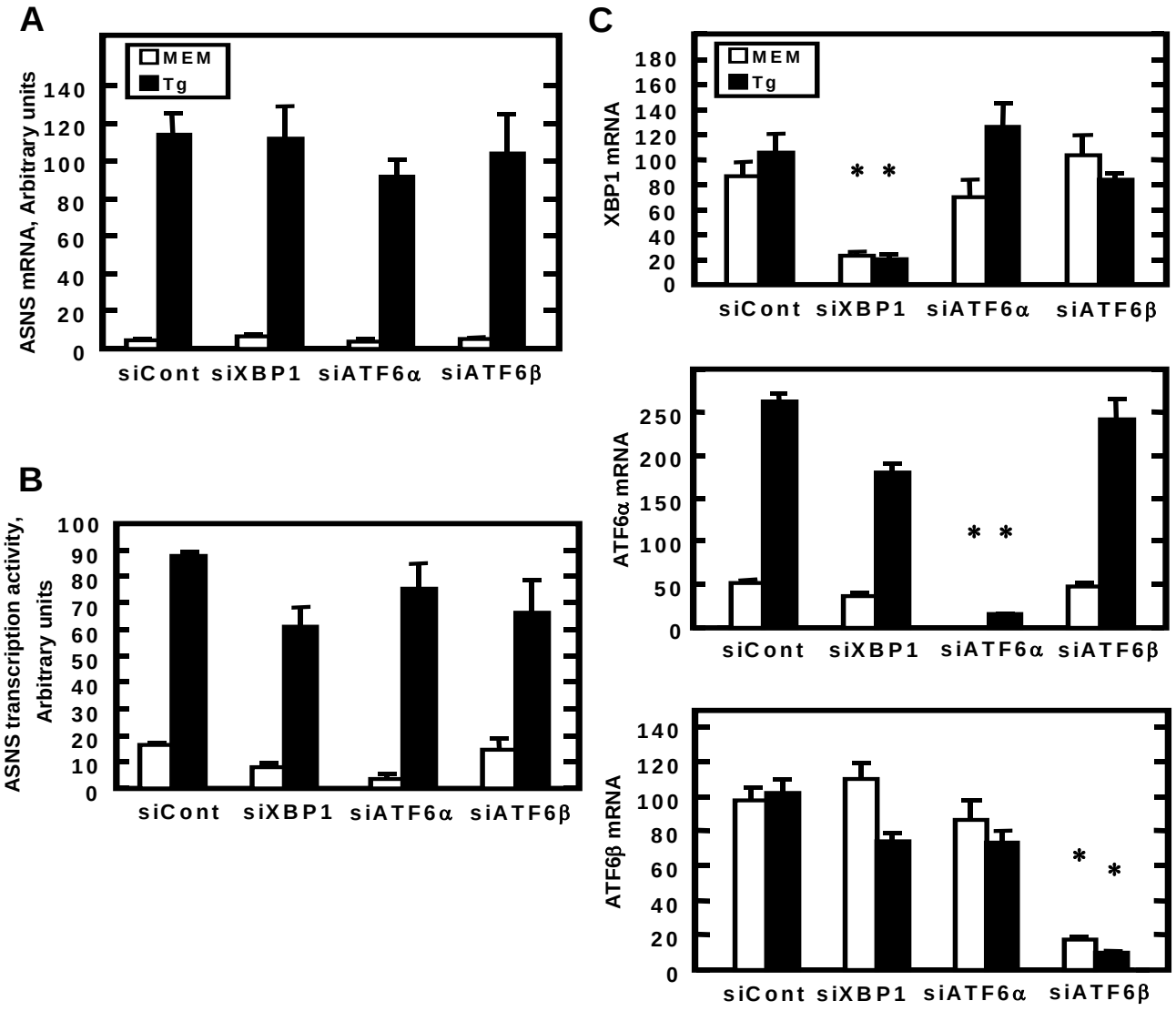

Figure 5-6. Knockdown of XBP1, ATF6α, or ATF6β expression by siRNA does not affect induction of *ASNS* transcription during ER stress. Short interference RNA (siRNA) transfections with a non-targeting siRNA (siCont) or against XBP1, ATF6α, or ATF6β were performed in HepG2 cells. After incubation in complete MEM, the cells were incubated in MEM control or MEM+Tg medium for 8 h to induce ER stress. Total RNA was isolated and ASNS steady state mRNA content (A), *ASNS* transcription activity (B), or XBP1, ATF6α, and ATF6β mRNA (C) were assayed. The qRT-PCR reactions were performed in duplicate for each sample and samples were collected from three independent experiments. Values are expressed as means ± S.E.M. and the asterisks denote a statistically significant difference ($p < 0.05$) relative to the respective siControl value.

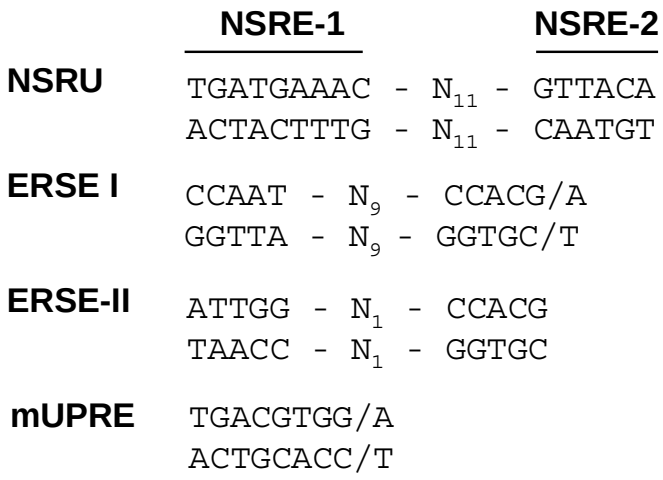

Figure 5-7. Comparison of the NSRU, ERSE-I, ERSE-II, and mUPRE sequences.

CHAPTER 6
GENERAL CONCLUSIONS AND FUTURE DIRECTIONS

Conclusions

Transcriptional control of gene expression has been shown to be an important modality of regulation for many genes. As mentioned in this study, the Kilberg laboratory has contributed substantially in documenting it for SNAT2, ASNS, C/EBPβ, ATF4 and ATF3 genes. Eukaryotic cells respond to amino acid deprivation or ER-stress by triggering signal transduction cascades. These pathways will upregulate transcription (SNAT2, ASNS, C/EBPβ) and/or translation (ATF4) of specific genes to adapt to the stress condition the cell is experiencing and eventually to redress the situation. Ultimately, if the cell's protective mechanisms are overcome, apoptosis is triggered. Induction of proapoptotic bZip transcription factor CHOP occurs during activation of programmed cell death. The CHOP gene is transcriptionally controlled by both amino acid starvation and endoplasmic reticulum stress. Most of the time the same pathways will be responsible for sending both survival and apoptotic signals. So, in order to elucidate timing of the events and to obtain a clearer picture of the phenomena that occur in the cell under stress conditions, it is required a better understanding of the molecular mechanisms involved, identification of unknown factors and discovery of new feedback or auto feedback mechanisms.

ER-stress is linked to the pathology of numerous diseases, such as: diabetes mellitus and insipidus, cardiovascular diseases, viral infection, cancer, cystic fibrosis, hemophilias A and B (clinically presented as blood coagulation deficiency), osteogenesis imperfecta (manifested by skeletal deformity), neurodegenerative diseases (Parkinson, Alzheimer) and bipolar disorder (a mood disorder). Immune response and aging processes implicate ER-stress as well.

Protein/aminoacid availability is critical in the early stages of development. Protein malnutrition during pregnancy causes intrauterine growth retardation (IUGR). It has been shown

that one component of the mechanism is changes in placental SNAT2 expression. Restricted protein diet is associated with an increase in the life expectancy. L-Asparaginase treatment of childhood Acute Lymphoblastic Leukemia (ALL) is used to deplete the whole body of asparagine. The therapeutic strategy is based on the observation that human leukemia cells in children have low expression levels of ASNS and consequently show high sensitivity to L-Asparaginase.

This study focused particularly on the differential transcriptional regulation of the SNAT2 gene by ER stress and amino acid limitation. The *SNAT2* transcription and transport activity are up-regulated during amino acid deprivation, hypertonic stress or hormonal stimulation (48,94,129). As shown in this work, UPR activation represses SNAT2 transcription activity. Considering the SNAT2 gene up-regulation in diabetes and cancer, identifying ways of selectively repressing the gene by the activation of the UPR could lead to potential therapeutic applications in the future. Identification of novel *cis*-acting regulatory elements, as DNase I hypersensitive sites, will contribute to the further characterization of the transcriptional control of the SNAT2 gene during different stress conditions.

The other important contribution of this study is the characterization of ASNS transcriptional control during UPR activation. Employing ChIP and siRNA strategies was demonstrated that PERK/eIF2α/ATF4 arm of the UPR pathway is the only one that contributes to ASNS induction in the presence of ER stress. The immediate implication of the findings is that the ASNS NSRU is a genomic element that in addition to ERSE I, II and mUPRE is perfectly capable of mediating transcriptional response to ER stress.

Given the ponderous role that UPR and AAR pathways play in causing or on the contrary, in alleviating the pathology related to disease, understanding of the underlined molecular

mechanisms becomes even more significant. Ultimately, the goal of this research project is to contribute with a comprehensive understanding of the fundamentals of gene regulation and inherently to improve the existing strategies and to discover new avenues in maintaining the healthy status of individuals or combating the disease when the latter occurs.

Future Directions

Identifying and exploring the function of coactivators or corepressors that are recruited to the SNAT2 gene during amino acid limitation or ER stress remains one of the most imminent future goals. A potential repressor/corepressor recruitment to the SNAT2 gene during UPR could explain the repression of the SNAT2 transcription. How do the C/EBP-ATF composite site and the ATF4-enhanceosome influence the PIC assembly and transcription activation from the promoter. Is a looping mechanism involved between the intronic enhancer and the promoter?

Another important possibility that would explain the differential transcriptional response of the SNAT2 gene to the activation of the AAR and UPR is a potential re-localization mechanism of the gene within the nucleus. The advantage of this hypothesis is that it represents a testable one. The association of the SNAT2 promoter with an actively transcribing transcription factory during AAR activation but not UPR activation would explain the distinct transcriptional response of the gene. Visualization of the repositioning inside the nucleus of the SNAT2 gene can be achieved by DNA-fluorescence in situ hybridization (FISH).

Investigation of chromatin changes during concurrent treatment with medium lacking histidine (–His) or containing HisOH to activate the AAR and TG to trigger the UPR in HepG2 cells will contribute to the elucidation of the nature of the repressive signal triggered during UPR. How is the acetylation or methylation of histones modified during concomitant activation of AAR and UPR? Crosstalk of the AAR and UPR with other pathways such as the MAPK

pathway have to be further explored as these links may hold the critical signaling molecules that are involved in stimulating SNAT2 transcription.

The ChIP data showed that levels of H3K4me3, a marker of transcription activation and an anchor of the TFIID complex, are decreased at the SNAT2 promoter during UPR activation. The role of the H3K4me3 modification and the possible recruitment of a H3K4me3 demethylase such as JARID1B (Plu-1) to the SNAT2 promoter during ER stress remains to be addressed by ChIP analysis.

Addressing the role of HDACs in the transcriptional activation of the ASNS and SNAT2 genes represents one of the important future directions. Clearly, the TSA treatment of HepG2 cells led to the inhibition of the AAR induced transcription of the SNAT2 gene. The ChIP analysis revealed that HDACs 1, 2, and 3 are constitutively bound to the ASNS promoter and SNAT2 gene (promoter and C/EBP-ATF site) and were depleted upon stress. How is the profile of histone acetylation for the SNAT2 or ASNS genes affected by the treatment with the HDAC inhibitor TSA? Does TSA prevent the recruitment of an HDAC that is required for SNAT2 activation during AAR? Experiments that include TSA treatment of cells followed by ChIP analysis will lead to the answers of these questions.

DNase I hypersensitivity assay revealed the existence of six hypersensitive (HS) sites. Functional characterization of the HS2, 4, 5 and 6 in HepG2 cells represents an important future objective. Site direct mutagenesis (cloning and transfecting the SNAT2 fragments, with these *cis*-elements that either contain or not mutations) followed by exposure of the cells to various stress conditions (amino acid limitation, ER stress, hormonal stimulation) will contribute to the identification of the function of these elements. Beside these experiments, exploring the role of HS2 as a potential boundary element between the SNAT2 enhancer and the promoter should

include the investigation of the binding of the insulator binding protein CTCF (CCCTC-binding factor) by ChIP analysis. Characterization of the SNAT2 DNase I HS sites in other cell lines and eventually a cell line that shows a closed chromatin conformation in basal conditions will allow for a clear contrast with the stressed activated open chromatin conformation of the gene. The next step includes the investigation of the DNase I HS sites of ASNS, C/EBPβ and other genes of interest. For the SNAT2 gene, high-resolution analysis such as *in vivo* footprinting represent the following analysis in the investigation of the cis elements of the gene. With regard to nucleosome positioning and MNase treatment, an important future objective would be the high resolution analysis (LM-PCR) of the SNAT2 promoter and C/EBP ATF site. The translational nucleosome positioning analysis can be applied to the ASNS gene and other genes of interest as well.

The elements that need to be addressed in the future regarding the ASNS induction by the UPR are related to the transcriptional complex that is assembled at the ASNS NSRU. Efforts of identifying these components are actually ongoing in the Kilberg laboratory. A question that remains to be addressed as for the SNAT2 gene is, are coactivators part of the protein complex formed at the ASNS promoter region during stress? Does the transcriptional complex formed differ in its composition depending on the initial stimulus, amino acid limitation or ER stress?

The specific role of NSRE-2 in mediating the transcriptional up-regulation of the ASNS gene to AAR and UPR remains to be determined. Given the fact that NSRE-2 confers UPR sensitivity to a C/EBP-ATF site such as that of CHOP leaves open the possibility of investigation of the involvement of this element to the ER stress response. The transcription factors that bind NSRE-2 have yet to be identified.

APPENDIX

Crosstalk Between the AAR and UPR with the MAP Kinase Pathway

Crosstalks between the AAR or UPR with the MAP kinase pathway were explored by inhibitor studies. The crosstalk between the AAR and the MAP kinase pathway has received special attention in the research of the Kilberg laboratory recently (171). In contrast the UPR and MAP kinase crosstalk has not been investigated. The immunoblotting results in Fig. A-1 showed that the MEK1/2 inhibitor PD98059 blocked ATF4 induction, but not the p-eIF2 alpha during ER stress. So, the MAP kinase pathway action is required for ATF4 induction during UPR and the crosstalk is downstream of p-eIF2α. These data are in contrast with those obtained during AAR activation, where the MAP kinase acts upstream of the p-eIF2α. and ATF4. The inhibition of the MEK1/2 by U0126 revealed that both the p-eIF2 alpha and ATF4 are blocked during either AAR or UPR activation (Fig. A-2). The explanation for the distinct results obtained from the use of PD98059 and U0126 during UPR could stand in the specificity of these inhibitors (i.e. PD98059 is considered a MEK1 inhibitor whereas U0126 is a MEK1/2 inhibitor). Other nonspecific actions of these inhibitors should be considered as well in the interpretation of the results.

Nucleosome Positioning on the Human SNAT2 Gene

Establishing the translational positioning of nucleosomes in the SNAT2 gene upstream and downstream the transcription start site (TSS) was the next goal in the investigation of chromatin structure. Are nucleosomes positioned on the SNAT2 gene? Does amino acid limitation or ER stress affect the nucleosome postioning of the SNAT2 gene? To answer these questions, a micrococcal nuclease (MNase) digestion of NP-40 permeabilized HepG2 cells was performed. The digestion by MNase in the linker DNA, between the nucleosomes, was used to map the position of nuclesomes in the SNAT2 region from nt -2320 to +2070. The Southern blotting

results shown in Fig. A-3 demonstrated the existence of a parental band of the right size (4.39kb), a nuclesome ladder was visible starting from mono- and di-nucleosomes toward the proximal promoter region where the resolution was lost. First, this result may denote no translational positioning of nucleosomes in this area. These might be situated randomly, and the end result represented by a smear can be reflective of the average of different MNase cut positions in a cell population. Second, the probe and/or assay conditions may not be optimized to resolve this area. It is noteworthy that in the SNAT2 proximal promoter region, where there is overall low resolution of the 200 bp nucleosome ladder, a band (2.15 kb in size) appeared during AAR activation by HisOH in the 1 and 5 unit MNase digested lanes. Based on the size, the site was mapped in the SNAT2 proximal promoter and is indicated by the thick black arrow in the diagram at the bottom of the blot (Fig. A-3). This result indicates a potential positioning of a nucleosome in the SNAT2 promoter region during HisOH activation of the AAR pathway. It is interesting to speculate that this nucleosome would play a pivotal role in the SNAT2 PIC assembly during exposure of HepG2 cells to amino acid limitation.

Recruitment of p300 at the BiP/GRP78 Promoter

Recruitment of the coactivators (Fig. A-4) p300 and PCAF at the BiP/GRP78 promoter region was assayed by ChIP analysis. The data showed that there is some recruitment of p300 and not PCAF during UPR activation only. This result is consistent with the BiP sensitivity to the UPR and its AAR insensivity. In contrast, ATF4 binding (although low values) at the BiP promoter was observed during both AAR and UPR activation. Another interesting observation was the BiP responsiveness to the AAR activation in the presence of the HDAC inhibitor trichostatin A (TSA). BiP transcription activity was induced two-fold by HisOH treatment in the presence of TSA. These results indicate a possible role of the HDACs as repressors of BiP transcription during the AAR despite increased ATF4 binding detected at the promoter.

Screening of HDAC Binding at the ASNS and SNAT2 Genes

The binding of HDACs1-7 and the co-repressor NcoR was investigated by ChIP analysis. The purpose of this experiment was the screening of the HDAC binding at the ASNS and SNAT2 genes. The results presented in Fig. A-5 showed that HDACs 1-4 occupy the SNAT2 promoter and C/EBP-ATF site and the ASNS promoter during basal conditions. The binding of HDACs 1-4 was decreased upon stress (AAR or UPR). HDACs 5,6,7 and NcoR did not bind the regions tested as demonstrated by the values equal to the non-specific IgG. The replicate experiments for HDAC1,2, 3 and 5 were performed and the data are shown and discussed in Chapter 5.

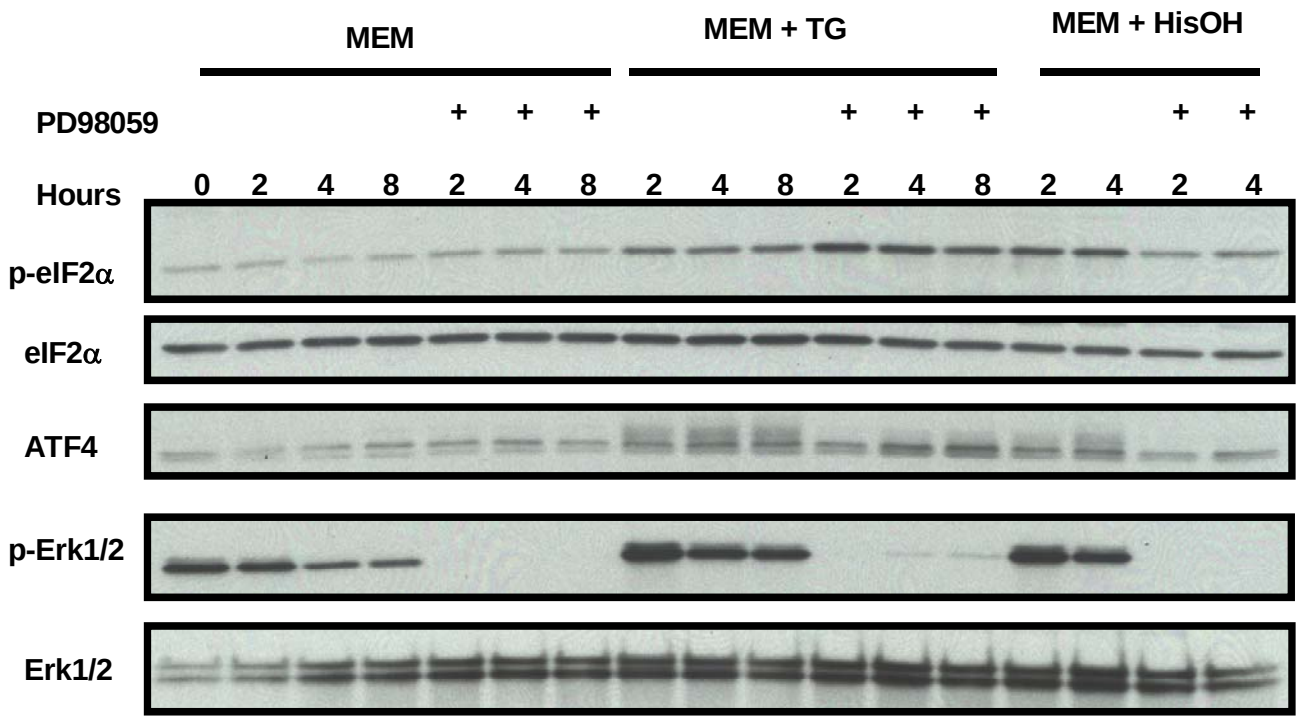

Figure A-1. Inhibition of MEK1/2 by PD98059 blocks ATF4 induction but not that of p-eIF2α during UPR. Whole cell extracts were prepared from HepG2 cells pre-treated or not for 1 h with 50 μM PD98059 followed by AAR or UPR activation using HisOH or TG respectively. Western blot analysis was performed using the indicated antibodies.

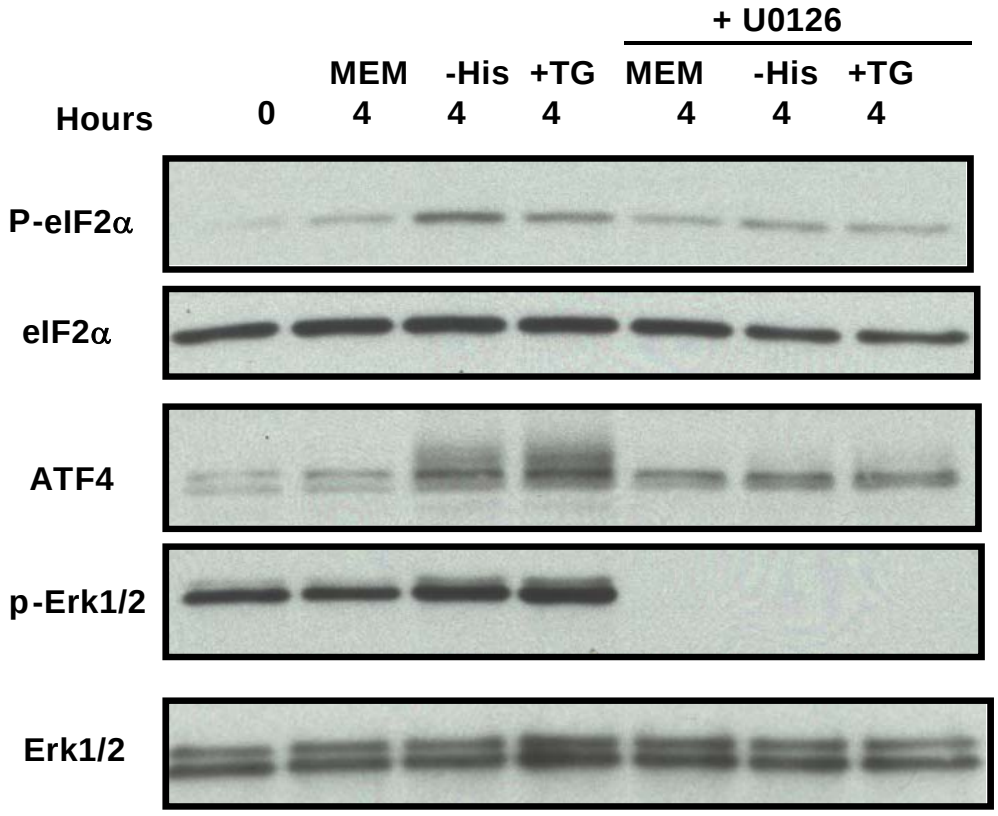

Figure A-2. Inhibition of MEK1/2 by U0126 blocks p-eIF2a and ATF4 induction during UPR. Whole cell extracts were prepared from HepG2 cells pre-treated or not for 1 h with 10mM U0126 followed by AAR or UPR activation using HisOH or TG respectively. Western blot analysis was performed using the indicated antibodies.

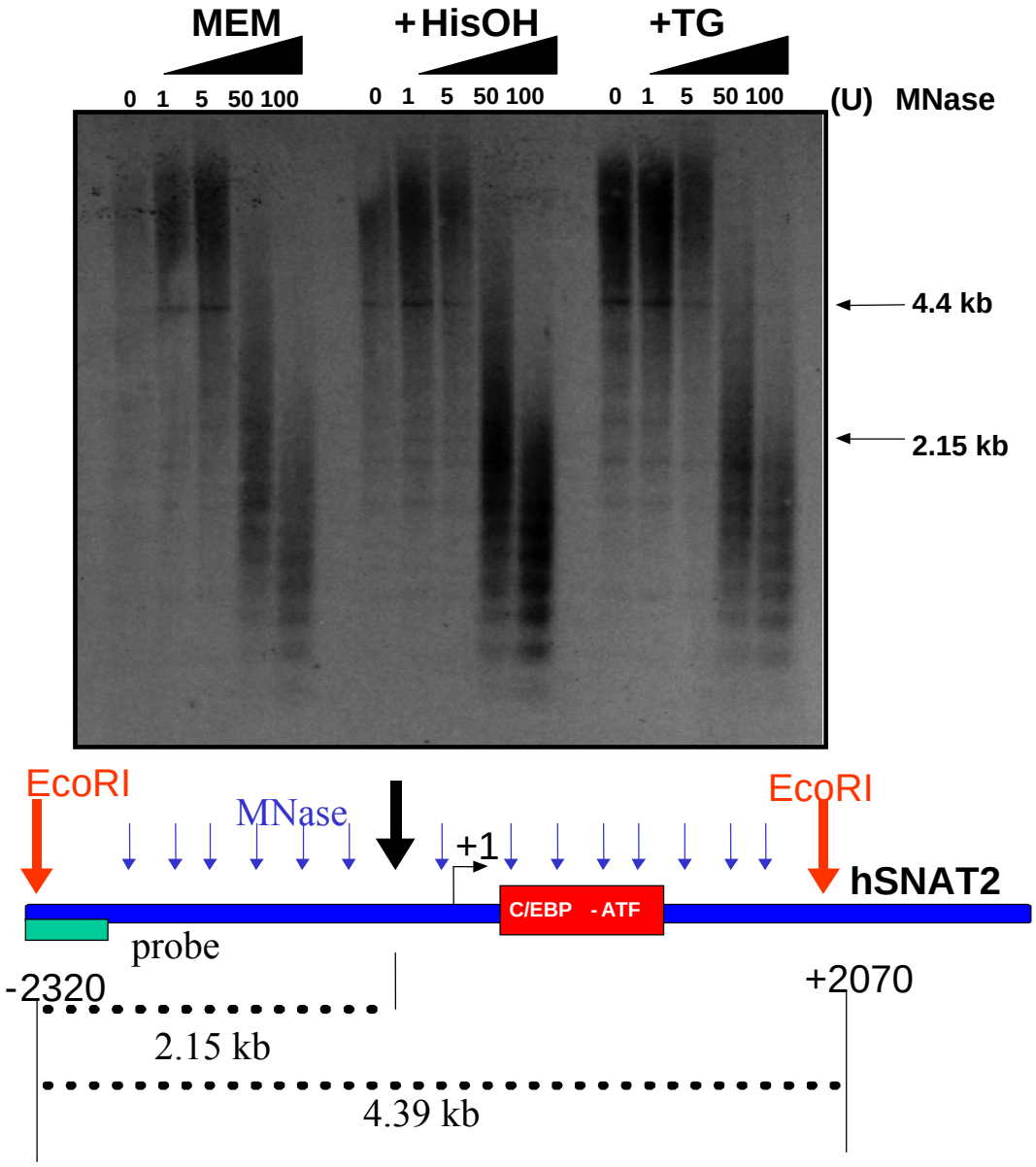

Figure A-3. Micrococcal nuclease treatment and indirect end-labelling. Incubation of HepG2 cells for 8 h in MEM, MEM+HisOH or MEM+TG was followed by MNase digest. Concentrations of MNase used are indicated on top of the gel. After mnase and *EcoR*I digestion 15 mg of DNA were loaded in each lane. For the detailed protocol see the materials and methods section. The diagram at the bottom indicates the position of the radiolabeled probe, the cutting positions of the *EcoR*I restriction enzyme, the length of the parental band (4.39kb) and of another restriction fragment (2.15 kb) observed only in lanes treated with 1 and 5 units of MNase during HisOH activation of the AAR pathway. The autoradiograph shown is representative of multiple blots.

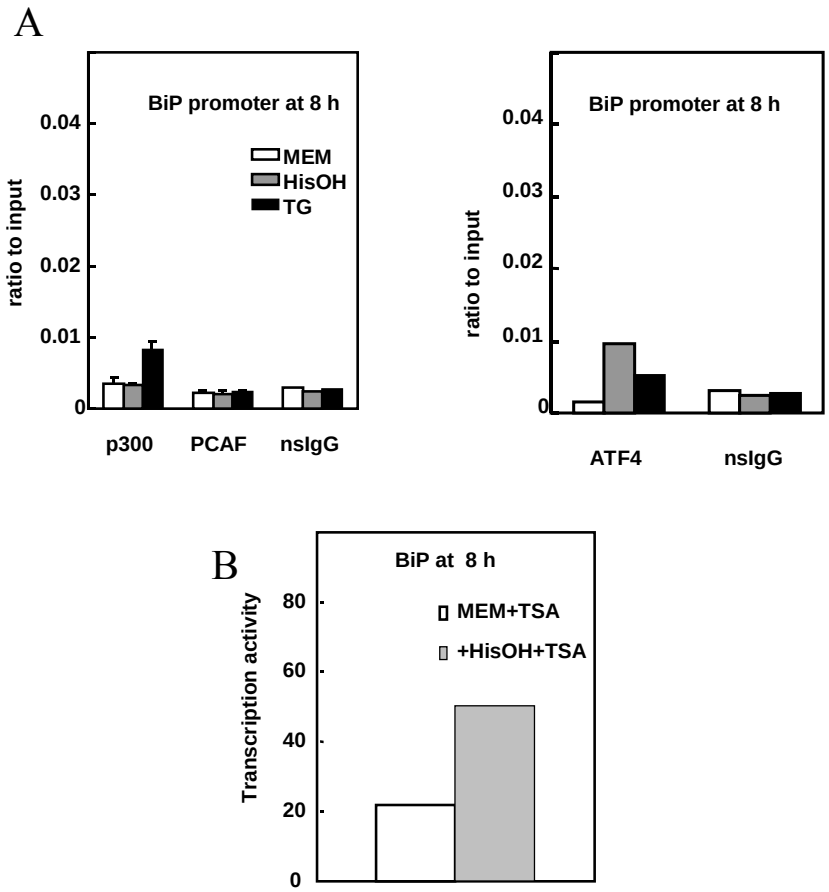

Figure A-4. Protein binding at the *BiP* promoter and *BiP* transcription activity. A) p300 and ATF4 binding to the BiP promoter region during activation of the AAR or UPR. HepG2 cells incubated with MEM only, MEM+HisOH or MEM+TG were used for the ChIP assays. B) BiP transcription activity was measured during AAR activation in the presence of TSA. The data for p300 and PCAF are from three independent experiments, whereas the ATF4 binding and BiP transcription activity data are from a single experiment.

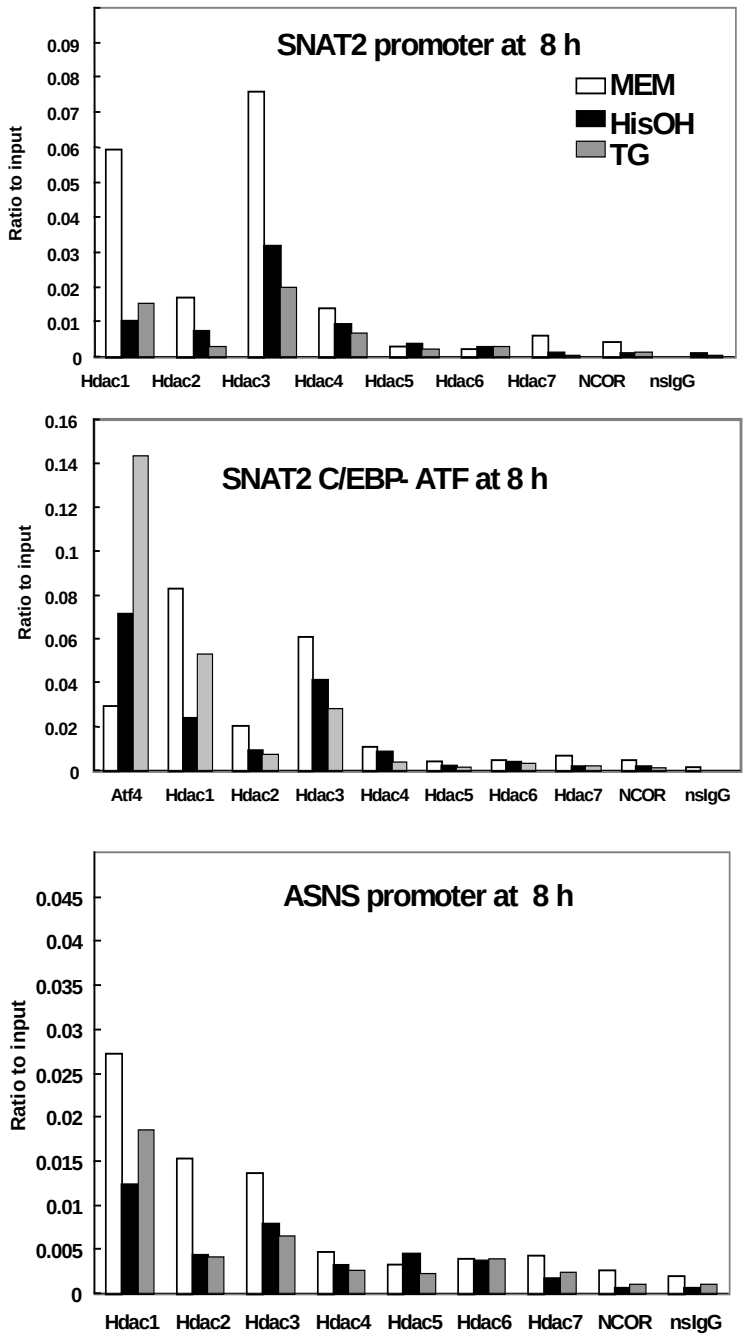

Figure A-5. The binding of HDACs at the *SNAT2* and *ASNS* genes. ChIP analysis was performed on HepG2 cells treated with HisOH or TG for 8 h. Antibodies against HDACs 1-7, ATF4 and nsIgG were used in the IP step of the ChIP assay. The data shown were collected from one experiment.

LIST OF REFERENCES

1. Mitchell, J. A., and Fraser, P. (2008) *Genes Dev* **22**, 20-25
2. Volpi, E. V., Chevret, E., Jones, T., Vatcheva, R., Williamson, J., Beck, S., Campbell, R. D., Goldsworthy, M., Powis, S. H., Ragoussis, J., Trowsdale, J., and Sheer, D. (2000) *J Cell Sci* **113 (Pt 9)**, 1565-1576
3. Johnson, B. R., Nitta, R. T., Frock, R. L., Mounkes, L., Barbie, D. A., Stewart, C. L., Harlow, E., and Kennedy, B. K. (2004) *Proc Natl Acad Sci U S A* **101**, 9677-9682
4. Zeng, C., Kim, E., Warren, S. L., and Berget, S. M. (1997) *Embo J* **16**, 1401-1412
5. Ishihama, Y., Tadakuma, H., Tani, T., and Funatsu, T. (2008) *Exp Cell Res* **314**, 748-762
6. Ragoczy, T., Bender, M. A., Telling, A., Byron, R., and Groudine, M. (2006) *Genes Dev* **20**, 1447-1457
7. Fraser, P., and Engel, J. D. (2006) *Genes Dev* **20**, 1379-1383
8. Shilatifard, A. (2006) *Annu Rev Biochem* **75**, 243-269
9. Ragoczy, T., Telling, A., Sawado, T., Groudine, M., and Kosak, S. T. (2003) *Chromosome Res* **11**, 513-525
10. Lanctot, C., Cheutin, T., Cremer, M., Cavalli, G., and Cremer, T. (2007) *Nat Rev Genet* **8**, 104-115
11. Mateos-Langerak, J., Goetze, S., Leonhardt, H., Cremer, T., van Driel, R., and Lanctot, C. (2007) *J Cell Biochem* **102**, 1067-1075
12. Chandy, M., Gutierrez, J. L., Prochasson, P., and Workman, J. L. (2006) *Eukaryot Cell* **5**, 1738-1747
13. Macfarlane, W. M. (2000) *Mol Pathol* **53**, 1-7
14. Birney, E., Stamatoyannopoulos, J. A., Dutta, A., Guigo, R., Gingeras, T. R., Margulies, E. H., Weng, Z., Snyder, M., Dermitzakis, E. T., Thurman, R. E. (2007) *Nature* **447**, 799-816
15. Bazett-Jones, D. P., Leblanc, B., Herfort, M., and Moss, T. (1994) *Science* **264**, 1134-1137
16. Thanos, D., and Maniatis, T. (1995) *Cell* **83**, 1091-1100
17. Agalioti, T., Lomvardas, S., Parekh, B., Yie, J., Maniatis, T., and Thanos, D. (2000) *Cell* **103**, 667-678
18. Jones, K. A., and Kadonaga, J. T. (2000) *Genes Dev* **14**, 1992-1996
19. Taatjes, D. J., Marr, M. T., and Tjian, R. (2004) *Nat Rev Mol Cell Biol* **5**, 403-410
20. Wright, K. J., Marr, M. T., 2nd, and Tjian, R. (2006) *Proc Natl Acad Sci U S A* **103**, 12347-12352
21. Marr, M. T., 2nd, Isogai, Y., Wright, K. J., and Tjian, R. (2006) *Genes Dev* **20**, 1458-1469
22. Butler, J. E., and Kadonaga, J. T. (2002) *Genes Dev* **16**, 2583-2592
23. Nikolov, D. B., Chen, H., Halay, E. D., Usheva, A. A., Hisatake, K., Lee, D. K., Roeder, R. G., and Burley, S. K. (1995) *Nature* **377**, 119-128
24. Basehoar, A. D., Zanton, S. J., and Pugh, B. F. (2004) *Cell* **116**, 699-709
25. Muller, F., Demeny, M. A., and Tora, L. (2007) *J Biol Chem* **282**, 14685-14689
26. Bushnell, D. A., Westover, K. D., Davis, R. E., and Kornberg, R. D. (2004) *Science* **303**, 983-988
27. Kornberg, R. D. (2007) *Cell Death Differ* **14**, 1989-1997
28. Svejstrup, J. Q., Vichi, P., and Egly, J. M. (1996) *Trends Biochem Sci* **21**, 346-350
29. Kobor, M. S., and Greenblatt, J. (2002) *Biochim Biophys Acta* **1577**, 261-275
30. Sharma, M., George, A. A., Singh, B. N., Sahoo, N. C., and Rao, K. V. (2007) *J Biol Chem* **282**, 20887-20896

31. Yan, Q., Moreland, R. J., Conaway, J. W., and Conaway, R. C. (1999) *J Biol Chem* **274**, 35668-35675
32. Gopalakrishnan, S., Van Emburgh, B. O., and Robertson, K. D. (2008) *Mutat Res*
33. Imhof, A., and Bonaldi, T. (2005) *Mol Biosyst* **1**, 112-116
34. Horn, P. J., and Peterson, C. L. (2002) *Science* **297**, 1824-1827
35. Lomberk, G., Bensi, D., Fernandez-Zapico, M. E., and Urrutia, R. (2006) *Nat Cell Biol* **8**, 407-415
36. Lee, T. I., Jenner, R. G., Boyer, L. A., Guenther, M. G., Levine, S. S., Kumar, R. M., Chevalier, B., Johnstone, S. E., Cole, M. F., Isono, K., Koseki, H., Fuchikami, T., Abe, K., Murray, H. L., Zucker, J. P., Yuan, B., Bell, G. W., Herbolsheimer, E., Hannett, N. M., Sun, K., Odom, D. T., Otte, A. P., Volkert, T. L., Bartel, D. P., Melton, D. A., Gifford, D. K., Jaenisch, R., and Young, R. A. (2006) *Cell* **125**, 301-313
37. Boyer, L. A., Lee, T. I., Cole, M. F., Johnstone, S. E., Levine, S. S., Zucker, J. P., Guenther, M. G., Kumar, R. M., Murray, H. L., Jenner, R. G. (2005) *Cell* **122**, 947-956
38. Kurdistani, S. K., Tavazoie, S., and Grunstein, M. (2004) *Cell* **117**, 721-733
39. Bernstein, B. E., Liu, C. L., Humphrey, E. L., Perlstein, E. O., and Schreiber, S. L. (2004) *Genome Biol* **5**, R62
40. Barrera, L. O., and Ren, B. (2006) *Curr Opin Cell Biol* **18**, 291-298
41. Soutoglou, E., and Talianidis, I. (2002) *Science* **295**, 1901-1904
42. Zhang, P., McGrath, B. C., Reinert, J., Olsen, D. S., Lei, L., Gill, S., Wek, S. A., Vattem, K. M., Wek, R. C., Kimball, S. R. (2002) *Mol Cell Biol* **22**, 6681-6688
43. Sood, R., Porter, A. C., Olsen, D. A., Cavener, D. R., and Wek, R. C. (2000) *Genetics* **154**, 787-801
44. Harding, H. P., Calfon, M., Urano, F., Novoa, I., and Ron, D. (2002) *Annu Rev Cell Dev Biol* **18**, 575-599
45. Chen, H., Pan, Y. X., Dudenhausen, E. E., and Kilberg, M. S. (2004) *J Biol Chem* **279**, 50829-50839
46. Palii, S. S., Thiaville, M. M., Pan, Y. X., Zhong, C., and Kilberg, M. S. (2006) *Biochem J* **395**, 517-527
47. Kilberg, M. S., Pan, Y. X., Chen, H., and Leung-Pineda, V. (2005) *Annu Rev Nutr* **25**, 59-85
48. Kilberg, M. S., Stevens, B. R., and Novak, D. A. (1993) *Annu Rev Nutr* **13**, 137-165
49. Kilberg, M. S., Hutson, R. G., and Laine, R. O. (1994) *Faseb J* **8**, 13-19
50. Kimball, S. R., and Jefferson, L. S. (2005) *Semin Cell Dev Biol* **16**, 21-27
51. Kimball, S. R., and Jefferson, L. S. (2006) *Am J Clin Nutr* **83**, 500S-507S
52. Kimball, S. R., and Jefferson, L. S. (2004) *Nutr Metab (Lond)* **1**, 3
53. Garcia-Barrio, M., Dong, J., Ufano, S., and Hinnebusch, A. G. (2000) *Embo J* **19**, 1887-1899
54. Dong, J., Qiu, H., Garcia-Barrio, M., Anderson, J., and Hinnebusch, A. G. (2000) *Mol Cell* **6**, 269-279
55. Hansen, B. S., Vaughan, M. H., and Wang, L. (1972) *J Biol Chem* **247**, 3854-3857
56. Vaughan, M. H., and Hansen, B. S. (1973) *J Biol Chem* **248**, 7087-7096
57. Vattem, K. M., and Wek, R. C. (2004) *Proc Natl Acad Sci U S A* **101**, 11269-11274
58. Dever, T. E., Feng, L., Wek, R. C., Cigan, A. M., Donahue, T. F., and Hinnebusch, A. G. (1992) *Cell* **68**, 585-596
59. Siu, F., Bain, P. J., LeBlanc-Chaffin, R., Chen, H., and Kilberg, M. S. (2002) *J Biol Chem* **277**, 24120-24127

60. Natarajan, K., Meyer, M. R., Jackson, B. M., Slade, D., Roberts, C., Hinnebusch, A. G., and Marton, M. J. (2001) *Mol Cell Biol* **21**, 4347-4368
61. Hinnebusch, A. G., and Natarajan, K. (2002) *Eukaryot Cell* **1**, 22-32
62. Vallejo, M., Ron, D., Miller, C. P., and Habener, J. F. (1993) *Proc Natl Acad Sci U S A* **90**, 4679-4683
63. Podust, L. M., Krezel, A. M., and Kim, Y. (2001) *J Biol Chem* **276**, 505-513
64. Schroder, M., and Kaufman, R. J. (2005) *Annu Rev Biochem* **74**, 739-789
65. Schroder, M., and Kaufman, R. J. (2005) *Mutat Res* **569**, 29-63
66. van Anken, E., and Braakman, I. (2005) *Crit Rev Biochem Mol Biol* **40**, 269-283
67. Rutkowski, D. T., and Kaufman, R. J. (2004) *Trends Cell Biol* **14**, 20-28
68. Harding, H. P., Zhang, Y., Bertolotti, A., Zeng, H., and Ron, D. (2000) *Mol Cell* **5**, 897-904
69. Ron, D. (2002) *J Clin Invest* **110**, 1383-1388
70. Wek, R. C., and Cavener, D. R. (2007) *Antioxid Redox Signal* **9**, 2357-2371
71. Cullinan, S. B., and Diehl, J. A. (2006) *Int J Biochem Cell Biol* **38**, 317-332
72. Cullinan, S. B., Zhang, D., Hannink, M., Arvisais, E., Kaufman, R. J., and Diehl, J. A. (2003) *Mol Cell Biol* **23**, 7198-7209
73. Haze, K., Yoshida, H., Yanagi, H., Yura, T., and Mori, K. (1999) *Mol Biol Cell* **10**, 3787-3799
74. Yoshida, H., Okada, T., Haze, K., Yanagi, H., Yura, T., Negishi, M., and Mori, K. (2000) *Mol Cell Biol* **20**, 6755-6767
75. Lemin, A. J., Saleki, K., van Lith, M., and Benham, A. M. (2007) *FEBS Lett* **581**, 1819-1824
76. Thuerauf, D. J., Marcinko, M., Belmont, P. J., and Glembotski, C. C. (2007) *J Biol Chem* **282**, 22865-22878
77. Yamamoto, K., Sato, T., Matsui, T., Sato, M., Okada, T., Yoshida, H., Harada, A., and Mori, K. (2007) *Dev Cell* **13**, 365-376
78. Lee, K. P., Dey, M., Neculai, D., Cao, C., Dever, T. E., and Sicheri, F. (2008) *Cell* **132**, 89-100
79. Ron, D., and Hubbard, S. R. (2008) *Cell* **132**, 24-26
80. Back, S. H., Schroder, M., Lee, K., Zhang, K., and Kaufman, R. J. (2005) *Methods* **35**, 395-416
81. Iwawaki, T., and Akai, R. (2006) *Biochem Biophys Res Commun*
82. Kaufman, R. J. (1999) *Genes Dev* **13**, 1211-1233
83. Hollien, J., and Weissman, J. S. (2006) *Science* **313**, 104-107
84. Ron, D. (2006) *Science* **313**, 52-53
85. Zhao, L., and Ackerman, S. L. (2006) *Curr Opin Cell Biol* **18**, 444-452
86. Romisch, K. (2005) *Annu Rev Cell Dev Biol* **21**, 435-456
87. Schubert, U., Anton, L. C., Gibbs, J., Norbury, C. C., Yewdell, J. W., and Bennink, J. R. (2000) *Nature* **404**, 770-774
88. Johnson, A. E., and van Waes, M. A. (1999) *Annu Rev Cell Dev Biol* **15**, 799-842
89. Helenius, A., and Aebi, M. (2004) *Annu Rev Biochem* **73**, 1019-1049
90. Ma, Y., and Hendershot, L. M. (2004) *J Biol Chem* **279**, 13792-13799
91. Yamamoto, K., Yoshida, H., Kokame, K., Kaufman, R. J., and Mori, K. (2004) *J Biochem (Tokyo)* **136**, 343-350
92. Hampton, R. Y., Gardner, R. G., and Rine, J. (1996) *Mol Biol Cell* **7**, 2029-2044
93. Reimer, R. J., Chaudhry, F. A., Gray, A. T., and Edwards, R. H. (2000) *Proc Natl Acad Sci U S A* **97**, 7715-7720

94. Mackenzie, B., and Erickson, J. D. (2004) *Pflugers Arch* **447**, 784-795
95. Oxender, D. L., and Christensen, H. N. (1963) *J Biol Chem* **238**, 3686-3699
96. Thomas, E. L., Shao, T. C., and Christensen, H. N. (1971) *J Biol Chem* **246**, 1677-1681
97. Gazzola, G. C., Franchi, R., Saibene, V., Ronchi, P., and Guidotti, G. G. (1972) *Biochim Biophys Acta* **266**, 407-421
98. Sugawara, M., Nakanishi, T., Fei, Y. J., Huang, W., Ganapathy, M. E., Leibach, F. H., and Ganapathy, V. (2000) *J Biol Chem* **275**, 16473-16477
99. Yao, D., Mackenzie, B., Ming, H., Varoqui, H., Zhu, H., Hediger, M. A., and Erickson, J. D. (2000) *J Biol Chem* **275**, 22790-22797
100. Hatanaka, T., Huang, W., Wang, H., Sugawara, M., Prasad, P. D., Leibach, F. H., and Ganapathy, V. (2000) *Biochim Biophys Acta* **1467**, 1-6
101. Bain, P. J., LeBlanc-Chaffin, R., Chen, H., Palii, S. S., Leach, K. M., and Kilberg, M. S. (2002) *J Nutr* **132**, 3023-3029
102. Kilberg, M., and Häussinger, D. (1993) *Mammalian Amino Acid Transport*, Plenum Publishing Corporation
103. Hyde, R., Christie, G. R., Litherland, G. J., Hajduch, E., Taylor, P. M., and Hundal, H. S. (2001) *Biochem J* **355**, 563-568
104. Franchi-Gazzola, R., Dall'Asta, V., Sala, R., Visigalli, R., Bevilacqua, E., Gaccioli, F., Gazzola, G. C., and Bussolati, O. (2006) *Acta Physiol (Oxf)* **187**, 273-283
105. Franchi-Gazzola, R., Gaccioli, F., Bevilacqua, E., Visigalli, R., Dall'Asta, V., Sala, R., Varoqui, H., Erickson, J. D., Gazzola, G. C., and Bussolati, O. (2004) *Biochim Biophys Acta* **1667**, 157-166
106. Kilberg, M. S., Barber, E. F., and Handlogten, M. E. (1985) *Curr Top Cell Regul* **25**, 133-163
107. Bhat, H. K., and Vadgama, J. V. (2002) *Int J Mol Med* **9**, 271-279
108. Ensenat, D., Hassan, S., Reyna, S. V., Schafer, A. I., and Durante, W. (2001) *Biochem J* **360**, 507-512
109. Gaccioli, F., Huang, C. C., Wang, C., Bevilacqua, E., Franchi-Gazzola, R., Gazzola, G. C., Bussolati, O., Snider, M. D., and Hatzoglou, M. (2006) *J Biol Chem* **281**, 17929-17940
110. Hyde, R., Peyrollier, K., and Hundal, H. S. (2002) *J Biol Chem* **277**, 13628-13634
111. Guerrini, L., Gong, S. S., Mangasarian, K., and Basilico, C. (1993) *Mol Cell Biol* **13**, 3202-3212
112. Barbosa-Tessmann, I. P., Chen, C., Zhong, C., Siu, F., Schuster, S. M., Nick, H. S., and Kilberg, M. S. (2000) *J Biol Chem* **275**, 26976-26985
113. Zhong, C., Chen, C., and Kilberg, M. S. (2003) *Biochem J* **372**, 603-609
114. Palii, S. S., Chen, H., and Kilberg, M. S. (2004) *J Biol Chem* **279**, 3463-3471
115. Bruhat, A., Jousse, C., Carraro, V., Reimold, A. M., Ferrara, M., and Fafournoux, P. (2000) *Mol Cell Biol* **20**, 7192-7204
116. Pan, Y. X., Chen, H., Thiaville, M. M., and Kilberg, M. S. (2007) *Biochem J* **401**, 299-307
117. Thastrup, O., Cullen, P. J., Drobak, B. K., Hanley, M. R., and Dawson, A. P. (1990) *Proc Natl Acad Sci U S A* **87**, 2466-2470
118. Tkacz, J. S., and Lampen, O. (1975) *Biochem Biophys Res Commun* **65**, 248-257
119. Lipson, K. E., and Baserga, R. (1989) *Proc Natl Acad Sci U S A* **86**, 9774-9777
120. Kilberg, M. S. (1989) *Methods Enzymol* **173**, 564-575
121. Lu, P. D., Harding, H. P., and Ron, D. (2004) *J Cell Biol* **167**, 27-33

122. Harding, H. P., Novoa, I., Zhang, Y., Zeng, H., Wek, R., Schapira, M., and Ron, D. (2000) *Mol Cell* **6**, 1099-1108
123. Harding, H. P., Zhang, Y., Zeng, H., Novoa, I., Lu, P. D., Calfon, M., Sadri, N., Yun, C., Popko, B., Paules, R. (2003) *Mol Cell* **11**, 619-633
124. Ameri, K., and Harris, A. L. (2008) *Int J Biochem Cell Biol* **40**, 14-21
125. Liang, G., and Hai, T. (1997) *J Biol Chem* **272**, 24088-24095
126. Yang, X., Matsuda, K., Bialek, P., Jacquot, S., Masuoka, H. C., Schinke, T., Li, L., Brancorsini, S., Sassone-Corsi, P., Townes, T. M., Hanauer, A., and Karsenty, G. (2004) *Cell* **117**, 387-398
127. De Angelis, R., Iezzi, S., Bruno, T., Corbi, N., Di Padova, M., Floridi, A., Fanciulli, M., and Passananti, C. (2003) *FEBS Lett* **547**, 15-19
128. Fawcett, T. W., Martindale, J. L., Guyton, K. Z., Hai, T., and Holbrook, N. J. (1999) *Biochem J* **339 (Pt 1)**, 135-141
129. McGivan, J. D., and Pastor-Anglada, M. (1994) *Biochem J* **299 (Pt 2)**, 321-334
130. Barber, E. F., Handlogten, M. E., Vida, T. A., and Kilberg, M. S. (1982) *J Biol Chem* **257**, 14960-14967
131. Saier, M. H., Jr., Daniels, G. A., Boerner, P., and Lin, J. (1988) *J Membr Biol* **104**, 1-20
132. Kilberg, M. S., and Barbosa-Tessmann, I. P. (2002) *J Nutr* **132**, 1801-1804
133. Gjymishka, A., Palii, S. S., Shan, J., and Kilberg, M. S. (2008) *J Biol Chem* **283**, 27736-27747
134. Yoshida, H., Haze, K., Yanagi, H., Yura, T., and Mori, K. (1998) *J Biol Chem* **273**, 33741-33749
135. Roy, B., and Lee, A. S. (1999) *Nucleic Acids Res* **27**, 1437-1443
136. Barbosa-Tessmann, I. P., Pineda, V. L., Nick, H. S., Schuster, S. M., and Kilberg, M. S. (1999) *Biochem J* **339 (Pt 1)**, 151-158
137. Chen, C., Dudenhausen, E., Chen, H., Pan, Y. X., Gjymishka, A., and Kilberg, M. S. (2005) *Biochem J* **391**, 649-658
138. Pan, Y., Chen, H., Siu, F., and Kilberg, M. S. (2003) *J Biol Chem* **278**, 38402-38412
139. Jousse, C., Bruhat, A., Harding, H. P., Ferrara, M., Ron, D., and Fafournoux, P. (1999) *FEBS Lett* **448**, 211-216
140. Ma, Y., Brewer, J. W., Diehl, J. A., and Hendershot, L. M. (2002) *J Mol Biol* **318**, 1351-1365
141. Pirot, P., Ortis, F., Cnop, M., Ma, Y., Hendershot, L. M., Eizirik, D. L., and Cardozo, A. K. (2007) *Diabetes* **56**, 1069-1077
142. Peterson, C. L., and Laniel, M. A. (2004) *Curr Biol* **14**, R546-551
143. Vermeulen, M., Mulder, K. W., Denissov, S., Pijnappel, W. W., van Schaik, F. M., Varier, R. A., Baltissen, M. P., Stunnenberg, H. G., Mann, M., and Timmers, H. T. (2007) *Cell* **131**, 58-69
144. Lee, J., Thompson, J. R., Botuyan, M. V., and Mer, G. (2008) *Nat Struct Mol Biol* **15**, 109-111
145. Whetstine, J. R., Nottke, A., Lan, F., Huarte, M., Smolikov, S., Chen, Z., Spooner, E., Li, E., Zhang, G., Colaiacovo, M., and Shi, Y. (2006) *Cell* **125**, 467-481
146. Rosenfeld, M. G., Lunyak, V. V., and Glass, C. K. (2006) *Genes Dev* **20**, 1405-1428
147. Xiang, Y., Zhu, Z., Han, G., Ye, X., Xu, B., Peng, Z., Ma, Y., Yu, Y., Lin, H., Chen, A. P., and Chen, C. D. (2007) *Proc Natl Acad Sci U S A* **104**, 19226-19231
148. Guo, F., and Cavener, D. R. (2007) *Cell Metab* **5**, 103-114

149. Yoshida, H., Matsui, T., Yamamoto, A., Okada, T., and Mori, K. (2001) *Cell* **107**, 881-891
150. Sriburi, R., Jackowski, S., Mori, K., and Brewer, J. W. (2004) *J Cell Biol* **167**, 35-41
151. Yoshida, H., Matsui, T., Yamamoto, A., Okada, T., Mori, K., and 2001. *Cell* **107**, 881-891
152. Berlanga, J. J., Santoyo, J., and De Haro, C. (1999) *Eur J Biochem* **265**, 754-762
153. Wolfgang, C. D., Chen, B. P., Martindale, J. L., Holbrook, N. J., and Hai, T. (1997) *Mol Cell Biol* **17**, 6700-6707
154. Siu, F., Chen, C., Zhong, C., and Kilberg, M. S. (2001) *J Biol Chem* **276**, 48100-48107
155. Lopez, A. B., Wang, C., Huang, C. C., Yaman, I., Li, Y., Chakravarty, K., Johnson, P. F., Chiang, C. M., Snider, M. D., Wek, R. C., and Hatzoglou, M. (2007) *Biochem J* **402**, 163-173
156. Gjymishka, A., Su, N., and Kilberg, M. S. (2008) *Biochem J*
157. Thomas, M. C., and Chiang, C. M. (2006) *Crit Rev Biochem Mol Biol* **41**, 105-178
158. Sato, S., Tomomori-Sato, C., Parmely, T. J., Florens, L., Zybailov, B., Swanson, S. K., Banks, C. A., Jin, J., Cai, Y., Washburn, M. P., Conaway, J. W., and Conaway, R. C. (2004) *Mol Cell* **14**, 685-691
159. Takagi, Y., and Kornberg, R. D. (2006) *J Biol Chem* **281**, 80-89
160. Fan, X., Chou, D. M., and Struhl, K. (2006) *Nat Struct Mol Biol* **13**, 117-120
161. Andrau, J. C., van de Pasch, L., Lijnzaad, P., Bijma, T., Koerkamp, M. G., van de Peppel, J., Werner, M., and Holstege, F. C. (2006) *Mol Cell* **22**, 179-192
162. Zhu, X., Wiren, M., Sinha, I., Rasmussen, N. N., Linder, T., Holmberg, S., Ekwall, K., and Gustafsson, C. M. (2006) *Mol Cell* **22**, 169-178
163. Novoa, I., Zhang, Y., Zeng, H., Jungreis, R., Harding, H. P., and Ron, D. (2003) *Embo J* **22**, 1180-1187
164. Barbosa-Tessmann, I. P., Chen, C., Zhong, C., Schuster, S. M., Nick, H. S., and Kilberg, M. S. (1999) *J Biol Chem* **274**, 31139-31144
165. Yamamoto, K., Sato, T., Matsui, T., Sato, M., Okada, T., Yoshida, H., Harada, A., Mori, K., and 2007. *Dev Cell* **13**, 365-376
166. Yoshida, H., Matsui, T., Hosokawa, N., Kaufman, R. J., Nagata, K., and Mori, K. (2003) *Dev Cell* **4**, 265-271
167. Lee, A. H., Iwakoshi, N. N., and Glimcher, L. H. (2003) *Mol Cell Biol* **23**, 7448-7459
168. Chen, C., Dudenhausen, E. E., Pan, Y. X., Zhong, C., and Kilberg, M. S. (2004) *J Biol Chem* **279**, 27948-27956
169. Fernandez, J., Lopez, A. B., Wang, C., Mishra, R., Zhou, L., Yaman, I., Snider, M. D., and Hatzoglou, M. (2003) *J Biol Chem* **278**, 50000-50009
170. Bruhat, A., Averous, J., Carraro, V., Zhong, C., Reimold, A. M., Kilberg, M. S., and Fafournoux, P. (2002) *J Biol Chem* **277**, 48107-48114
171. Thiaville, M. M., Pan, Y. X., Gjymishka, A., Zhong, C., Kaufman, R. J., and Kilberg, M. S. (2008) *J Biol Chem* **283**, 10848-10857

BIOGRAPHICAL SKETCH

Altin Gjymishka was born in 1975 in the city of Peshkopi, Albania. After he finished high school in Albania, he was admitted in 1994 to the Carol Davila University of Medicine and Pharmacy in Bucharest, Romania, where he studied general medicine. After graduating from medical school and becoming licensed as an M.D. in September 2000, he continued his residency training in general surgery. Always wanting to expand his scientific knowledge, he joined in fall 2004 the Interdisciplinary Program in Biomedical Sciences at the University of Florida. Altin completed his Ph.D. in medical sciences--biochemistry and molecular biology under the guidance of Dr. Michael S. Kilberg in fall 2008.